2018

A Role for PI31-Mediated Proteasome Regulation in Proteostasis and Neuronal Health

Sandra Jones

A ROLE FOR PI31-MEDIATED PROTEASOME REGULATION IN PROTEOSTASIS AND NEURONAL HEALTH

A Thesis Presented to the Faculty of

The Rockefeller University

in Partial Fulfillment of the Requirements for

the degree of Doctor of Philosophy

by

Sandra Jones

June 2018

A ROLE FOR PI31-MEDIATED PROTEASOME REGULATION IN PROTEOSTASIS AND NEURONAL HEALTH

Sandra Jones, Ph.D.

The Rockefeller University 2018

The specific and timely degradation of proteins is achieved by the Ubiquitin-Proteasome System (UPS), which governs a variety of cellular processes such as apoptosis, cell cycle progression, protein quality control, and metabolism. Using this system, cells maintain homeostasis by quickly and irreversibly altering signaling pathways in response to changing environmental stimuli. Protein degradation by UPS requires two consecutive steps, 1) the covalent attachment of the substrate by ubiquitin and 2) the delivery of the substrate to the 26S proteasome for breakdown and recycling of reusable ubiquitin. The 26S proteasome is a 2.5-MDa multicatalytic protease consisting of two subcomplexes: a 20S core particle (CP) and a 19S regulatory particle (RP) that caps one or both ends of the 20S proteasome. Most investigations on proteasome regulation have focused on substrate recognition, binding, deubiquitination, unfolding, and translocation. However, evidence shows that the 26S complex itself can be regulated by the abundance of available subunits, rates of assembly and disassembly, post-translational modification, localization, and a variety of interacting proteins. Yet, this data is limited and an extensive amount of knowledge remains to be uncovered regarding 26S proteasome regulation since it differs depending on the tissue and cellular context. Aging, for example, leads to reduced proteasome activity but it is unknown how proteasomes are affected throughout the aging process.

In this thesis, the aim is to reveal how proteasomes are regulated by changes in nicotinamide adenine dinucleotide (NAD+) metabolism and how this impacts neurodegeneration.

Using *Drosophila melanogaster*, I describe the necessity for the proteasome regulator, DmPI31, in neuronal maintenance and show that dietary restriction and NAD+ repletion, can regulate both DmPI31 and proteasome activity. Generation of *dmPI31* mutant clones in the *Drosophila* eye show rapid degeneration of photoreceptor cells and RNAi knockdown of DmPI31 leads to eclosion defects and shortened lifespan. I demonstrate the ability of NAD+ repletion to increase proteasome activity and DmPI31 protein levels and show NAD+ acts via DmPI31 to increase 26S proteasome activity. The importance of this pathway is illustrated by the finding that elevated levels of DmPI31 can extend lifespan and partially rescue neuronal degeneration in a *Drosophila* model of spinocerebellar ataxia type 1(SCA1). These results demonstrate a link between NAD+ and proteasomes that may ultimately prove useful for developing interventions that counter the effects of neurodegeneration and allow for an understanding why this system begins to fail in aging and age-associated diseases.

Acknowledgments

First and foremost, I would like to thank my advisor, Dr. Hermann Steller, for welcoming me into the lab and providing guidance and support for both personal and scientific growth throughout the years. Additional thanks to my committee members, Dr. Shai Shaham and Dr. Michael Young, who have provided challenging and useful commentary during my studies that have expanded my knowledge on approaching scientific questions. To Dr. Nancy Bonini, thank you for accepting my invitation to sit as my external committee member and providing your feedback.

I am so grateful for everyone in the Dean's office here at The Rockefeller University, Kristen Cullen, Marta Delgado, Cristian Rosario, and Stephanie Fernandez, have all been such a great support when I needed anything. Thank you to Emily Harms and Andrea Morris for providing me with amazing opportunities in teaching and mentorship. All the Steller lab members, past and present, who have made the lab a great place to work and each contributed to my growth as a scientist – Ainhoa Perez, Cristinel Sandu, Anshuman Kelkar, Park Cho, Sigi-Benjamin-Hong, Kai Liu, Joe Rodriguez, Yetis Gultekin, Irit Shachrai, Tommy Hsiao, Sam Sharma, Junko Shimazu, Adi Minis, Linda Liu. Thanks to the two high school summer students I had the privilege of mentoring– Catherina Mobini and Amy Liu– who were so intelligent, fun, and eager to learn.

Furthermore, I owe my passion and pursuit of science to my Spelman College mentors – Dr. Leyte Winfield and Dr. Kimberley Jackson– who introduced me to research, nominated me for countless fellowships, and continue to encourage me all these years later. To Dan Jarosz,

whose mentorship during my summer at MIT was exceptional and not only introduced me to Rockefeller but taught me that there is no such thing as a ‘failed’ experiment.

Finally, thanks to my friends and family. I don’t think my Gilliam/EXROP support system knows how much they mean to my sanity. Seeing everyone once a year wasn’t enough but always reawaken my passion for science. To Troy, for all the laughs, motivation, patience, and updates on the outside world. My biggest thanks goes to my parents, William and Soon Jones who have pushed me since I could remember to take on a challenge and have supported me in everything I’ve ever pursued.

Table of Contents

List of Figures and Illustrations

List of Abbreviations

- aa –amino acid
- AD – Alzheimer's disease
- Atx-1 – ataxin-1 protein
- cADPR – cyclic ADP-ribose
- CNS – Central nervous system
- CP –core particle
- DmPI31 – *Drosophila melanogaster* Proteasome Inhibitor 31
- DR – Dietary restriction
- DUB – deubiquitinating enzyme
- HbYX – Hydrophobic Tyrosine-X
- Na – Nicotinic acid
- NAD+ -- Nicotinamide adenine dinucleotide
- Nam – Nicotinamide
- OL – Optic lobe
- PARPs – Poly ADP-ribose polymerase
- PD – Parkinson's disease
- PE -- Post eclosion
- PIP – proteasome interacting protein
- Redox – oxidation reduction reactions
- RP – regulatory particle
- SCA-1—Spinocerebellar ataxia type-1
- UPS – Ubiquitin Proteasome System

1. Introduction

1.1 Protein Degradation by the Ubiquitin-Proteasome System (UPS)

1.1.1 The Ubiquitin-Proteasome System

The concept of a tightly controlled and highly regulated mechanism for intracellular protein degradation was until a few decades ago underappreciated by many scientists. Now, the dynamic state of the proteome, by regulated synthesis and degradation, are recognized as being crucial for diverse cellular processes. The two major pathways of protein degradation in eukaryotic cells are the lysosomal proteolysis pathway and the ubiquitin-proteasome system (UPS). Lysosomal proteolysis is a bulk process that involves the uptake of extracellular proteins, cytoplasmic organelles, or cytosolic proteins into membrane bound vesicles that will fuse with the lysosome. Once inside these membrane-bound organelles, engulfed proteins are exposed to several digestive enzymes that will non-selectively degrade them at approximately the same rate. In this way, long lived cytoplasmic proteins are eventually degraded. The degradation of short-lived intracellular proteins however is primary conducted by the UPS. This system requires proteins to be tagged with a chain of an evolutionarily conserved polypeptide termed ubiquitin via a highly regulated enzymatic cascade. These polyubiquitinated proteins are then targeted for delivery to the multisubunit protease complex termed the proteasome. Both the attachment of ubiquitin and degradation of proteins by the proteasome are energy dependent processes that require ATP (Glickman and Ciechanover, 2002; Nedelsky et al., 2008). It was the discovery of this intricate cascade and the targeted degradation of proteins that transformed the field. It is now clear that targeted protein degradation plays a major role in a variety of cellular processes such as

apoptosis, cell cycle progression, differentiation, DNA repair, protein quality control, and metabolism. However, much remains to be learned about the regulation of protein degradation by the UPS. Uncovering mechanisms that regulate proteasomal degradation under varied cellular contexts and determining how aberrations in this process bring about disease leave much to be discovered.

1.1.2 Composition of the UPS

The UPS is a selective pathway that degrades cytoplasmic and nuclear proteins. It requires two consecutive steps 1) the covalent attachment of the substrate by ubiquitin and 2) the delivery of the substrate to the 26S proteasome for breakdown and recycling of reusable ubiquitin. Ubiquitin (Ub) is a highly conserved 76-amino acid polypeptide that is attached to lysine residues to form polyubiquitin chains on proteins targeted for degradation by the 26S proteasome. Conjugation of ubiquitin usually occurs at lysine residues and requires 3 types of enzymes: E1 (ubiquitin-activating enzyme), E2 (ubiquitin-conjugating enzyme), and E3 (ubiquitin ligase). Ubiquitin is activated in an ATP dependent manner by the E1 activating enzyme, which generates a high-energy thiol ester intermediate. Next, one of several E2 conjugating enzymes receives the ubiquitin from E1 and forms a similar thiol ester intermediate before binding to one of many E3 ubiquitin ligases. From here the E3 ubiquitin ligase binds to a specific substrate and catalyzes the transfer of ubiquitin from the E2 enzyme to the substrate. E3 ubiquitin ligases thus hold the key to substrate specificity in the UPS. The subsequent addition of ubiquitin to lysine residues on previously conjugated enzyme forms the polyubiquitin chain that is recognized by the 26S proteasome (Glickman and Ciechanover 2002; Hershko and Ciechanover 1998).

After tagging with ubiquitin, proteins are targeted to the 26S proteasome. This complex is a sophisticated 2.5-MDa multicatalytic protease consisting of two subcomplexes: a barrel shaped 20S core or catalytic particle (CP) and a 19S regulatory particle (RP) that caps one or both ends of the 20S proteasome. Both subcomplexes are made up of distinct subunits. The 20S CP is made from the stacking of two identical outer alpha rings and two identical inner beta rings, each of which has seven distinct subunits. The N-terminal tails of the alpha subunits form a "gate" into the center of the core where the proteolytic beta subunits reside. The beta subunits, beta1, beta2, beta5, contain the three distinct catalytic functions, caspase-like, trypsin-like, and chymotrypsin-like activity, respectively, so named due to the types of peptides they generate. These active sites are located deep within the barrel of the narrow entrance channel, 13 Å, thus proteins must be at least partially unfolded for translocation into the core particle prior to degradation (Groll et al., 2000). The 19S RP is important for translocation of proteins into the CP but also functions in the recognition of ubiquitinated proteins and deubiquitination of substrates. It is composed of a base with three non-ATPases (Rpn1, Rpn2, Rpn13), six ATPases (Rpt1-6) and a lid with nine non-ATPase subunits (Rpn3, Rpn5-9, Rpn11-12, Rpn15) and Rpn10, which is assumed to sit between the interface of the base and the lid (Murata et al., 2009). The six ATPases are responsible for gate opening and facilitating substrate entry. The C-termini of the six ATPase subunits contain a three-residue HbYX (Hydrophobic-tyrosine-X) motif that upon ATP binding allows for docking of these subunits into the pockets between the alpha subunits of the 20S CP to promote gate opening (Smith et al., 2007a). Subunits of the base including Rpn1, Rpn13, Rpt4, and Rpn10 sequester ubiquitinated proteins directly or through intermediaries that contain both ubiquitin-like domains (UBL) and ubiquitin-associated domains (UBA). The only subunit with a known biochemical function in the lid is Rpn11, which facilitates de-ubiquitination of substrates to

further their degradation (Coux et al., 1996, Glickman and Ciechanover, 2002). The other functions of the lid subunits remain elusive.

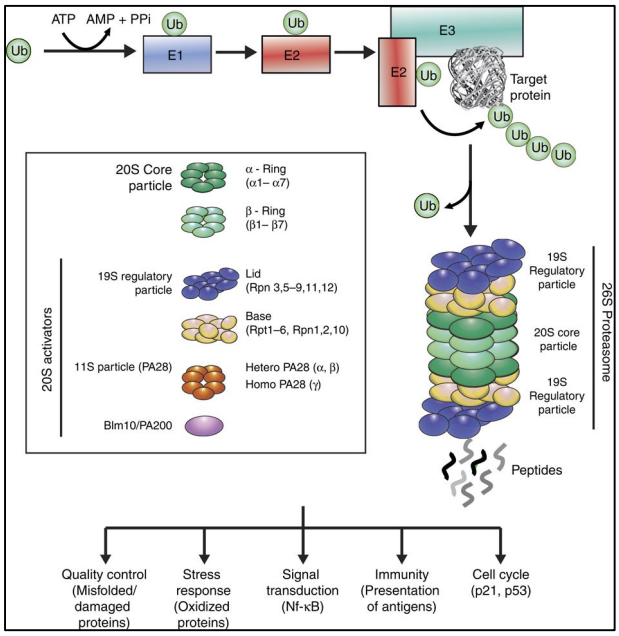

Figure 1.1 Structure and function of the UPS

Two steps are critical for degradation of substrates by the proteasome. First, substrates must be tagged with ubiquitin (ub), a 76 aa polypeptide. This involves three distinct classes of enzymes, E1, E2, and E3s, that work in concert to attach distinct ub chains. The ub-activating enzyme, E1, uses ATP to activate ub before transfer to the E2, ub-conjugating enzyme. The last step involves the E3 ub-ligase that takes ub and typically links it to a lysine residue on the target substrate. The specificity of degradation comes from E3 ub-ligases which are abundant and recognize one or a few specific protein motifs. After ubiquitination, substrates are targeted to the proteasome for degradation. The majority of active proteasomes reside as 26S proteasomes which are formed from the attachment of the 20S CP with the 19S RP. This complex works to recognize, deubiquitinate, unfold, and translocate substrates into the proteolytic barrel for cleavage. However, alternative activators exist such as the 11S and PA200 that support hydrolysis of small peptides. Due to the abundance of proteasome substrates, the proteasome is involved in a variety of cellular processes such as quality control, cell cycle, and signal transduction. Figure is adapted from (Vilchez et al., 2014).

1.1.3 Regulation of the UPS

The regulation of the ubiquitin proteasome system can occur at the level of substrate ubiquitination and/or at the level of proteasome activity. Much of the earlier studies focused on regulation at the level of substrate ubiquitination. Protein substrates can be monoubiquitinated, multiubiquitinated, or polyubiquitinated and how each of these contributes to various cellular processes is being actively investigated. The attachment of ubiquitin to lysine residues gives flexibility to branching in the formation of polyubiquitin chains. This branching is highly regulated and results in different physiological processes such as protein degradation by the proteasome when ubiquitin is attached to Lys-48 and modification of signal transduction when attached to Lys-63 (de Bie and Ciechanover, 2011). However, it is now obvious that proteasomes themselves can be regulated by alternative activators, various interacting proteins, translational control, and post translation modifications. Currently, the direct regulation of proteasome activity is not well understood probably owing to tissue and context-specific regulators. Although the primary proteasome machinery found in eukaryotic cells is composed of the 20S CP and 19S RP to form the 26S holoenzyme, the population of proteasomes in any given cell may be heterogeneous. For instance, many 20S CP can be capped on one side by the 19S RP and a different complex, e.g., PA28, on the other. Impairment or failure of the UPS leads to defects in the proteostasis network often resulting in diseases such as cancer and neurodegeneration, thus properly assembled proteasomes directed to the appropriate locales are a necessity. Since proteasomal degradation is required for numerous cellular functions, the regulation of proteasome activity must be delicately and specifically tuned to meet the needs of specific cells at a given moment. Due to its role in modulating a variety of different cellular outcomes the UPS has arisen as an attractive target for the development of therapeutics. The drug Bortezomib is the

first therapeutic proteasome inhibitor to be used in humans. It is used to treat multiple myeloma by preventing proteasome mediated degradation of proapoptotic proteins and many times is given in combination therapy to overcome drug resistance (Chen et al., 2011). A major side effect that occurs in 30% of patients on Bortezomib is peripheral neuropathy and suggests that synapses may be particularly sensitive to proteasome inhibition (Alé et al., 2015). Studying how the UPS is regulated can aid in the development of effective treatments for a variety of diseases and provide clues as to how these diseases may develop.

1.1.3.1 Alternative activators of the proteasome

The most common and often referred to as "default" activator of the proteasomes is the 19S core particle. This activator is ATP dependent and mostly mediates the degradation of ubiquitinated substrates. However, alternative activator complexes and alternative catalytic subunits exist that can regulate the activity of the proteasome as well. There are three well known alternative activators that can replace or work in concert with the 19S RP: PA28 (also known as REGα,β or 11S), REGγ and PA200/Blm10. PA28 is composed of two homologous subunits PA28α and PA28β that *in vitro* form a heptameric ring that stimulates the hydrolysis of small peptides by the 20S. Unlike the 19S cap, PA28 lacks ATPase activity and ubiquitin binding ability. It is thought to optimize MHC class I presentation and is upregulated in response to interferon γ stimulation (Cascio et al., 2002). REGγ shares a similar size to PA28, both being heptameric assemblies that have no ATPase activity or ubiquitin-sensing receptors to support unfolding of proteins, however is not induced by interferon γ. It has been reported to degrade key cell cycle inhibitors such as p21, p19, p16 and the regulatory protein steroid receptor coactivator-3 (SRC-3) in a ubiquitin and ATP-independent manner. This alternative regulator is overexpressed in some cancers and linked to defects in mitosis and apoptosis (Li et al., 2006; Liu

et al., 2013) . The third activator PA200/Blm10 is a large protein that binds to the CP as a monomer but takes on a circular shape (Schmidt and Finley, 2013). Blm10 again does not utilize ATP and is thus implicated in hydrolyzing peptides. It is suggested to act as an adaptor that functions under circumstances of hybrid proteasomes and is reported to have a role in a wide variety of processes such as spermatogenesis, DNA repair, mitochondrial inheritance, and possibly 20S assembly (Savulescu and Glickman, 2011; Stadtmueller and Hill, 2011). One study has also reported Blm10 to be necessary for sequestering 20S CP into proteasome storage granuli (PSG) during quiescence in yeast (Weberruss et al., 2013). Fairly recently, CDC48/p97 has also been described as a proteasome activator that binds to the 20S CP in archaea. CDC48 is a AAA+ ATPase that contains a HbYX domain much like the Rpt base subunits of the 19S and can bind to the 20S CP, induce gate opening, unfolding of substrates, and ultimately result in degradation (Barthelme and Sauer, 2012). Since many alternative activators may be transiently associated, context specific, or substoichiometric it is likely that with the advancement of tools more proteasome activators will be discovered.

1.1.3.2 Transcriptional Regulation

Transcriptional control is another means by which proteasome activity can be regulated. Proteasome subunits are thought to reside within cells only in relation to their respective their respective complexes, 19S or 20S, with the exception of Rpn10/S5a which has been found in a free state (Piterman et al., 2014). However, studies on the basal rate of proteasome subunit biosynthesis are lacking. Under stress however, proteasome subunits undergo a coordinated upregulation pointing to common signaling pathways regulating their gene expression (Livneh et al., 2016). Proteasome inhibition is reported to cause upregulated proteasome synthesis across

several species from humans to *Drosophila*. The two most well studies transcription factors involved are the mammalian Nrf1/Nrf2, orthologs of *C. elegans* SKN-1, and Rpn4 in yeast. In mammals, Nrf1 is found bound to the endoplasmic reticulum but in response to partial proteasome inhibition, it is processed and translocated to the nucleus. Here, it results in the transcription of all 26S subunits as well as CDC48/p97 (Sha and Goldberg, 2014). Nrf2 is similar to Nrf1 as they both recognize a common promoter element, antioxidant response element (ARE), in the genes they control. However, they differ in their regulation and subcellular localization, with Nrf2 being mitochondrial and then cytoplasmic upon induction. Also, from knockout studies in mice it is clear that Nrf1 plays a role in development while Nrf2 is important for response to oxidative stress and protection from neurodegeneration (Schmidt and Finley, 2013). In yeast, Rpn4 is a short-lived protein that is quickly degraded by the proteasome. However, when proteasome activity is comprised Rpn4 levels accumulate and this protein acts as a transcription factor, binding to PACE (proteasome associated control elements) sequences upstream of proteasomal subunits. In this way Rpn4 is under negative feedback control and acts as a sensor for impaired proteasome biogenesis. Additionally, RPN4 gene transcription can be induced by Hsf1, under heat stress, Yap1, during oxidative stress, and Pdr1/3, during drug resistance. Thus, these conditions promote proteasome biogenesis through upregulation of Rpn4.

Upregulation of single proteasome subunits has also been shown to coordinate the upregulation of other subunits and proteasome activity itself. For instance, upregulation of the β5 subunit acts in a number of human cell lines to increase proteasome assembly and subsequent activity. This upregulation was shown to protect cells from oxidative stress by leading to higher degradation rates (Chondrogianni et al., 2005). Similarly, upregulation of Rpn6 under the transcriptional control of DAF-16/FOXO4 in C. elegans and humans, was shown to elevate

proteasome activity. This did not coincide with global proteasome subunit upregulation but is instead thought to enhance activity by accelerating the association between 20S and 19S particles (Pathare et al., 2012; Vilchez et al., 2012). Conversely, upregulation of the 26S proteasome subunit S5b via the TNFα/NFκB inflammatory signal is reported as an inhibitor of 26S activity by interfering with assembly. Interestingly, overexpression of S5b resulted in shorten lifespan and onset of aging phenotypes in mice while *Drosophila* mutants for S5b show rescue of tau induced rough eye and prolonged lifespan in tauopathy (Shim et al., 2012). These results show that proteasome regulation is complex, context dependent, and may be differentially controlled between cell types and species.

1.1.3.3 Proteasome associated proteins

Proteasome activity is required for a wide variety of cellular process with demands that may change depending upon tissue type, nutrient availability and developmental stage. Thus, in addition to the core proteasome subunits, proteasomes are associated with a wide variety of proteasome interacting proteins (PIPs). Several PIPs have been found to be involved in efficient assembly of proteasomes in mammalian cells such as p28, s5b, and p27 (Heinrichs, 2009). However, weakly associated or transiently associated factors that may have essential roles may prove difficult to identify. Additionally, the use of different purification techniques can cause the number of PIPs identified to range from 24 putative interactors (Verma et al., 2000) to a network of more that 471 proteins (Guerrero et al., 2008). The functions of these proteins vary and include E3 ligase activity, shuttling of ubiquitinated substrates to the proteasome, DUB activity, altered proteasome stability, and inhibition of the 20S CP. Although most PIPs are found at substoichiometric amounts, a few including Ecm29 are reported to be co-regulated with proteasome subunits and found at nearly the same levels. This protein, which is found

exclusively in the cytosol (Tai et al., 2010), is also shown to bind and stabilize the interaction between 20S and 19S particles (Leggett et al., 2002; Tai et al., 2010) and preferentially associates with mutant proteasomes (De La Mota-Peynado et al., 2013). Recent reports have shown the Ecm29 can inhibit proteasome-mediated protein degradation and disassemble the 26S proteasome in response to oxidative stress (Wang et al., 2017). Although the exact mechanisms are still under investigation, this protein likely functions to ensure that abnormal proteasomes remain inactive.

Numerous studies have also demonstrated the association of neuronal proteins with the proteasome. Parkin, an E3 ubiquitin ligase, is capable of activating 26S proteasomes via its N-terminal ubiquitin-like domain which enhances association with 19S subunits. Interestingly, mutations in *parkin* are linked to early-onset familial Parkinson's disease (PD) and proteasome dysfunction (Um et al., 2010) implicating an essential role for proteasome activity in maintaining healthy neurons. Moreover, constituents of aggregates in PD namely α-synuclein and amyloid beta (Aβ) interact with the proteasome and inhibit UPS function *in vitro* and *in vivo* (Chen et al., 2006; Gregori et al., 1995; Snyder et al., 2003; Stefanis et al., 2001) indicating a role for proteasome dysfunction in the progression of PD.

Another group of PIPs in the brain, identified by mass spectrometry in the rat cortex, are the 14-3-3 family members γ, ζ, and δ. In general, 14-3-3 protein family members have a broad range of functions in the brain stemming from their known interaction with over 200 proteins. They participate in cell signaling, cell cycle, apoptosis and neural development. Interestingly, some isoforms are enriched within the synapse to regulate transmission and plasticity. In concert with this is the finding that the phosphobinding protein14-3-3γ is only found on synaptic proteasomes (Tai et al., 2010) and presumably regulates protein turn over at synapses. Another

14-3-3 family member, 14-3-3ζ, binds to PA28, a proteasome activator, and suppresses proteasome assembly and increases sensitivity of multiple myeloma cell lines to proteasome inhibition (Gu et al., 2018). Unpublished results from our lab by Dolors Ferres-Marco also indicate 14-3-3ζ plays a role in proteasome inhibition and showed that this protein modulates proteasome-mediated dendritic pruning of sensory neurons during development.

Last, interacting proteins can regulate proteasome activity by localizing proteasomes to areas of proteolytic demand. This is especially true in neurons where cell bodies can be up to a meter away from sites of synaptic activity in the axon, where proteasomes are needed. Recently, the *Drosophila* homolog of the LC8 dynein light chains, Cut up (Ctp), was shown to interact with 19S and 20S proteasome subunits in motor neurons of *Drosophila* 3rd instar larvae. This interaction facilitates the transport of proteasomes and it was found to be independent of synaptic vesicle proteins. This report shows that proteasomes also exhibit more anterograde movement than retrograde and mutations in *ctp* severely affect transport leading to an increase in the number of satellite boutons (Kreko-Pierce and Eaton, 2017). These studies demonstrate a critical need for proteasome regulation at the synapse and show that defects in proteasome localization lead to irregular synapse formation and function.

1.1.3.4 Posttranslational modifications

Several posttranslational modifications can modify proteasome activity. More than 345 modifications of 11 different types were shown to associate with the yeast 26S proteasome with many sites being a target for more than one modification. This indicates that communication between post-translational modifications may regulate proteasome activity (Hirano et al., 2016). Many of the functional consequences of these post-translational modifications have not been

identified. Of interest to this thesis are posttranslational modifications that have been identified to alter proteasome function in response to metabolic changes. These modifications point to pathways that might alter proteasome activity depending on nutrient availability and the metabolic status of the cell. In *Drosophila*, 26S proteasomes are modified by O-linked N-acetyl glucosamine (O-GlcNAc) that inhibits proteasome activity (Sümegi et al., 2003). O-GlcNAc transferase (OGT) adds the O-GlcNAc moiety to the Rpt2 subunit of the 19S cap, specifically affecting the ATPase activity of the proteasome and leading to an inhibitory affect. Yet another example of metabolically regulation proteasome function is through Protein kinase A (PKA) phosphorylation. PKA activity is dependent on cyclic AMP (cAMP) levels in the cell. Using purified 26S proteasomes it was shown that 26S proteasome activity is enhanced via PKA phosphorylation of Rpt6, an AAA+ ATPase located in the 19S regulatory cap (Zhang et al., 2007a). Lastly, the Steller lab has shown another potential mechanism by which proteasomes are metabolically regulated. This mode of regulation does not directly target a proteasomal subunit but instead targets the PIP, PI31. TNKS is shown to mediate the ADP-ribosylation of PI31which reduces its binding affinity for 20S α subunits. The model predicts that this modification relieves 20S repression thus promoting 26S assembly. The necessity for ADP-ribose subunits links this pathway to metabolism since these subunits are derived from intracellular nicotinamide adenine dinucleotide (NAD+) pools (Cho-Park and Steller, 2013). NAD+ is a metabolite for a variety of cellular processes and redox reactions within the cell but also acts as a substrate for NAD+ consuming enzymes such as poly ADP-ribose polymerases (PARPs) like TNKS. The role of NAD+ in regulating proteasome activity will be explored in this thesis and the neuroprotective function of NAD+ discussed in a later section.

1.1.4 DmPI31 is an essential proteasome regulator

An essential regulator of proteasome activity was identified in a screen for defective caspase activation in *Drosophila* spermatogenesis. A novel F-box protein termed nutcracker, that is the ortholog of mammalian FBXO7, was isolated and shown to interact with SkpA and Cullin-1, components of an Skp/Cullin/F-box (SCF) ubiquitin ligase complex. *Nutcracker* mutants are defective in caspase activation and proteasome activity (Bader et al., 2010). A biochemical screen for proteins interacting with Nutcracker identified DmPI31. It was shown that nutcracker binds to DmPI31 via a conserved Fbxo7/PI31 (FP) domain and stabilizes DmPI31 (Bader et al., 2011; Chu-Ping et al., 1992). DmPI31 is homologous to mammalian PI31, a 31kD proline rich protein, which was initially isolated as an inhibitor of 20S proteasomes. DmPI31 shares over 45% homology with mammalian PI31 proteins. The interaction between these proteins was shown to be necessary for caspase activation, proteasome activity and ultimately spermatogenesis in *Drosophila.* Although, PI31 was initially found to be an inhibitor of 20S proteasomes *in vitro* that competes with PA28 for binding (Chu-Ping et al., 1992), (Zaiss et al., 1999) *in vivo* activation of DmPI31 stimulated proteasome activity and rescued proteasome defects. Loss-of-function studies in *Drosophila* result in defects in protein breakdown further defining the role for DmPI31 in stimulating proteasome function. Thus, DmPI31 serves as an activator of the 26S proteasome and its activity is essential for normal protein breakdown and organismal survival. This protein is also shown to be an activator of 26S proteasomes while inhibiting 20S proteasomes *in vitro*. *DmPI31* mutants also display reduced proteasome activity and lethality during the 3rd instar larvae to pupal transition (Bader et al., 2011). The full activity of DmPI31 is dependent on the HbYX motif located at its C-terminus. This motif is shared by

other modulators of proteasome activity such as the AAA+ ATPase Rpt subunits of the 19S proteasome and CDC48/p97.

In search for regulators of DmPI31 activity, TNKS, an ADP-ribosyltransferase, was identified as a direct binding partner that modulates PI31 activity through ADP-ribosylation. TNKS is a member of the PARP superfamily of proteins and it widely known for its role in binding the negative regulator of telomere length, TRF1. It localizes to many subcellular locations including telomeres, spindle poles, and the cytoplasm and several binding partners of TNKS have been identified that containing an RXXPDG motif or a degenerate form, including PI31. Similarly, the ADP-ribosylation of PI31 by TNKS is shown to be necessary as TNKS inhibition decreases proteasome activity *in vivo*. ADP-ribosylation of PI31 blocks the binding of PI31 to the α subunits of the 20S proteasome and thus relieves 20S inhibition by PI31. Additionally, ADP-ribosylation promotes the binding of dp27 and dS5b to PI31, which sequesters them from the 19S RP to promote 26S assembly. The C-terminal HbYX motif is required for DmPI31 binding to TNKS and the assembly chaperones dp27 and dS5b (Cho-Park and Steller, 2013). These data provide a mechanism by which PI31 acts as a regulator of proteasome assembly that is potentially under metabolic control (Figure 1.2).

Native gel analysis shows that recombinant GST tagged PSMF1/PI31 can form trimers, hexamers, and nonamers. In silico modeling of PSMF1/PI31 predicts that this protein may form a heptameric ring that binds to the 20S in replacement of the 19S RP and inhibits substrate entry into the 20 CP (Clemen et al., 2015). *In vitro*, PI31 was shown to bind 26S proteasomes but has no effect on activity nor did PI31 overexpression or RNAi cause cellular proteasome defects. However, this paper also reports that the 10 -22 residue C-terminal peptides of PI31 can activate 20S hydrolysis in a HbYX dependent manner but that the C-terminus of PI31 itself inhibits the

20S CP. Interesting, the N-terminus of PI31 alone does not shown any inhibition of 20S CP suggesting that PI31 can regulate proteasome activity via its C-terminal tail mediating gate opening (Li et al., 2014).

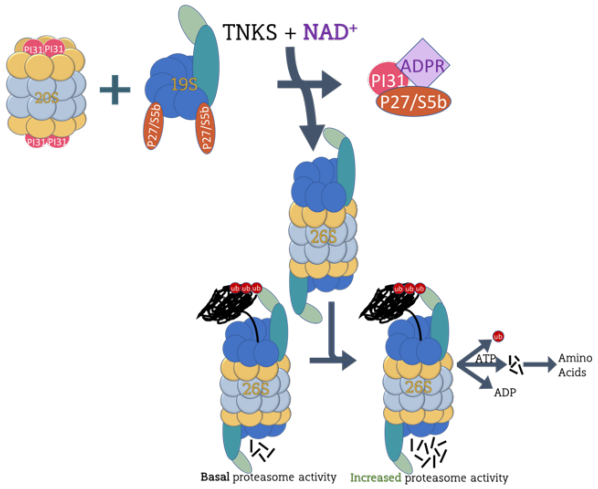

Figure 1.2 Current Model for Increased Proteasome Assembly by ADP-ribosylation of PI31
The current model for increased proteasome activity by ADP-ribosylation of PI31 shows that TNKS uses NAD+ as a donor for ADP-ribose groups. TNKS directly binds to PI31 to transfer ADP-ribose and this binding requires the HbYX domain of PI31. This model predicts that PI31 sits on the 20S CP blocking the entry chamber but that upon ADP-ribosylation of PI31, 20S binding is relieved and PI31 binding to 19S chaperones increases. These two events allow the 20S and 19S to come together more efficiently under conditions that require increased 26S proteasome activity. Figure adapted from (Cho-Park and Steller, 2013).

How DmPI31 interacts with the proteasome to regulate its function is still unclear given the difference between activities *in vitro* and *in vivo*. An *Arabidopsis* homologue of PI31, named proteasome regulator 1 (PTRE1), was shown to be a positive regulator of 26S proteasomes and mediates auxin suppression of proteasome activity. Mutations in *ptre1* result in severe developmental defects in plants and auxin is thought to mediate proteasome activity by altering

PTRE1 localization (Yang et al., 2016). Unpublished data from our lab by Kai Liu also indicate that DmPI31 functions as a modulator of proteasome localization. However, whether PTRE1 interacts with other proteins or undergoes post-translational modifications requires further investigation. The yeast ortholog of PI31, Fub1, was shown to co-immunoprecipitate with both the 20S and 26S proteasome but not free 19S particles. Fub1 also shows an inhibitory effect on 20S *in vitro* but did not show any inhibitory effects on proteasome degradation *in vivo*. In fact, neither deletion not overexpression of Fub1 *in vivo* had any deleterious effects on proteasome function. It was only when ΔFub1 was combined with deletion of a 20S assembly chaperone, Δpba4, did lethality occur and this lethality could be rescued by Δa3, a CP subunit, or deleteion of the N-terminal of Δa7 (Yashiroda et al., 2015). However, the generation of alternative proteasome complexes, where deleted subunits can replace others, complicates the interpretation of Fub1 function *in vivo*. Thus, an understanding of the structure of PI31 interaction with 20S and 26S proteasome *in vivo* will elucidate its role in regulating proteasomes.

1.2 Protein homeostasis in neurodegeneration

In late-onset neurodegenerative diseases such as Alzheimer's, Parkinson's, and Huntington's disease there is an accumulation of ubiquitin conjugated aberrant proteins into aggregates in the brain. These aggregates often show accumulation of chaperones and proteasome subunits suggesting that UPS activity was initiated but proteasomes fail to degraded these proteins. For instance, defining traits of AD include the accumulation of Aβ neurite plaques and tau containing neurofibrillary tangles. These protein aggregates can also be seen in the brain during the normal aging process suggesting an important role for cellular degradation systems in the clearance of proteotoxic aggregates during aging (Gray et al., 2003).

A possible explanation for the accumulation of toxic proteins and subsequent aging phenotypes is the impairment of the UPS. Indeed, many reports describe a decrease in proteasome activity in aged organisms. This decrease has been associated with altered expression of proteasome subunits and impairment in proteasome assembly (Dasuri et al., 2009; Rogers et al., 2012; Vernace et al., 2007; Vilchez et al., 2014). Loss-of-function mutations that result in decreased proteasome activity also shown enhance neurodegenerative phenotypes. Mutations in FBXO7, the mammalian homolog of *Drosophila* nutcracker that binds to and stabilizes DmPI31, was found to cause early onset Parkinsonian-pyramidal disease (PPD) (Di Fonzo et al., 2009) FBXO7 was shown to interact with the PSMA2/alpha2 subunit of the proteasome and modifies it via ubiquitination. Additionally, mutations in *Parkin*, a ubiquitin ligase, lead to a failed interaction between this protein and its substrate α-synuclein resulting in the formation of Lewy bodies and eventually in familial PD. Parkin expression is also downregulated in AD and may contribute to accumulation of intracellular Aβ (Zheng et al., 2016). Spinocerebellar ataxia type 3 (SCA3) is a polyglutamine disorder caused by the CAG expansion of in the gene encoding Ataxin-3. Ataxin-3 itself if a DUB containing a ubiquitin interacting motif that when overexpressed in *Drosophila* can protect from polyQ induced neurodegeneration (Winborn et al., 2008). Another member of the ataxia family of neurodegenerative disorders is that of Spinocerebellar ataxia-type 1 (SCA1). This polyQ disease is caused by a CAG repeat in the gene product, ataxin-1. In this model, proteasome activity has been shown to be directly impaired by decreased degradation of a short-lived fluorescent protein (Park et al.). Modifier screens have been conducted in *Drosophila* models of both SCA1 and SCA3 to look for suppressors of neurodegeneration. In these studies the role for proper protein folding and protein degradation are highlighted as the majority of modifiers fell into the chaperone or UPS category.

1.2.1 Role of the UPS in Wallerian degeneration

Wallerian degeneration is the result of damage to nerve fibers that can be seen early on in diseases such as Alzheimer's, Parkinson's, and multiple sclerosis. It occurs in response to infections, diabetes, and normal aging. The Wallerian degeneration slow mouse (wld^s) is an autosomal dominant genetic alteration that encodes for the first 70 amino acids of the ubiquitination factor Ufd2a and full length Nmnat1. It shows resistance to nerve cell damage both *in vitro* and *in vivo*. Overexpression of Nmnat1, an enzyme that catalyzes that last step in NAD+ biosynthesis, has been shown to protect axon degeneration induced by transection in the dorsal root ganglion neurons (Mack et al., 2001). The protection seen in the wld^s mouse could be a result of protecting NAD+ levels since depletion of NAD+ and ATP is accompanied with axonopathy. This protection of NAD+ provides a possible role for proteasomes in the protection of axon degeneration due to TNKS mediated ADP-ribosylation of PI31. PARP-1 inhibitors may also play a role in protection from neuronal death. Excessive activation of PARP-1 leads to the depletion of cytosolic NAD+ which has been linked to PARP-1 mediated neuronal cell death. Reports have shown that the induction of DNA strand breaks in PARP-$1^{-/-}$ neurons saves cytosolic NAD+ levels and rescues neuronal death. In addition, replenishing NAD+ levels in neurons that have suffered DNA damage can prevent PARP-1 induced neuronal death (Alano et al., 2010). Thus, the beneficial effects of NAD+ in neuronal protection may in part be related to the ADP-ribosylation of PI31 and subsequent proteasome assembly.

1.2.2 Age-associated decline in proteostasis

In *Drosophila melanogaster*, aging is associated with a decline in proteasome activity and this appears to be due to reduced assembly of the 26S proteasome (Tonoki et al., 2009). Aged

flies show an accumulation of ubiquitinated proteins and a decline in the level of 26S proteasome protein compared to young flies. This age-related reduction in 26S proteasomes can be overcome with the overexpression of *Rpn11*, a component of the 19S RP known for its de-ubiquitinating activity. The overexpression of this subunit also suppresses the accumulation of poly-ubiquitinated proteins with age, increases fly lifespan, and rescues SCA3 induced neurodegeneration (Tonoki et al., 2009). Another recent study in *Drosophila* showed that impairment of the proteasome with the feeding of proteasome inhibitors promoted the aging phenotype and reduced lifespan. However, this study uncovers a proteasomal regulatory circuit that upregulates proteasome mRNAs and subunits in response to impaired proteasome functionality. This upregulation is dependent on Nrf2, which is a transcription factor that is traditionally known for its role in mediating responses to oxidative stresses (Tsakiri et al., 2013).

Additional evidence for a critical role for proteasomes in aging comes from studies of elevated proteasome activity. In such a study conducted in *Saccharomyces cerevisiae*, UPS capacity was manipulated with the use of the Rpn4 transcription factor. Cells deleted for *RPN4* show a decrease in proteasome levels, while loss of the ubiquitin ligase that regulates Rpn4 turnover, *UBR2*, upregulates Rpn4 and thereby increases in proteasome components. The replicative life span in this yeast model was significantly extended with increased UPS capacity while a decrease in UPS capacity shortens replicative life span. In yeast models for neurodegenerative diseases, a loss of *UBR2* results in improved clearance of toxic huntingtin fragments suggesting that increased proteasome capacity prolongs lifespan through the elimination of toxic proteins (Kruegel et al., 2011).

1.2.3 Proteasome transport to the synapse

Efforts to identify the causes and mechanisms underlying neurodegenerative diseases have undoubtedly uncovered defective proteostasis as a major cause for the progression of neurodegeneration. However, whether the various types of toxic aggregates lead to progressive impairments in proteostasis that only manifest in disease overtime or whether some other factors play a role is still a major question. AD is of major interest since it is the most common brain degenerative disorder and begins with impairments in cognitive function that prevent the formation of new memories followed by progressive loss of previously encoded memories. Since patients at the early stages have intact motor and sensory neurological function it is suggested that failure at the synapses required to form new memories are the cause. Although Aβ plaques and tau tangles are hallmarks of the disease, early studies report dysfunction at the synapse as the initial target of AD. Indeed, deficits in a number of neurotransmitters accumulate with disease progression and loss of synapses correlate more robustly to cognitive decline than the number of Aβ plaques or tau tangles (Selkoe, 2002). This poses the question of how proteostasis is maintained at the synapse under physiological conditions. Many studies have shown a requirement for the UPS to maintain synaptic plasticity and that proteasome activity is distinctly regulated at the synapse (Hamilton and Zito, 2013; Tsai, 2014). One way in which proteasome activity is regulated here is by transport of proteasomes from the cell body to the synapse and within different synaptic compartments such as the dendritic shaft to dendritic spines. Both 19S and 20S proteasomes are previously described as being trafficked into dendritic spines upon activity and this is correlated with an increase in degradation of polyubiquitinated proteins in spines. Theses proteasomes are shown to be tightly associated with the actin cytoskeleton suggesting proteasomes can be actively transported to subcellular localizations where protein

degradation is needed (Bingol and Schuman, 2006). Since then several reports have established proteasome association with molecular motors and support the hypothesis that proteasomes move both anterograde and retrograde to carry out local degradation to maintain synapses (Otero et al., 2014; Hsu et al., 2015; Kreko-Pierce and Eaton, 2017). Evidence of local dysfunction in proteasome degradation results in early phases of tauopathies and the formation of ubiquitin conjugated tau aggregates (Tai et al., 2012). Thus, mechanisms that disrupt the transport of proteasomes to axons could initially lead to synaptic dysfunction which compounds overtime and leads to neurodegenerative phenotypes.

1.2.4 Neuroprotective role of NAD+ metabolism

Nicotinamide adenine dinucleotide (NAD+), it phosphorylated form (NADP+) and reduced forms (NADH and NADPH) have crucial roles in processes such as transcription, cell cycle control, DNA repair, and metabolism. There are two major pathways via which cells produce NAD+, the de novo pathway that uses tryptophan and the NAD+ salvage pathway that recycles nicotinamide and nicotinic acid from the diet. This molecule serves as a substrate for three classes of enzymes: poly (ADP-ribose) polymerases (PARPs), cADP-ribose synthases, and Sirtuins. PARPs are NAD+ consuming enzymes that produce an ADP-ribosyl protein modification and/or form ADP-ribose polymers. The addition of each unit of ADP-ribose to an acceptor protein requires one molecule of NAD+ creating a considerable challenge for cellular NAD homeostasis when ADP-ribosylation is activated. One of the major causes of cell death due to genotoxic stress is the hyperactivation of PARP-1, which depletes cytoplasmic and nuclear NAD+. The depletion of NAD+ also results in the inability for a cell to generate ATP, which is a major requirement for 26S proteasome mediated degradation. cADP-ribose synthases, CD38 and

CD157, are ectoenzymes that use NAD+ as a substrate to generate second messengers, such as cADP-ribose, which contributes to calcium mobilization. Sirtuins are enzymes whose function to deacetylate lysine residues of transcription factors and histones is dependent on the NAD+/NADH redox ratio. These enzymes have emerged in the regulation of cell survival and longevity. Specifically, Sir2 has been shown to mediate lifespan expansion in *S. cerevisiae*, *C.elegans*, and *D. melanogaster* (Belenky et al., 2007). Recent studies have shown that genetic or pharmacological inactivation of the PARP1 homolog, pme-1, in *C. elegans* increases NAD+ pools and extends lifespan through *sir-2.1*, the worm sirtuin homolog, and boosts mitochondrial metabolism (Mouchiroud et al., 2013).

The therapeutic potential of NAD+ metabolism is well recognized, as pathophysiological states such as neurodegeneration can be suppressed by increasing NAD+ production or associated enzymes. For instance, overexpression of Nmnat1 in dorsal root ganglion (DRG) neuronal explant cultures protected axons from both mechanical transection, ischemia, and toxins such as vincristine (Araki et al., 2004, Coleman and Perry, 2002)(Gillingwater et al., 2004). The addition of exogenous NAD+ 24 hours prior to axonal transection also delays axonal degeneration although this protection is less effective than lentiviral expression of Nmnat1 (Araki et al., 2004). It was also found that degenerating axons show a decrease in NAD+ levels and protection of this NAD+ pool efficiently protects axons from degeneration (Wang et al., 2005). Overexpression of Nmnat has also been shown to suppress tauopathy by reducing the number of hyperphosphorylated tau oligomers. This protection is independent of its NAD+ synthase activity and was shown that Nmnat can directly interact with phosphorylated tau and promote its ubiquitination and clearance (Ali et al., 2011). *Drosophila* models of spinocerebellar ataxia 1 (SCA1) showed that both Nmnat as well as an enzymatically inactive form of Nmnat are

neuroprotective. This study found that Nmnat acts independent of its NAD+ synthase activity and instead acts as a chaperone for neuronal maintenance and protection (Zhai et al., 2008). NAD+ levels vary significantly between tissues and are dramatically altered by dietary levels of nicotinic acid and nicotinamide (Belenky et al., 2007; Elhassan et al., 2017). Dietary niacin has shown to confer protection from the development of AD and cognitive decline (Morris et al., 2004). Recent data has found that the reduced form of NAD+, NADH can directly bind 26S proteasomes via a putative binding motif found on 19S subunits. Interestingly, addition of 0.1 or 0.5 mM NAD+ to NIH3T3 cells increased the levels and activity of 26S proteasomes. This was likely due to increased assembly as there was no change in proteasome subunit expression (Tsvetkov et al., 2014). In *Drosophila pink1* mutants, increasing the NAD+ salvage pathway via supplementation of nicotinamide prevents neurodegeneration and rescues mitochondrial defects (Lehmann et al., 2017). This precursor was also shown to ameliorate mitochondrial dysfunction and motor deficits in a *Drosophila* model for PD (Jia et al., 2008). These findings point to a pathway that may link neuroprotection, NAD+, and the proteasome. The exact mechanisms by which Nmnat and NAD+ confer neuroprotection and whether they are independent of each other remain to be determined.

Dietary Restriction (DR) without malnutrition was first describe by McCay et al. in 1935 to extend mean and maximal lifespan of rats and since then its beneficial effects have been described as reducing cancer incidence and delaying the onset of aging phenotypes. Interestingly, DR increases intracellular NAD+ levels (Guarente and Picard, 2005) providing yet another connecting to possible regulation of proteasome activity via DmPI31. DR is thus far the only non-genetic way in which to increase lifespan in every model organism studied from primates to yeast. Many hypotheses for how dietary restriction contributes to longevity have been proposed

such as enhancement of apoptosis, increased physical activity, reduced metabolic rate, attenuation of insulin IGF-1 signaling, and protein turnover (Xiang and He, 2011). In yeast, dietary restriction was shown to extend replicative lifespan through a mechanism that was dependent on Sir2 and Npt1, a nicotinic acid phosphor-ribosyltransferase. Interestingly, NAD+ salvage pathway proteins and nicotinamide induced NAD+ increase can mediate neuroprotection and longevity (Lin et al., 2000; McClure et al., 2012; Ocampo et al., 2013).

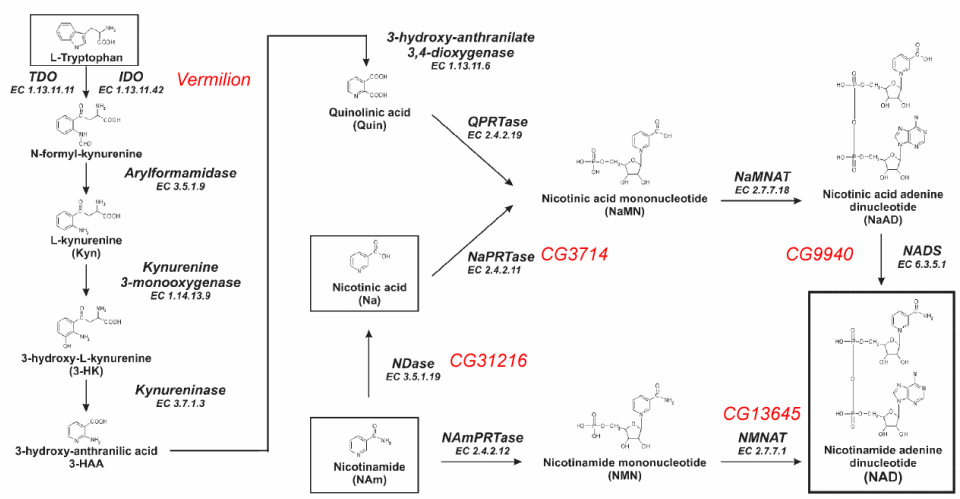

Figure 1.3 NAD+ *de novo* synthesis and salvage pathways in *Drosophila*

NAD+ is an essential coenzyme crucial for a variety of cellular processes, redox reactions, and cellular respiration. It is also the substrate for three major classes of enzymes, sirtuins, cADPRs, and PARPs. NAD+ can be synthesized from the aa tryptophan via de novo synthesis or from dietary intake of metabolites Na and Nam via the NAD+ salvage pathway. Byproducts of NAD+ digestion are recycled back into useful forms by enzymes in the salvage pathway, available enzymes in flies are indicated in red with CG number. NMNAT is essential for neuronal health and mammals have 3 genes corresponding to different subcellular localization while flies have one gene, CG13645. This salvage pathway is also essential in humans as lack of dietary metabolite intake results in the vitamin deficiency disease pellagra.

1.3 Relevance

The therapeutic potential of NAD+ metabolism is well recognized, as pathophysiological states such as neurodegeneration can be suppressed by increasing NAD+ production or associated enzymes. Additional data shows that TNKS mediated ADP-ribosylation of PI31, which requires NAD+ can promote 26S proteasome assembly. Natural aging may predispose to neurodegeneration as both proteasome assembly and NAD+ are shown to decline with age in worms and mice (Tonoki et al., 2009, Mouchiroud et al., 2013, Gomes et al., 2013, Yoshino et al., 2011, Ramsey et al., 2008). Both of these findings suggest a mechanism by which declining NAD+ levels can cause decreased proteasome activity and lead to the progression of age associated neurodegeneration. The overarching aim is to bridge metabolic and genetic mechanisms of proteasome regulation to expand the scientific body of knowledge on how proteolysis impacts aging and neurodegenerative diseases. Understanding protein degradation during the progression of neurodegeneration and the regulators involved will uncover potential therapeutic targets to delay the onset of these diseases. This thesis will address the role of DmPI31 in *Drosophila* neurons during development and in maintaining neuronal health in addition to studying how NAD+ metabolism influences PI31 mediated proteasome activity.

2. Characterization of DmPI31 in neuronal maintenance and longevity

2.1 Summary

Neuronal remodeling and maintenance are processes that require a tight balance between protein synthesize and degradation. The UPS mediates proteolysis in neurons in a highly regulated fashion by tagging specific proteins with ubiquitin and targeting them to the proteasome for degradation. Proteasomes are regulated in a diverse manner through interactions with alternative activators, post-translational modifications, and changes in localization. This chapter characterizes the role of a proteasome-interacting protein, *Drosophila* PI31 (DmPI31), within neurons of both larvae and adult flies. This protein is shown to localize to distinct brain regions where it co-expresses with proteasome subunits. Generation of mitotic clones mutant for *dmPI31* revealed that this protein is essential for protein degradation in adult photoreceptor neurons, as these cells accumulate poly-ubiquitinated proteins and rapidly degenerate. Targeted RNAi-mediated knockdown of PI31 in neurons resulted in eclosion and motor neuron defects further suggesting an essential role for DmPI31 in neurons. Lastly, the crucial role of regulating expression of this protein is shown as a result of its impact on *Drosophila* lifespan. Together, these results uncover previously unknown roles for DmPI31 in the *Drosophila* nervous system.

2.2 Rationale

In a screen for regulators of caspase activation during *Drosophila* spermatogenesis, a proteasome regulatory complex composed of nutcracker and DmPI31 was found to be necessary for proper sperm differentiation. Nutcracker interacts with and promotes DmPI31 stability and

together they participate in non-apoptotic caspase activation that drives cellular remodeling in the testes. DmPI31 mRNA transcripts are highly expressed in the testes while females and mutants lacking germline cells express reduced amounts (Bader et al., 2011). However, *dmPI31* mutants display pupal lethality suggesting a role for this protein outside of the testes as well. Initially reported as an inhibitor of 20S proteasomes in vitro, PI31 has a conserved HbYX (Hb= Hydrophobic amino acid, Y = Tyrosine, and X= any amino acid) motif shared by Rpt subunits for binding or activation of 20S proteasomes (Smith et al., 2007b; Kumar et al., 2010). Indeed, DmPI31 was shown to function *in vivo* as a proteasome activator that can rescue the dominant-negative temperature sensitive proteasome alleles *DTS5* and *DTS7*, mutations in subunits B2 and B5 respectively. The HbYX motif at the C-terminal tail of DmPI31 is necessary for full proteasome activation but deletions in this region still manage to increase 26S proteasome activity *in vitro* and *in vivo* (Bader et al., 2011). However, knowledge on the *in vivo* role of DmPI31 outside the testes is lacking. Similar to sperm, neurons go through periods of cellular remodeling where proteolysis must play a critical function.

In this chapter, I explore the role of DmPI31 in neuronal function by characterizing the localization of this protein as well as associated mutant phenotypes. The localization of proteasomes within neurons plays a key role in regulating protein degradation during processes such as dendritic pruning, synaptic plasticity, and neuronal maintenance (Wójcik and DeMartino, 2003; Janse et al., 2004; Patrick, 2006). Endogenous PI31 displays both cytoplasmic and nuclear localization but expresses more highly the central brain of 3rd instar larva. In adult flies, DmPI31 localizes to a subset of neurons in the central brain as well as photoreceptor axons. Using loss of function mutants and driving RNAi of PI31 in specific neuronal subtypes, I show that PI31 is essential for neuronal maintenance. Polyubiquitinated proteins accumulate, neurons rapidly

degeneration, and the number of active zones is reduced. These studies clarify the role of DmPI31 as a proteasome activator *in vivo* and illustrate the importance of PI31 in neuronal maintenance.

2.3 Results

2.3.1 DmPI31 is expressed in the *Drosophila* central brain and adult photoreceptor axons

It was reported that the majority of adult DmPI31 mRNA resides in the testes (Bader et al., 2011). However DmPI31 mRNA is present at low levels in the adult female and is expressed throughout the *Drosophila* life cycle (Arbeitman et al., 2002). Furthermore, mass spectrometry from an enriched membrane fraction of adult *Drosophila* heads identified DmPI31 along with other proteasome subunits (Aradska et al., 2015) confirming the presence of DmPI31 in locales beyond the testes. In order to determine the role of DmPI31 in neuronal function, I explored the expression and localization of this protein in the brains of 3rd instar larval and adult flies. To probe for the localization of this protein *in vivo*, I took advantage of a transgenic line expressing a mCherry-DmPI31 fusion protein driven by the endogenous promoter for DmPI31 (PI31::mCherry-PI31). This fusion protein was previously shown to properly localize in the testes and to rescue mutant phenotypes (Bader et al., 2011). Confocal z-stack images of 3rd instar larval brains show that DmPI31 is highly expressed in the central brain (CB) and ventral nerve cord (VNC) relative to the optic lobes (OLs) (Figure 2.1). Both the larval CB and VNC contain large neural stem cells termed neuroblasts that are multipotent and generate the neuronal and glial diversity in the adult central nervous system (CNS) (Egger et al., 2008; Homem and Knoblich, 2012). Proteasome function has been reported to play a crucial role in neuroblasts and neurogenesis. Mutations in the 19S proteasome subunit Rpn10 show strong mitosis defects in

larval neuroblasts (Szlanka et al., 2003) while *Prosβ2^{1}*, a dominant temperature-sensitive mutation (DTS5) in the β2 subunit of the 20S proteasome, caused mild mitotic defects in these cells (Neuburger, 2006). To determine whether DmPI31 is specifically localized to larval neuroblasts, I stained PI31::mCherry-PI31 larval brains with the neuroblast markers deadpan (Dpn), which marks the nuclei of large neuroblasts, and prospero (Pros), which marks the smaller nuclei of ganglion mother cells (GMCs). Although DmPI31 is fairly ubiquitous in the CB, Dpn positive cells show a higher expression of DmPI31 in the CB compared to Pros positive cells (Figure 2.2a). Proteasome expression levels within the larval brain were determined by assaying the expression of a GFP-tagged α2 subunit under the endogenous promoter since proteasome subunits are rarely found as single components. α2-GFP is ubiquitous but highly expressed in the perinuclear region of the neuroblasts and cytoplasm. This protein is also seen to localize to the cytoplasm of neural progeny (Figure 2.2b). To determine whether DmPI31 co-localizes with the proteasome in neuroblasts, flies expressing GFP-tagged α2 or Rpt3 subunits under their endogenous promoters (Ma et al., 2002) were crossed to PI31::mCherry PI31 lines. Confocal z-stacks of 3rd instar larval brains were analyzed and showed more expression of DmPI31 within α2 and Rpt3 positive cells (Figure 2.2c,d). However, not all α2GFP expressing cells showed elevated PI31 indicating that this protein is actively regulated depending upon the cellular state. Both α2GFP and Rpt3GFP display nuclear and cytoplasmic localization consistent with previous reports on proteasome localization in *Drosophila* (Ma et al., 2002) although Rpt3 has a broader cytoplasmic expression pattern (Figure 2.2d). The increase in expression of these subunits within neuroblasts may be attributed to proteasome demand being higher in actively dividing cells (Wójcik and DeMartino, 2003). To determine DmPI31 localization in the adult brain, whole-mount brain dissections from age matched PI31::mCherry-PI31 adults were fixed

alongside Oregon-R brains to control for background fluorescence(Figure 2.3a). The expression pattern of DmPI31 in the central brain is consistently localized to a specific subgroup of cells in the central brain that is yet unexplored (Figure 2.3b,c). I cannot rule out that these neurons are undergoing apoptosis or PE remodeling and thus show upregulated DmPI31 that may suggest upregulate proteasome activity. However, mcherry-PI31 additionally localizes to the R7 and R8 photoreceptor axons found in the adult medulla (Figure2.3d-e). This localization points to the possibility that DmPI31 is being actively transported to axons, since these axons project a fair distinct from their cell bodies. Visualizing the outermost axon terminals shows high levels of PI31 expression overlapped with the cell specific marker for the R7/R8 axons (Figure 2.3f) providing further evidence to support the idea that PI31 is transported to these distal locations.

Figure 2.1 DmPI31 expression is highly localized to the central brain and ventral nerve cord in 3rd instar larval CNS

(**a**) Schematic of 3rd instar larval central nervous system. Central brain (CB), ventral nerve cord (VNC), optic lobe (OL), outer proliferation center (OPC), inner proliferation center (IPC), neuroblasts in optic lobe and central brain (NB), medulla (me), neuroepithelium (NE), lamina furrow (LF). (**b-f**) Ventral view of confocal z-stack projections of 3rd instar larval brains expressing PI31-mCherry fusion protein under the PI31 endogenous promoter. (**b**) Composite image shows DmPI31 expression in red relative to neural progenitors marked by anti-deadpan (Dpn) in green, neural progeny labeled with anti-prospero (Pros) in white and DAPI in blue labelling nuclei. (c) Endogenous PI31 expression localizes to the CB and VNC where its expression is higher in large cells, called neuroblasts, marked by anti-Dpn. (d) anti-Dpn staining marking neural progenitors in the CB and VNC. (e) anti-Pros staining marking the neural progeny in a stereotype fashion that does not overlap with anti-Dpn. (f) DAPI staining shows nuclei of all cells in the CB, OL, and VNC. (g-k) Dorsal view of the larval CNS. (g) Composite confocal projection showing DmPI31 expression from the dorsal side overlapping with anti-Dpn in green and with anti-Pros in white. (h) Endogenous mCherry-PI31 (i) anti-Dpn (j) anti-Pros (k) DAPI. All images are shown at 20X magnification.

a.
LF
IPC
NE
NB
OL
CB
me
VNC
OPC
;Pl31::mcherryPl31;
b.
CB
OL
VNC
50 µm
c.
Pl31
d.
Deadpan
e.
Prospero
f.
Dapi
Ventral
g.
CB
VNC
OL
50 µm
h.
Pl31
i.
Deadpan
j.
Prospero
k.
Dapi
Dorsal

Figure 2.2 DmPI31 and proteasome subunits co-express in the central brain of 3rd instar larval CNS

(a-d) Confocal z-stack projections show the CB and OL at 63X magnification. (a) mCherry tagged PI31 is expressed ubiquitously in the CNS but more notably in the nucleus and cytoplasm of large neuroblast cells in the CB. Confocal z-projections show the specific staining pattern of anti-Pros (white), anti-Dpn (green), PI31(red), and DAPI (blue). (b) The alpha2-GFP tagged subunit of the 20S proteasome is expressed in the cytoplasm and perinuclear region of the neuroblasts. This protein is also seen to localize to the cytoplasm of neural progeny. The composite image shows alpha2-GFP (green), anti-Pros (white), anti-Dpn (red), and DAPI (blue). (c) 3rd instar larval brains co-expressing both endogenous mCherry-PI31(red) and endogenous alpha2-GFP (green) a 20S proteasome subunit. Brains were stained with anti-Dpn (purple) marking neuroblast nuclei and Dapi (blue) staining all nuclei. The vast majority of neuroblasts express both PI31 and alpha2GFP however there are a few exceptions (white arrows). (d) 3rd instar larval brains co-expressing both endogenous mCherry-PI31 and endogenous RPT3-GFP, a 19S regulatory subunit. RPT3 is highly expressed in the cytoplasm and perinuclear region of the neural progenitors as well as in the cytoplasm of neural progeny along with PI31.

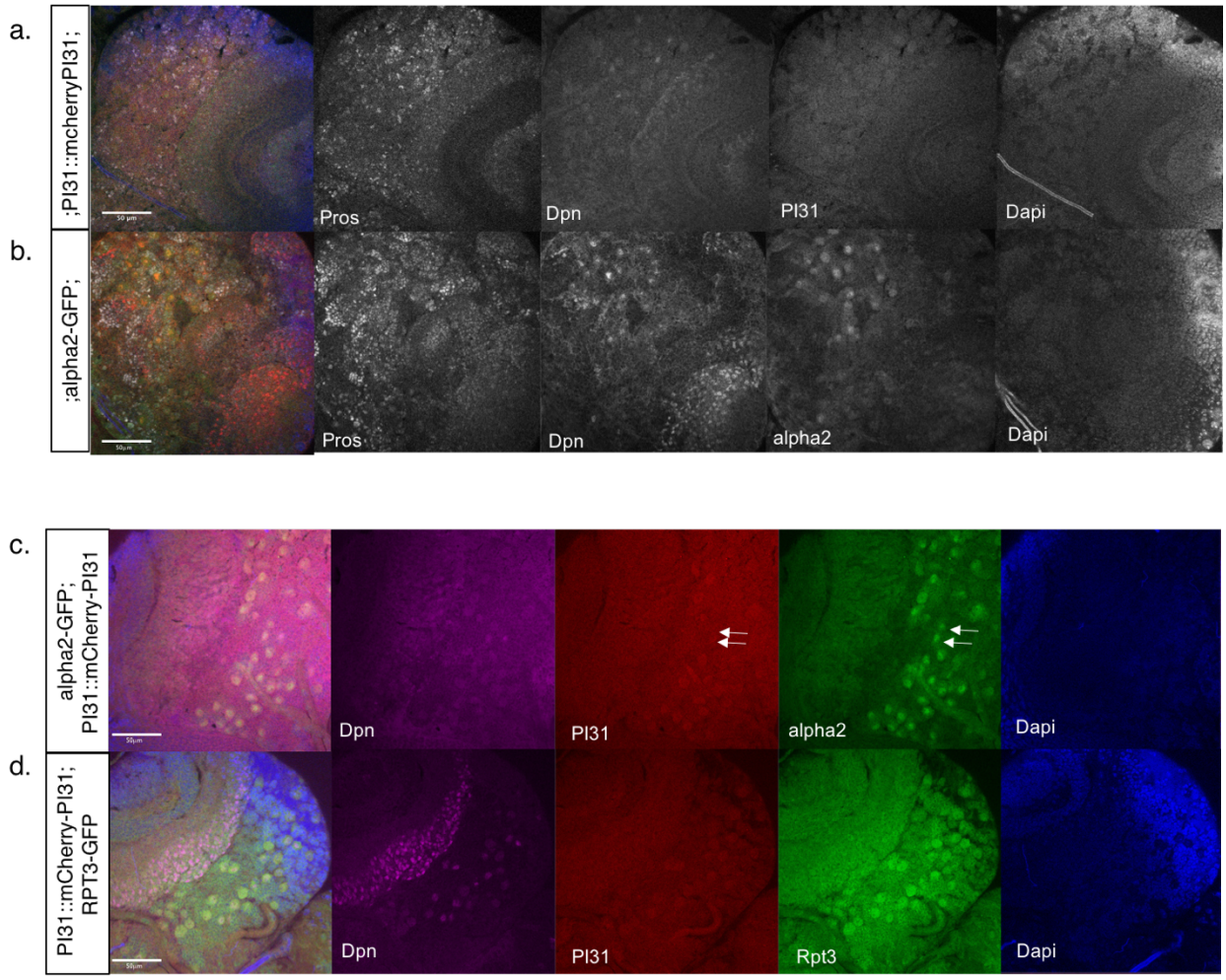
a.
;PI31::mcherryPI31;
Pros
Dpn
PI31
Dapi
b.
;alpha2-GFP;
Pros
Dpn
alpha2
Dapi
c.
alpha2-GFP;
PI31::mCherry-PI31
Dpn
PI31
alpha2
Dapi
d.
PI31::mCherry-PI31;
RPT3-GFP
Dpn
PI31
Rpt3
Dapi

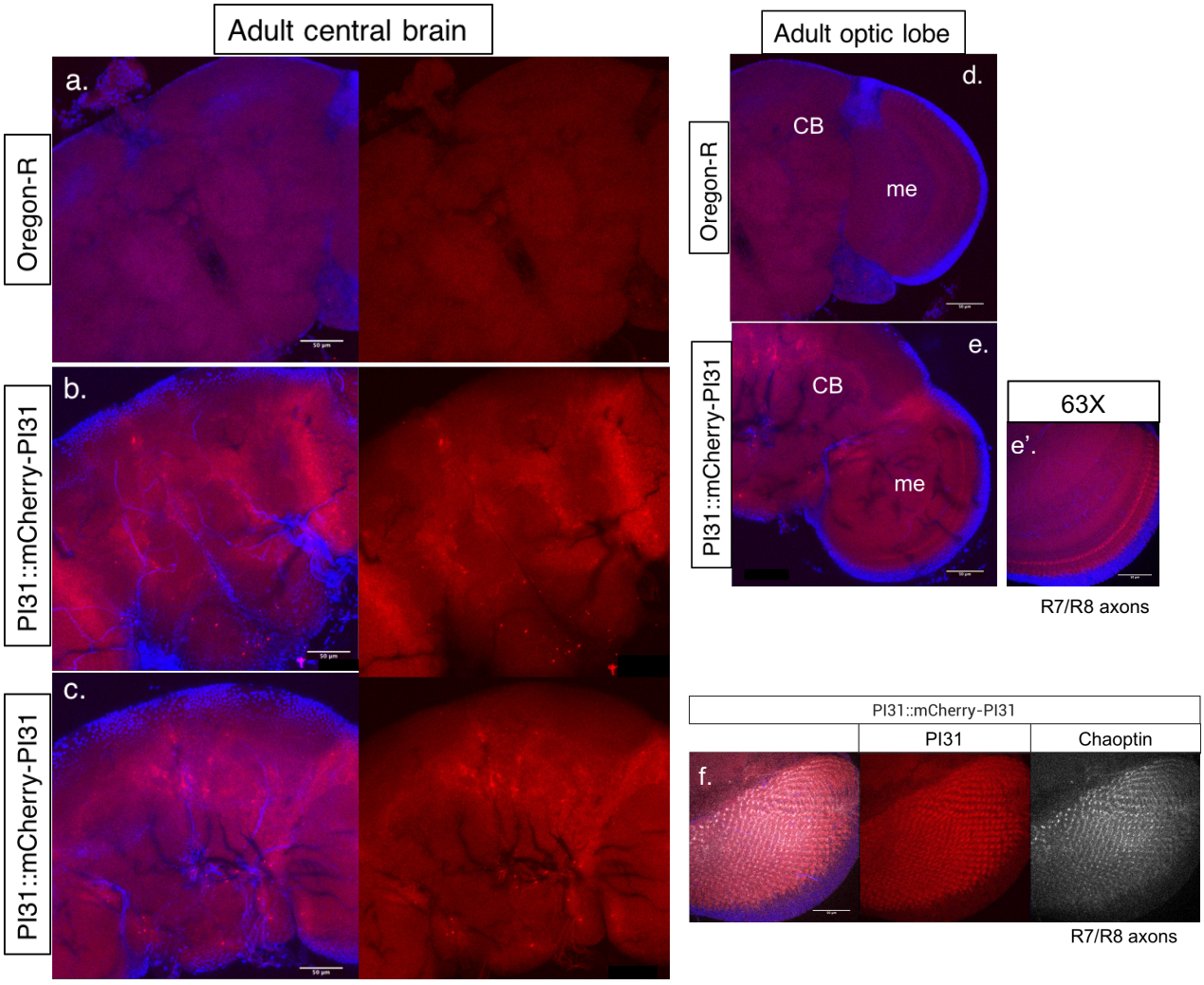

Figure 2.3 DmPI31 expresses within the adult CNS

(a-e) Confocal z-stack projections at 20x magnification of whole-mount adult *Drosophila* brains. (a) Wildtype brains show the mCherry background signal along with DAPI staining. (b) DmPI31 expresses in a stereotyped fashion in a subset of neurons. (c) A similar pattern of neuronal expression is seen within a different set of optical sections in a separate brain. (d) Optic lobe image of wildtype flies labeled with DAPI. (e and e') Optic lobe images show high expression of mcherry-PI31 in the R7/R8 medulla axons at 20X and (e') 63X. (f) Z-stack projections at 63X of the optic lobe medulla show PI31(red) highly expressed in the R7/R8 axon terminals labeled with anti-chaoptin (white).

2.3.2 DmPI31 mutants display mitotic defects and accumulate polyubiquitinated proteins

DmPI31 was found to cause accumulation of polyubiquitinated proteins and cell-cycle defects in the male-germline (Bader et al., 2011). However, whether DmPI31 functions in a similar manner in neuronal tissue is unknown. To learn more about the function of DmPI31, I stained brains from *dmPI31* mutants which survive into the pupal stage, for the presence of polyubiquitinated proteins (FK2), an apoptosis marker (Dcp-1), and the cell cycle factor (cyclin B). Since heterozygous mutants for dmPI31 are viable and show no obvious phenotype, it is expected that proteasomes are not impaired and thus this line was used as a control for FK2 staining. However, FK2 did not show an accumulation in dmPI31$^{-/-}$ larval brains compared to the dmPI31$^{-/+}$ (Figure 2.4a',b'). It is possible that the impairment of proteasomes activates a compensatory degradation machinery, such as autophagy, in these cells that acts to degrade any accumulated proteins (Lőw et al., 2013; Nedelsky et al., 2008). To determine whether there was increased apoptosis in these mutants, I stained for cleaved Dcp-1, the active form of a critical effector caspase. A slight accumulation of cleaved DCP-1 is observed but brain size between control and mutant groups was not affected (Figure 2.4c,d). Staining for cyclin B however showed a slight accumulation in the cytoplasm of cells in both the optic lobes when compared to wild-type controls (Figure2.4 c,d). Cyclin B is a substrate for the proteasome so this accumulation suggests defective proteasome activity. Interestingly, degradation of cyclin B is required for exit from mitosis (Castro et al., 2005). Likewise, dmPI31 mutant brains show altered localization of the stem cell markers Deadpan and Prospero (Figure 2.4 e,f). In control lines, Pros staining is restricted to the nucleus of GMCs and does not overlap with nuclear Dpn staining. Dpn also shows restricted localization and typically marks mitotic areas of the optic lobes. In mutants, Pros staining is diffuse, cytoplasmic, and overlaps with Dpn, whose expression pattern

is greatly expanded. (Figure 2.4 e,f). Pros is a transcriptional repressor that is restricted to the nucleus to downregulate cell cycle genes and restrict GMCs to one terminal mitosis. Dpn on the other hand plays an important role in neuroblast self-renewal and specification. Reports have shown that ectopic expression of Dpn promotes ectopic self-renewing divisions of neuroblast (Zhu et al., 2012). Thus, it appears that dmPI31 plays a role in cell cycle exit and loss of this protein results in cell cycle defects, accumulation of Dpn, and over-proliferation of neuronal stem cells.

In order to determine the consequences of loss of PI31 through all stages of development, I took advantage of the FLP/FRT technique that is used to generate mitotic clones in a heterozygous animal in specific tissues and stages (Golic *et al*., 1997). The FLP/FRT technique can yield mosaic wild-type, heterozygous, and homozygous mutant cells in a specific tissue of an animal heterozygous for a wild-type and mutant allele. Using a heat shock inducible flippase, I generated *dmPI31* mutant clones by subjecting heterozygous larvae to 3 rounds of 1hr heat shock over 72 hours. Similar to results obtained with antibody staining in *dmPI31* mutant larva, larval mutant clones did not show aggressive accumulation of poly-ubiquitinated proteins in the brain or eye discs (Figure 2.5a). However, leg discs with patches of mutant clones showed marked accumulation of poly-ubiquitinated proteins (Figure 2.5a,b). This may point to a more essential role for PI31 in this tissue or a compensatory mechanism held by the brain and eye discs to overcome proteotoxic stress. Of note, is the finding that DmPI31 was shown to be essential for leg development, thus the effect of loss of PI31 in this compartment may be more detrimental to proteasome function (Grubbs et al., 2013).

Additionally, I assayed PI31 function in adult tissues by generating mutant clones in the adult photoreceptors using an eye specific flippase. I found that photoreceptors which lack

dmPI31 rapidly degenerate and accumulate poly-ubiquitinated proteins, suggesting a defect in proteasome function (Figure 2.6c). However, heterozygous photoreceptor axons also appear affected with many displaying twisted and degenerative phenotypes as shown by GFP expression in these axons (Figure 2.6c). Photoreceptor clones induced by eye specific flippase in a different context also showed rapid degeneration. Live images of photoreceptors clones were taken with the cornea neutralization technique using transgenes that express GFP specifically in photoreceptors 1-6. Generation of mutant clones for *Nmnat*^{1}, an essential enzyme in the NAD+ salvage pathway, does not show degeneration at 1 day PE and mutant cells can be seen by lack of Tomato (red) but maintenance of GFP (green) (Figure 2.6a). These mutant cells are reported to degenerate with age. However, *dmPI31* mutant clones showed rapid degeneration of rhabodmeres as early as 1 day PE (Figure 2.6b) suggesting an essential role for PI31 in maintaining cellular health in this context.

Figure 2.4 *dmPI31* mutants display elevated cyclin B and DCP-1

(a) 3rd instar larva of heterozygous *dmPI31* mutants were used as a control to show the OL and CB stained for anti-DCP-1 (an effector caspase, red), FK2 (green), and DAPI (blue). (a') anti-FK2, a marker for conjugated ubiquitin, stains large cells which are likely, neural progenitors. (b) *dmPI31* null mutant OL and CB stained for DCP-1 (red), FK2 (green), and DAPI (blue). (b') anti-FK2 staining shows cytoplasmic staining of large neural progenitors but no difference in signal accumulation when compared to heterozygous larva. (c) Oregon-R strains were used as a control for anti-cyclin B, anti-DCP-1, and anti-Dpn staining. Compared to the control strain, *dmPI31* mutants show accumulation of cyclin B and a slight accumulation of DCP-1 in a subset of cells. Dpn expression, which typically marks mitotic areas of the optic lobe and is nuclear in neuroblasts, is altered and appears in a large number of smaller cells, whose localization coincides with neural progeny. (e) DmPI31 mutants show diffuse anti-pros (white) and anti-Dpn (green) in the cytoplasm of cell clusters pointing to potential proliferation defects. Note that anti-Dpn again stains more cells and appears cytoplasmic in clusters of cells. (f) Control brains show distinct anti-pros (white) staining that is high in neural progeny surrounding the neuroblasts, which are marked by nuclear Dpn staining. All confocal images were taken at 63X magnification.

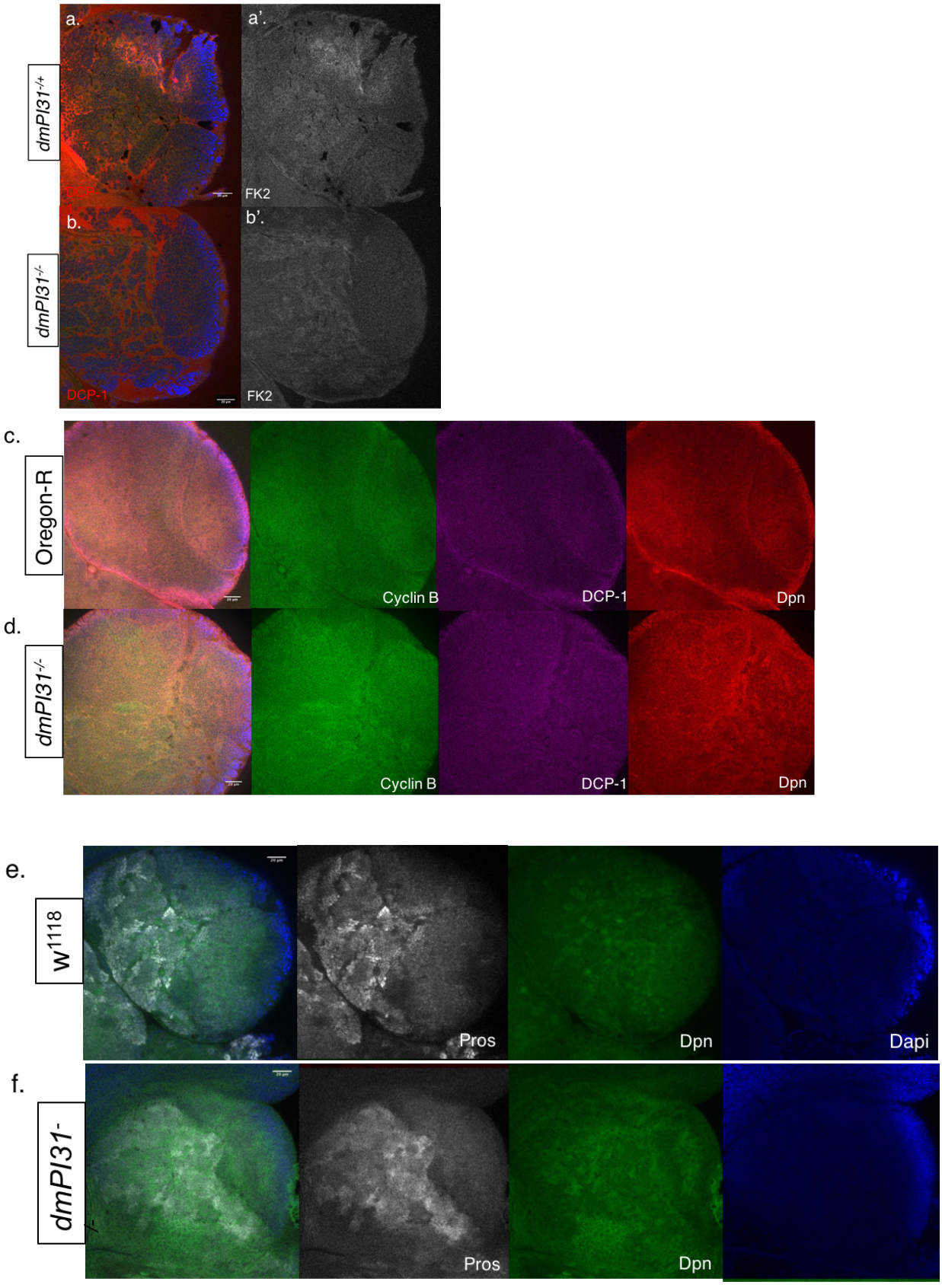
a.
a'.
dmPl31-/+
DCP-1
FK2
b.
b'.
dmPl31-/-
DCP-1
FK2
c.
Oregon-R
Cyclin B
DCP-1
Dpn
d.
dmPl31-/-
Cyclin B
DCP-1
Dpn
e.
w1118
Pros
Dpn
Dapi
f.
dmPl31-
Pros
Dpn

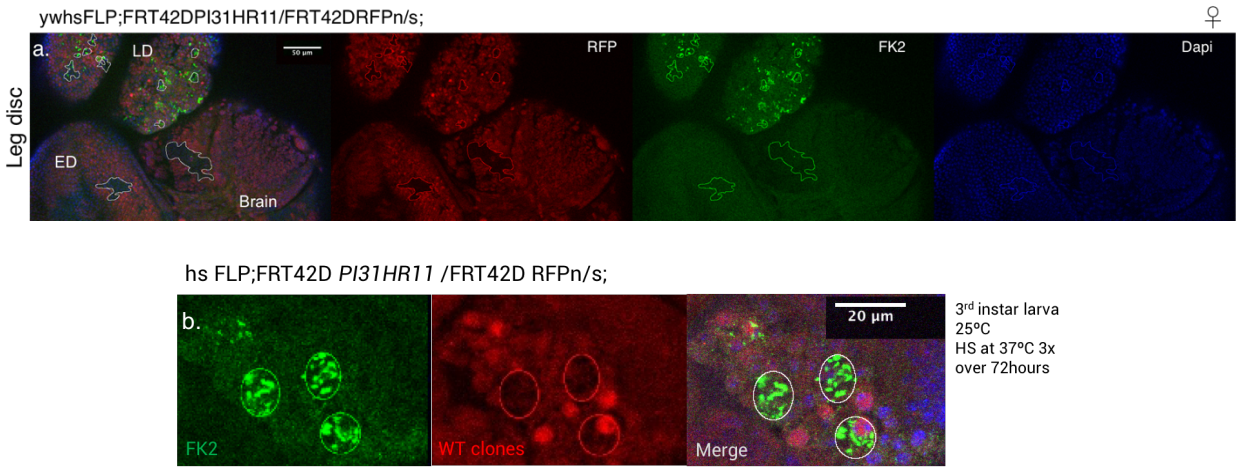

Figure 2.5 *dmPI31* mutant clones show accumulation of ubiquitin in leg imaginal discs

DmPI31 mutant clones were generated using a heat shock promoter driven flippase to generate clones in various tissues and assay accumulation of conjugated ubiquitin using anti-FK2. Larvae were heat shocked for 1 hour in a 37°C incubator 3 times over 72 hours. (a) Confocal z-stack images show anti-FK2 (green) accumulation in leg imaginal discs (LD) of 3rd instar larva. Wild-type clones are marked by RFP. Mutant clones in the eye disc (ED) and brain are outlined but FK2 does not show significant accumulation in these tissues. Image is viewed at 20X magnification. (b) Z-stack projections at 63X zoom show FK2 (green) accumulation in larval leg disc clones mutant for PI31. Wildtype clones are labeled in red and do not show accumulation of ubiquitinated proteins.

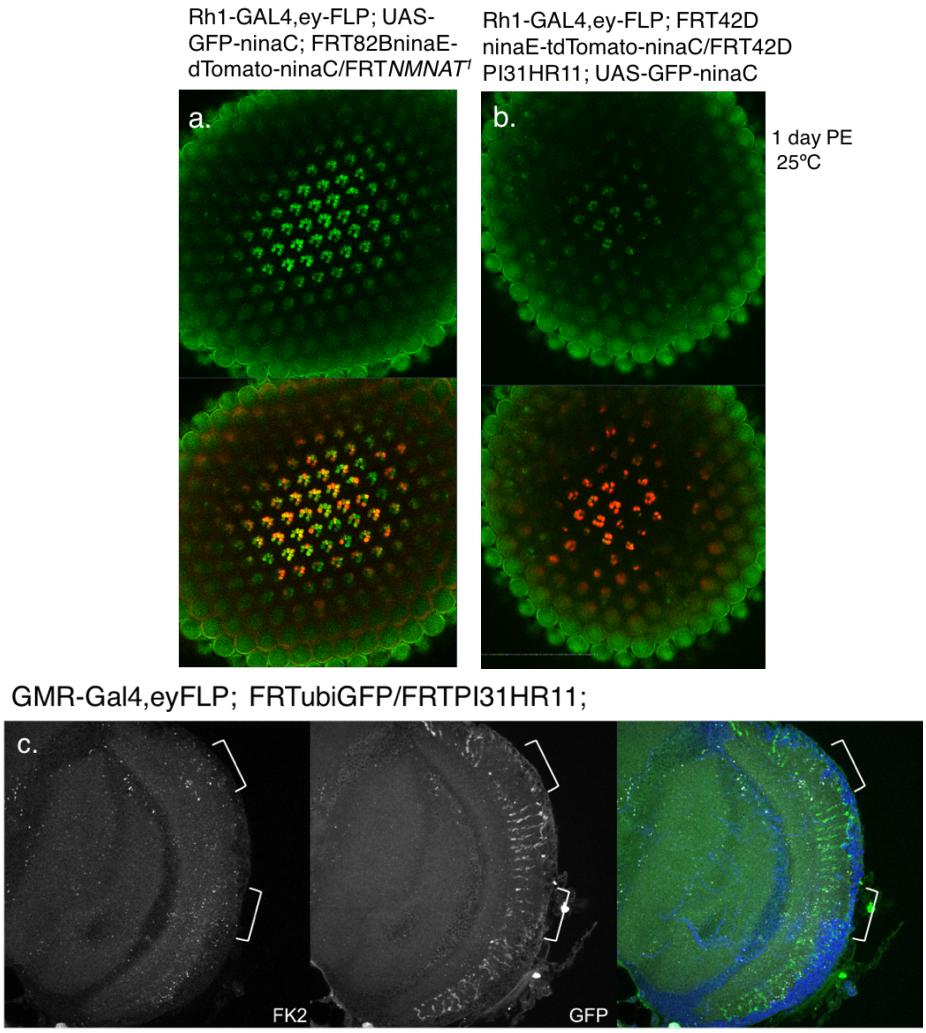

Figure 2.6 *dmPI31* mutants show various neuronal degeneration phenotypes

(a-b) Confocal images from the retina of living flies using the cornea neutralization technique. Mosaic clones were generated by flippase-mediate recombination driven in the eye with ninaC-GFP being expressed in the R1-R6 photoreceptors. (a) Mosaic clones of NMNAT, an essential enzyme in the NAD+ salvage pathway, show the retention of photoreceptors (green) in 1 day old flies. These photoreceptors are reported to degenerate with age. Tomato (red) marks wild-type clones. (b) Mosaic clones of *PI31*$^{-/-}$ show that only wild type clones (red) retain photoreceptors (green) while mutant photoreceptors rapidly degenerate and lack ninaC-GFP (green). (c) PI31 mutant mosaic clones were generated in the eye and whole mount staining of adult optic lobes show the accumulation of conjugated ubiquitin (FK2) in mutant photoreceptor axons (lack of GFP and marked with brackets) from R7 and R8 photoreceptors. These mutant axons also show severe degeneration indicating an essential role for DmPI31.

2.3.3 Neuron specific knockdown of dmPI31 results in eclosion and motor neuron defects

DmPI31 mutant larva are reported to develop melanotic tumors (Bader et al., 2011) but also show impairments in crawling and response to mechanical touch. I sought to address whether DmPI31 has additional neuronal functions outside of the brain. The larvae motor neurons are a well-defined system and display stereotyped projections thus making altered phenotypes identifiable through immunostaining. I assayed *DmPI31* mutant larva for defective motor neuron phenotypes. To do this, the motor neurons between muscle 6 and muscle 7 were stained for HRP, labeling neuronal membranes, and Bruchpilot (Brp) that labels the presynaptic active zones (AZs). *DmPI31* mutant motor neurons show less AZs on average compared to controls (w^{1118}: 421.5 +/- 150 foci, $dmPI31^{-/-}$: 271.9 +/- 84.4 foci, *p= 0.021) without any significant differences in branching or bouton number (w^{1118}: 58 +/- 21 boutons, $dmPI31^{-/-}$: 45.3 +/- 22 boutons, p=0.053; w^{1118}: 12.4 +/- 3.6 branches, $dmPI31^{-/-}$: 13.1 +/- 4.7 branches, p=0.8) (Figure2.7a-b). The reduction in AZs points to a role for dmPI31 in neurons and specifically at the axon terminals. To address the specific effect of DmPI31 on the adult neurons, I used RNAi against PI31 driven by a pan-neuronal driver nervana2 and found that homozygous flies fail to eclose completely from the pupal casing. The head and thorax of these flies emerge but they continue to struggle and never escape the casing while their heterozygous counterparts emerge within seconds (data not shown). Since this phenotype is depicted, I considered the possibility that the motor neurons were being affected in the hind legs (L3). To test these hypothesis, I manually removed partially eclosed living flies from their pupal casing and dissected the L3 legs. The femurs were stained with HRP which labels neurons and the amount of innervation was assayed by counting branch length and number (Figure 2.7c-e). Interestingly, PI31 knockdown resulted in shorter branched motor neurons with a tangled phenotype that did not extend the

length of the femur as in control lines (Figure 2.7d). Overepxression of PI31 showed a similar branch length and motor neuron morphology as the control (Figure 2.7e) and these results were quantified and shown to be significant (Figure 2.7f). It is of note, that the cell bodies of these motor neurons reside in the adult VNC located in the thorax and the staining here identifies the axons that project into the L3 legs.

Figure 2.7 Neuronal knockdown of DmPI31 results in eclosion and motor neuron defects
(a) Wandering 3rd instar larva neuromuscular junction (NMJ) from control flies and (a') PI31 mutant larva were stained with anti-HRP (red) and anti-Brp (green) to mark the presynaptic neuron and presynaptic active zones, respectively. Representative photos of the NMJs between muscles 6 and 7 are shown and taken at 63x magnification. PI31 mutant larva display less active zones while the bouton number and branch number do not significantly change. (b) Quantification of active zone number (w^{1118}: 421.5 +/- 150 foci, $dmPI31^{-/-}$: 271.9 +/- 84.4 foci, *p= 0.021), bouton number (w^{1118}: 58 +/- 21 boutons, $dmPI31^{-/-}$: 45.3 +/- 22 boutons, p=0.053), and branch number (w^{1118}: 12.4 +/- 3.6 branches, $dmPI31^{-/-}$: 13.1 +/- 4.7 branches, p=0.8). n=9 (c-e) Whole mount dissection of adult L3 leg were stained with anti-HRP to mark neurons. (c) Control L3 legs show neurons that are elongated and branched. Purple overlap shows a set of traces that were used for analysis in ImageJ which indicate the average branch length as 143.1 pixels. (d) RNAi mediated knockdown of PI31 results in shorter and twisted neurons with an average length of 100.9 pixels. These neurons also appear to show less elongated branch numbers. (e) PI31 overexpression in neurons shows elongated neurons similar to the control with an average length of 136.61 pixels.(f) Quantification of branch length for n=3 for adult L3 legs shows that RNAi of PI31 significantly reduced branch length.

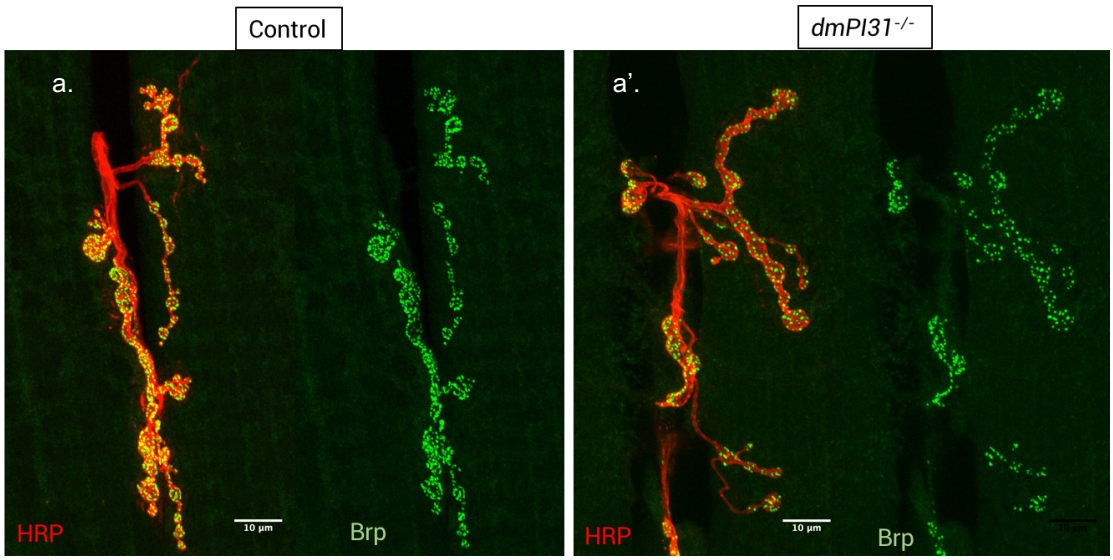
Control
dmPI31-/-
a.
a'.
HRP
Brp
10 µm

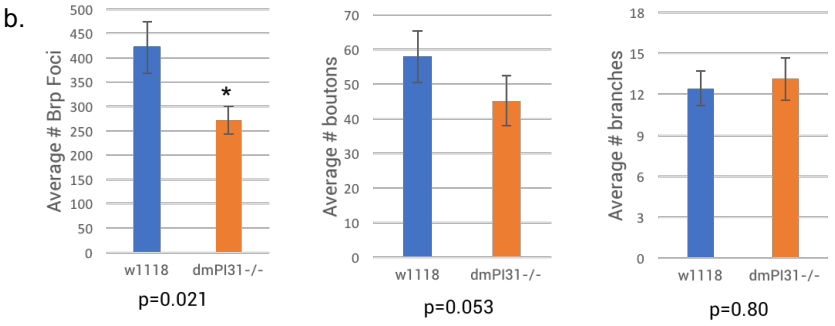
b.
Average # Brp Foci
Average # boutons
Average # branches
w1118
dmPI31-/-
*
p=0.021
p=0.053
p=0.80

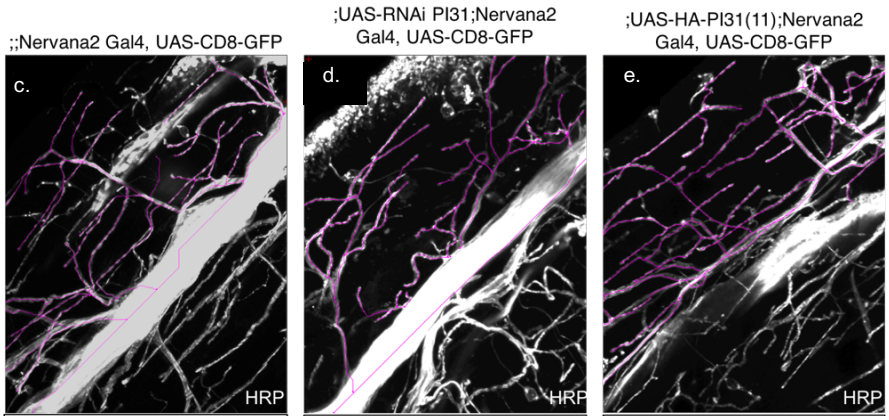
;;Nervana2 Gal4, UAS-CD8-GFP
;UAS-RNAi PI31;Nervana2 Gal4, UAS-CD8-GFP
;UAS-HA-PI31(11);Nervana2 Gal4, UAS-CD8-GFP
c.
d.
e.
HRP

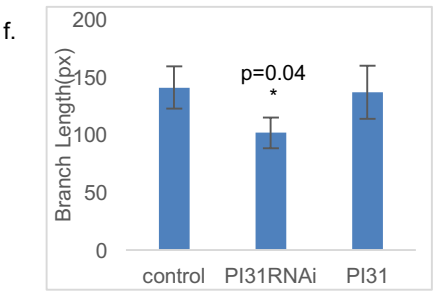
f.
Branch Length(px)
p=0.04
*
control
PI31RNAi
PI31

2.3.4 DmPI31 levels alter lifespan in Drosophila melanogaster

Drosophila have been a useful model to study the effect of proteins on aging and health-span due to their relatively short lifespan. Reports have shown that proteasome activity decreases with age and results from a decrease in proteasome assembly (Tonoki et al., 2009). TNKS, an ADP-ribosyltransferase, was identified as a direct binding partner that modulates PI31 activity through ADP-ribosylation. ADP-ribosylation of PI31 by TNKS is shown increase 26S proteasome assembly by reducing the affinity of PI31 to the alpha subunits of the 20S proteasome to relieve 20S inhibition (Cho-Park and Steller, 2013). DmPI31 provides a link between proteasome assembly and aging. Thus, I sought to address whether activating PI31 later in life could maintain the activity of proteasome and thus extend lifespan in *Drosophila*. To do this, I used a temperature sensitive Gal4 driver under the alpha tubulin promoter (Tubulin-Gal4, tubulin-Gal80^{ts}) to drive expression of various UAS transgenes. Tubulin-Gal80ts inhibits the expression of Gal4 until flies are moved to the restrictive temperature, 30°C. Using these lines, I was able to turn on and off gene expression in a temporal fashion and determine whether overexpression of dmPI31 late in life can extend lifespan. Age matched embryos were collected and distributed into bottles, so as to prevent overcrowding. Early eclosers were discarded, and age matched flies were collected and allowed to sexually mature for 3 days before male and females were separated into respective vials containing 30 flies each. Lines were allowed to develop at room temperature and flipped every 3 days until switched to higher temperatures of 25°C at day 25. At this temperature, it is excepted that Gal80ts is partially degraded but still restricts some transgene expression. This was done since, dmPI31 overexpression is shown to be lethal at high levels. In both males and females expression of RNAi against PI31 decreases average lifespan (RNAi PI31 in males 33 +/- 1.74 days, RNAi PI31 females 27 +/- 1.41 days)

compared to control (male 38 +/- 0.69 days, female 36 +/- 0.60 days) (Figure 2.8a,b). Interestingly, males but not females display lifespan extension when overexpressing dmPI31 (UAS dmPI31 males 46 +/- 0.91 days, UAS dmPI31 females 34.14 +/- 0.83 days) (Figure 2.8a,b). In a more stringent assay, age matched female flies were developed and aged at 18°C until being switched at day 47 to either 25°C or 29°C. At 25°C , the lifespan of female flies overexpressing dmPI31 does not significantly increase compared to control lines however, at 29°C both females showed increased lifespan under PI31 overexpression compared to control (Figure 2.8c). This experiment points to levels of dmPI31 being important for lifespan extension since higher temperatures result in greater induction of the transgenes. The differences seen between male and female flies could be due to expression differences between the sexes as it is known that dmPI31 is highly expressed in the testes.

Figure 2.8 DmPI31 levels influence lifespan in *Drosophila*

Lifespan assays were conducted with transgenic flies expressing various PI31 constructs under a temperature sensitive tubulin Gal4 promoter. OASIS 2 online application was used for survival analysis and to conduct statistical analysis on the lifespan of PI31 knockdown and overexpression flies compared to controls. (a-b) Flies were aged matched at RT, and females (a) and males (b) were reared separately at RT after reaching sexual maturity. At day 25 flies were switched to 25°C to drive expression of transgenes. (a) In female flies, knockdown of PI31 resulted in shortened average lifespan (27 days) compared to control (36 days), *$p=3.6 \times 10^{-4}$. Overexpression of PI31 did not significantly alter lifespan (34 days) compared to control, p=3.84. (b) Male flies also show reduced lifespan when PI31 is knocked down (33 days) compared to control (38 days), *p=0.0025. In males however, overexpression of PI31 extend lifespan (46 days) compared to control (38 days), *$p=2.8 \times 10^{-9}$. (c) Female flies were subject to more stringent induction of PI31 transgene expression with temperature sensitive lines developed and reared at 18°C and then switched to 25°C or 29°C at 47 days PE. At 25°C, average lifespan between control (73 days) and PI31 overexpression lines (78 days) is extended by 5 days. With higher transgene expression at 29°C, PI31 overexpression results in an 18 day increase in lifespan compared to control (57 days).

a.

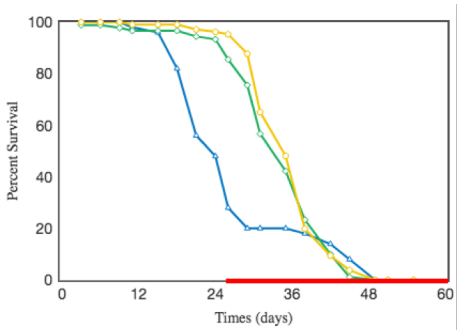

Tubulin-Gal4, Tubulin-Gal80ts

x

Name	# of subjects	Average lifespan (Days)	S.E.	95% C.I.	25%	50%	P values
UAS-RNAi-PI31	50	27.00	1.41	24.23 ~ 29.77	21.00	24.00	0.0024
UAS-PI31	90	34.14	0.83	32.51 ~ 35.78	31.00	35.00	0.384
Tub Gal4 Gal80ts	106	35.63	0.60	34.46 ~ 36.80	31.00	35.00	3.6×10^{-4}

b.

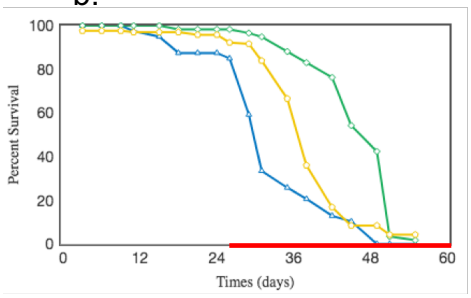

Tubulin-Gal4, Tubulin-Gal80ts

x

Name	# of subjects	Average Lifspan (Days)	S.E.	95% C.I.	25%	50%	P values
UAS-RNAi PI31	40	33.15	1.74	29.73 ~ 36.56	29.00	31.00	8.5×10^{-5}
UAS-PI31	59	46.00	0.91	44.21 ~ 47.79	45.00	49.00	2.8×10^{-9}
Tub Gal4 Gal80ts	168	38.00	0.69	36.65 ~ 39.34	35.00	38.00	0.0025

Developed and reared at RT
25 days PE switched to 25ºC

c.

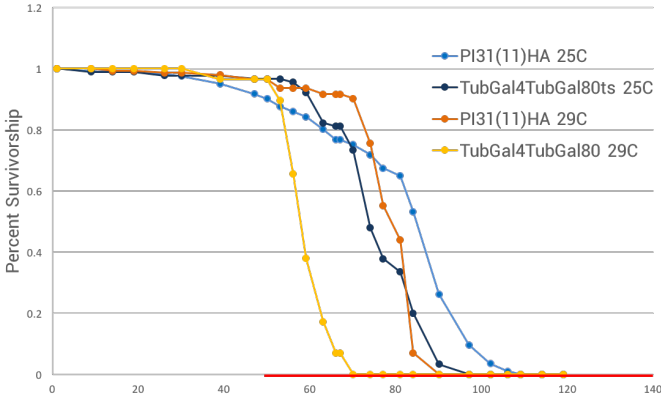

Temperature	Name	# of subjects	Average Lifespan (Days)
25	PI31(11)HA	150	77.6
25	TubGal4TubGal80ts	90	72.5
29	PI31(11)HA	146	75.1
29	TubGal4TubGal80ts	30	56.8

Developed and reared at 18ºC
47 days PE switched to 25ºC or 29ºC

2.4 Discussion

The essential role of DmPI31 in the *Drosophila* nervous system was highlighted in this chapter through studies on localization and mutant phenotypes. It was shown that DmPI31 expression appears ubiquitous but is most abundant in the larval and adult central brain. In addition, DmPI31 expresses in the photoreceptor axons of the adult optic lobes meaning there is a possible mechanism that transports DmPI31 to these distal locations. Within the central brain in larvae, DmPI31 expresses highly in the neuroblasts, which are the neuronal stem cells that self-renew and asymmetrically divide to produce the diversity of neurons in the *Drosophila* brain. Here in the neuroblasts, DmPI31 is shown to co-express with the proteasome subunits α2 and Rpt3. It is likely that neuroblasts require higher levels of proteasomes to keep up with the demands of proliferation and these proteasomes require a stringent level of regulation. In line with this is the observation that *dmPI31* mutants accumulate cyclin B and show expanded numbers of Dpn positive cells. Cyclin B is typically degraded by the 26S proteasome to initiate the termination of mitosis (Tokumoto et al., 1997). The accumulation of cyclin B indicates impaired 26S proteasome activity in *dmPI31* mutants leads to aberrant mitosis. Since the size of the brain does not appear to change, it would be interesting to check the balance between apoptosis and proliferation with TUNEL staining and EdU (5-ethynyl-2'-deoxyuridine) incorporation respectively. It is possible that DmPI31 in brain tissue is regulated in a different manner than in the leg discs, since polyubiquitinated proteins do not accumulate to the same extent. The decreased number of active zones in the larval NMJ and decreased branch number in the adult motor neurons points to dmPI31 playing a role in synaptic remodeling as well. Whether this is through proteasome mediated degradation of specific substrates is yet to be determined but

a screen for modifiers of the photoreceptor degeneration seen using the cornea neutralization technique in dmPI31 clones could lead to potential candidates.

This chapter emphasis that proteasome activity needs to be temporal and spatially restricted to prevent nonselective protein degradation. The subcellular localization of dmPI31 and mutant phenotypes link this proteasome interacting protein to essential functions in neuronal maintenance and health. Lifespan assays show that reduced levels of PI31 lead to shorten lifespan while overexpression can extend lifespan in males, and at very high levels in females. However, whether alterations in DmPI31 levels causes differential proteasome assembly during lifespan extension phenotypes is not yet known.

2.5 Materials and Methods

Fly stocks and culturing

All stocks were maintained on a standard cornmeal-molasses medium containing 3% yeast at 25°C unless otherwise indicated. John Belote generously provided the alpha2-GFP and Rpt3-GFP lines while PI31 mutants and tagged lines were generated previous in the lab by Maya Bader. RNAi for PI31 (105476) was obtained from VDRC. Rh1-GAL4,ey-FLP; UAS-GFP-ninaC; FRT82BninaE-dTomato-ninaC and Rh1-GAL4,ey-FLP; FRT42DninaE-dTomato-ninaC; UAS-GFP-ninaC were generated by former lab members Alexis Gambis and Bertrand Mollereau. Oregon-R or w1118 were used as control lines. Nervana^{2}Gal4 (6794), was obtained from Bloomington.

Brain dissection and immunostaining

3rd instar larva imaginal discs or adult brains were dissected in ice cold PBST (0.1% Triton-X) and fixed in 4% paraformaldehyde (PFA) for 40min on ice. After fixation, CB and VNC were separated from other discs and washed 3X in cold PBST before incubation for 1 hour in 2% BSA blocking buffer. Primary antibodies were diluted in 2% blocking buffer plus 5% normal donkey serum and incubated overnight at 4°C. anti-Deadpan (1:100, 11D1BC7 abcam195173), anti-Prospero (1:100, MR1A), anti-cyclin-B(1:100, F2F4) were all obtained from DSHB while mouse monoclonal anti-FK2 (1:100, Stressgen), cleaved anti-DCP-1 (1:200, cell signaling technologies) were obtained from the respective companies. Secondary antibodies corresponding hosts were diluted (1:500) in blocking buffer and incubated overnight at 4°C before samples were washed 3X in PBST. Brains were mounted in Vectashield plus DAPI and imaged with Zeiss confocal microscope by taking z-stacks and making maximum intensity projections.

Generation of mitotic clones

Lines of yw hsflp; FRT42DubiRFPn/s were crossed to FRT42D *PI31HR11* and heat shocked at 37°C 24 hours after egg laying and every 24 hours for 3 days before 3rd instar larva were dissected for imaginal discs and fixed in 4% paraformaldehyde. Tissues were washed 3X with PBST and blocked in 2% BSA. For poly-ubiquitin staining, mouse monoclonal FK2 was used (1:100) and incubated overnight at 4°C. Primary antibody was washed 3X for 10min each at room temperature before addition of secondary Donkey anti-mouse-FITC (1:500) which was incubated overnight at 4°C. Tissues were washed 3X with PBST and mounted in Vectashield plus DAPI. Confocal z-stacks were taken of mitotic clones marked by the absence of RFP and subsets of images were taken before applying maximum intensity projections using ImageJ.

Motor neuron whole-mount immunostaining

3rd instar larva of either control or PI31 mutants lines were dissected and immunostaining of NMJs were carried out according to the following protocols (Brent et al., 2009a, 2009b). Briefly, larval were filleted open using minutien pins and organs were carefully removed. Body walls were fixed with 4% PFA in HL3 saline (NaCl 70mM, KCl 5mM, CaCl2 1.5mM, MgCl2 20mM, NaHCO3 10mM, sucrose 115mM, and Hepes 5mM) for 25min and then washed 3X with HL3 saline. After fixation samples were moved to 1.5mL Eppendorf tubes containing 2% BSA blocking buffer and blocked for 30min at RT. Then primary antibody a-Brp (1:500, nc82) and Cy3 Goat-Horseradish peroxidase (1:500, Jackson immunoresearch) were added and incubated overnight at 4°C. Subsequently, gentle washing with PBST 3X was done before adding secondary antibody Donkey anti-mouse FITC (1:500) overnight in cold room. Samples were washed and NMJs between muscle 6/7 were imaged with z-stacks at 63X magnification with Zeiss Confocal microscope.

Live imaging of Drosophila photoreceptors

Generation of mosaic adult Drosophila photoreceptor clones was done following the protocol described in (Dourlen et al., 2013). Briefly, Rh1-GAL4, ey-FLP; UAS-GFP-ninaC; FRT82B ninaE-dTomato-ninaC and Rh1-GAL4,ey-FLP; FRT42DninaE-dTomato-ninaC; UAS-GFP-ninaC were crossed to FRT82BNmnat[1] (BL 24886) and FRT42D *PI31HR11* respectively. Adult flies of the correct genotype were anesthetized and mounted in low melt agarose at 45-55°C by submerging one wing of the fly into the agarose along with half of the head to prevent movement during imaging. Clones were identified by confocal imaging using a 40X water objective.

Drosophila lifespan assays and OASIS analysis

Lifespan analysis was carried out on UAS lines crossed to the Tubulin Gal4, Tubulin Gal80 temperature sensitive driver at indicated temperature either 18, 25, or 29°C. Stock of these lines were made over balancers and isogenized by backcrossing to w1118 lines. The following protocols were followed for lifespan assay set up and data analysis (Han et al., 2016; Linford et al., 2013). Lines were expanded and age matched eggs were collected and put into bottles. Aged matched eggs were allowed to reach sexual maturity and male and females were separated 30 to each vial. Vials were flipped every 3 to 4 days and the number of dead flies in each vial were scored. Statistical analysis was carried out using OASIS 2 online software.

3. Metabolic influence on proteasome regulation by NAD+

3.1 Summary

An understanding of how 26S proteasomes are regulated in response to metabolic changes within the cell is lacking but are critical to understanding why this system begins to fail in aging and age-associated diseases. DmPI31 provides a potential target for metabolically regulated proteasome modulation because of its modification by TNKS-mediated ADP-ribosylation. In this chapter, I explore proteasome regulation during two metabolic states, dietary restriction (DR) by means of yeast dilution and NAD+ repletion through nicotinamide and nicotinic acid supplementation. *Drosophila* at various developmental time points were subject to diets with defined amounts of yeast or the NAD+ precursors, nicotinamide (Nam) and nicotinic acid (Na). Both DR and supplementation of NAD+ precursors are shown to boost proteasome activity. I show that DmPI31 is necessary for the increase in proteasome activity seen during NAD+ repletion and more specifically the activity of 26S proteasomes. The rise in proteasome activity coincides with an enhanced expression of DmPI31 and increased 26S proteasome assembly. These findings demonstrate that proteasomes are actively regulated during varied metabolic states and demonstrate a potential pathway by which proteasomes can quickly adapt to metabolic changes. I conclude the chapter with studies in the context of Nmnat, an essential enzyme involved in the synthesis of NAD+ from Na and Nam. Generation of *nmnat*$^{-/-}$ photoreceptor clones reveals a decrease of DmPI31 along with photoreceptor axon degeneration. However, DmPI31 appears not to physically interact with Nmnat. Instead, feeding the flies NAD+

precursors in an *nmnat*$^{-/-}$ background can rescue the loss of DmPI31 providing further evidence that DmPI31 and proteasomes are regulated by NAD+ metabolism.

3.2 Rationale

The degradation or cleavage of substrates by the UPS is essential for many cellular processes including apoptosis, cell cycle control, cell signaling, and protein quality control. The structure and function of proteasomes is well known but how they are regulated *in vivo* is not well understood, most likely due to tissue and context specific regulators. However, evidence that proteasomes are actively regulated during metabolic changes exists with examples of posttranslational modifications of proteasome subunits, the accumulation of metabolic abnormalities during proteasome inhibition, and a decline in proteasome function during aging (Zhang et al., 2003, 2007b, 2007a; Tomaru et al., 2012; Tonoki et al., 2009). A potential candidate to explore in this context is the proteasome regulator, DmPI31, which was found to be an activator of 26S proteasomes *in vivo* by increasing assembly. This increase in assembly comes about through the posttranslational ADP-ribosylation of DmPI31 by the ADP-ribosyltransferase, tankyrase (TNKS) (Cho-Park and Steller, 2013). The source of ADP-ribose units is nicotinamide adenine dinucleotide (NAD+), which has been shown in a variety of systems to be neuroprotective and increase healthspan (Lehmann et al., 2016; Ocampo et al., 2013; Verdin, 2015; Wang et al., 2008; Zhang et al., 2016). Thus, NAD+ provides a link between cellular metabolism and proteasome activity. In our natural diet, nicotinic acid, nicotinamide, and tryptophan can be used to synthesize, NAD+, which is a key substrate for NAD+ consuming enzymes and a co-enzyme for redox reactions where in its reduced state becomes NADH. Increasing intracellular NAD+ content is involved in maintaining neural integrity in a variety of

contexts (Lehmann et al., 2016; Ocampo et al., 2013; Verdin, 2015) and is capable of extending healthspan (Anderson et al., 2003; Yoshino et al., 2011; Zhang et al., 2016). Whether these effects are mediated by gene expression changes, improved mitochondrial health, or increased autophagy have been explored but do not provide a definitive picture. Thus, I sought to explore the role of NAD+ repletion on proteasome activity by supplementing the diets of *Drosophila* with the NAD+ precursors nicotinamide (Nam) and nicotinic acid (Na), at times collectively referred to as niacin. Dietary restriction is also explored since it is shown to increase NAD+ levels and is the only non-genetic manipulation to reproducibly increase healthspan across species.

Here, I describe a link between cellular metabolism and proteasome activity. Through dietary supplementation, I show that both nicotinamide and nicotinic acid can increase proteasome activity, proteasome assembly, and protein levels of DmPI31. These findings are corroborated by knockdown of Nmnat, a key enzyme in the synthesis of NAD+ metabolism, which also shows reduced proteasome activity and DmPI31 expression. These two proteins however are not shown to physically interact. Instead, I speculate that the loss of the neuroprotective, Nmnat, results in a signaling pathway that lowers the expression of dmPI31 to restrict proteasome activity in degenerating neurons.

3.3 Results

3.3.1 Nicotinamide and nicotinic acid increase proteasome activity and levels of DmPI31

NAD+ provides a potential link between cellular metabolism and proteasome activity. Both dietary restriction and NAD+ repletion via nicotinamide and nicotinic acid have been shown to be beneficial for extending lifespan and healthspan across species but few studies have shown

how these interventions might impact proteasome regulation. To test whether boosting NAD+ levels could improve proteasome activity, I age-matched *Drosophila* embryos and distributed them on diets supplemented with nicotinamide (Nam) or nicotinic Acid (Na) as indicated in Figure 3.1a. Both metabolites are NAD+ precursors in the NAD+ salvage pathway (Figure 1.3). A cornmeal-molasses based food recipe was developed and supplemented with varied concentrations of Nam or Na (Figure 3.1b). Wild-type Oregon-R strains were fed on either Nam or Na supplemented food and whole-body lysates were assayed for cleavage of the luminogenic peptide Suc-LLVY-aminoluciferin indicative of the chymotrypsin-like activity of the proteasome. MG132, a potent proteasome inhibitor, is used as a negative control to determine specificity of substrate cleavage for the proteasome. When flies are fed with 10mM Na, proteasome activity increases 23% compared to non-supplemented control (Figure 3.2a). Feeding with 10mM Nam does not cause a significant increase in activity however increasing the amount of Nam to 30mM increases proteasome activity by 25%. High levels of Na increase proteasome activity by 18% in this assay which is still significant but high levels of Na consistently show less activity which may indicate slight toxicity. All values were normalized as a percentage of non-supplemented controls (MG132: 38.06 +/- 7.69 RLU, ***$p=1.7x10^{-6}$; Na 10mM:123.06 +/- 8.71 RLU, **p=0.003; Nam 10mM: 102.39 +/- 11.02 RLU, p=0.39; Na 30mM: 118.07 +/- 10.08 RLU, *p=0.049; Nam 30mM: 125.65 +/- 10.09 RLU, *p=0.013) (Figure 3.2a). To further investigate the impact these metabolites have on proteasome activity, western analysis was carried out on head lysates from control, w^{1118}, flies fed on varied concentrations of Nam and Na. Endogenous levels of DmPI31 were assayed and interestingly DmPI31 protein expression is increased with each concentration of either Nam or Na. Strikingly a two-fold increase was observed with supplementation of Na 10mM (Figure 3.2b). The 20S proteasome subunit, α7,

was also assayed and showed a slight decrease in subunit expression except in the case of Nam 20mM. Interestingly in *dmPI31* mutants, where the whole larval lysate was taken, α7 expression is increased compared to tubulin. This is potentially due to an adaptive feedback loop caused by loss of DmPI31 or possibly differential α7 levels across tissues. Whole body lysates from males fed on control or 10mM Na again show a significant increase in DmPI31 expression indicating that NAD+ repletion may regulate DmPI31 in a range of tissues. Many of the experiments to follow will use a UAS driven HA tagged DmPI31, thus I also tested whether NAD+ supplementation could increase DmPI31 in this context. Using GMR-Gal4 to drive expression of HA-PI31 in the eye, head lysates from flies fed a Na dilution series were taken and resolved on SDS-PAGE gel to assay for changes in dmPI31 levels. Again, Na increases dmPI31 levels but high levels of Na typically show diminished expression most likely due to toxicity (Figure 3.2c). However, the increase in DmPI31 seen at Na 40mM could be due to many factors including reduced consumption of food by the flies, compensatory gene regulation caused by decreased DmPI31, or quenching of an intermediary that typically inhibitions DmPI31 expression.

In order to better understand the effect of dietary supplementation *in vivo*, I took advantage of the hs-EGFP-N^{intra} *in vivo* proteasome sensor. This transgenic line expresses a Notch intracellular domain (N^{intra}) with a PEST degradation signal, that is a known target of the UPS, fused to EGFP downstream of the heat-shock promoter. Upon heat shock, EGFP-Nintra signal accumulates and at 1 hour reaches peak levels. If proteasomes are functional the signal degrades and is only slightly detectable after 4 hours. To test whether Nam or Na could increase in vivo proteasome activity, flies expressing a dominant temperature sensitive proteasome mutation in the β2 subunit (DTS7) were cross to the sensor to give a baseline level of proteasome impairment. Upon heath shock these transgenic flies show stabilization of EGFP-Nintra at 1 hour

post eclosion. In parallel flies fed on 30mM nicotinamide were heat shocked and showed less accumulation of stable EGFP-Nintra signal (Figure 3.2d). This points to a means by which Nam either primes proteasomes prior to heat shock or increases the rate at which proteasome assembly and subsequent activity occurs. Either way it is important to consider whether to this is due to transcriptional or post-transcriptional changes that occurring during Nam feeding. Since ADP-ribosylation of dmPI31 is shown to increase 26S proteasome activity, I sought to investigate whether dmPI31 is necessary for the increased proteasome activity seen under Na and Nam. I tested whether increased proteasome activity is still observed in transgenic flies expressing RNAi against dmPI31 and flies expressing HbYX deleted dmPI31 upon feeding with 10mM Na. Proteasome activity was measured in lysates using the *in vitro* method and in both cases feeding did not significantly alter proteasome activity (Figure 3.2e). On the other hand, control lines fed 10mM Na and overexpression of full-length PI31 increased proteasome activity by about 40% compared to control. This suggests that dmPI31 is required for the increase in proteasome activity upon Na and Nam feeding. Consistent with previous findings, the HbYX motif is required for full proteasome activity promoted by full length dmPI31 but the PI31ΔHbYX still confers a modest increase compared to control, which becomes significant upon 10mM Na (Compared to Tubulin, MG132: 20.42 +/- 6.15 RLU, ***p=3.03x10^{-5}; Na 10mM: 142.12 +/- 11.85 RLU, *p=0.012; UAS-PI31: 133.37 +/- 10.48 RLU, *p=0.027; RNAi PI31 108.67 +/- 6.34 RLU, p=0.281; RNAi PI31 + Na 10mM: 122.11 +/- 24.693 RLU, p=0.422; PI31ΔHbyX: 119.967 +/- 12.281 RLU, p= 0.208; PI31ΔHbYX + Na 10mM : 130.739 +/- 9.033 RLU, *p=0.017). This is interesting because the HbYX motif was found to be necessary for TNKS binding to dmPI31, meaning that a potential TNKS independent pathway exists that increases proteasome activity upon NAD+ repletion. However, one caveat of the *in vitro* proteasome assay

is that it does not differentiate between 20S and 26S proteasome activity. Thus, average proteasome activity upon different feeding conditions may not be reflective of shifts that occur in 20S versus 26S activity.

a.

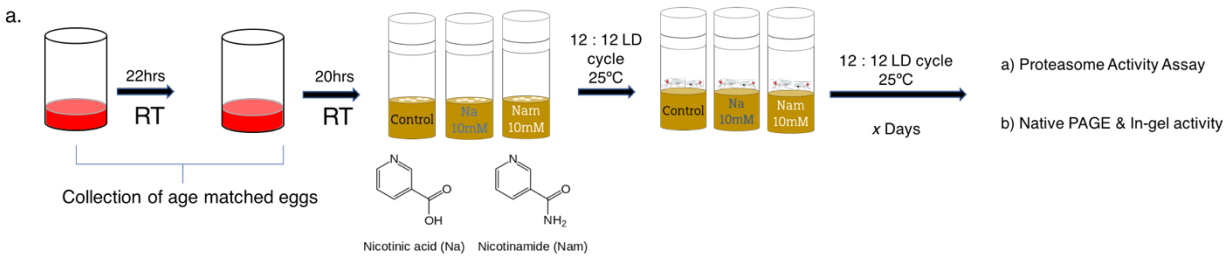

b.

Food Type	Molasses (mL/L)	Yeast (%)	Nicotinic Acid (g/L)	Nicotinamide (g/L)
Control	83	3%	0	0
Dietary Restricted	83	0.25%	0	0
Nicotinic Acid (NA) 10mM	83	3%	1.23	0
Nicotinic Acid (NA) 20mM	83	3%	2.46	0
Nicotinamide (Nam) 10mM	83	3%	0	1.22
Nicotinamide (Nam) 20mM	83	3%	0	2.44

Figure 3.1 Experimental design for nutrient supplementation

(a) Schematic of the experimental set up used to supplement different concentrations of NAD+ precursors. Flies were allowed to lay eggs on apple juice plates + yeast paste at RT for 22 hours. These eggs were discarded and fresh plates were used to collect age matched eggs for 20 hours. These eggs were harvest and divided onto standard cornmeal molasses medium supplemented with varying concentrations of NAD+ precursors, nicotinic acid and nicotinamide. After eclosion flies were allowed to reach sexual maturity and then transferred to fresh medium before being subjected to experimental assays. (b) Chart listing the concentrations of key components in the food. Note that 3% yeast was used as the standard concentration.

Figure 3.2 Nicotinamide and nicotinic acid increase proteasome activity and dmPI31
(a) Average luminescence produced by cleavage of peptide recognized by chymotrypsin-like activity of the proteasome. Values were normalized to the control in each experiment and MG132, a proteasome inhibitor was used as a control for proteasome specific activity. Na 10mM, Na 30mM, and Nam 30mM increase proteasome activity compared to the control, n=7. (b) Western analysis on wildtype lysates from adult flies subject to NAD+ supplemented diets. Quantification of DmPI31 normalized to tubulin shows an increase in PI31 with Nam 10mM, Nam 30mM and Na 10mM supplementation. Na 30mM did not show a significant increase in DmPI31 (c) Western blots from wild type male whole body lysates of flies show an increase in DmPI31 levels after supplementation of Na 10mM for 6 days PE compared to control. To address the effect of Na on DmPI31 levels more clearly a dilution series was conducted with transgenic lines expressing PI31 under the UAS promoter driven by GMR-Gal4 in the eye. Head lysates were taken and show that DmPI31 levels increase in a dose dependent manner until Na 20mM at then increase again at Na 40mM. Supplementation of NAD+ alone did not increase proteasome activity when added directly to lysates and does not show increases in PI31 protein level. (d) Transgenic flies expressing a truncated Notch ligand, Nintra-GFP, crossed to flies expressing mutant proteasome subunit, DTS7, under GMR-Gal4 promoter. 3rd instar larvae fed control or 30mM Nam were heat shocked for 30min at 37°C and allow to recover for 1 hour. Control fed larva show accumulation of GFP in eye discs but Nam fed flies show rapid degradation of GFP. e) Proteasome activity did not increase between control and Na 10mM fed fly lysates from a PI31 RNAi or PI31DHbYX background. On the other hand, control lines fed 10mM Na and overexpression of full-length PI31 increased proteasome activity by about 40% compared to control. Statistical analysis was carried out using a two-tailed, paired, t test (Compared to Tubulin, MG132: 20.42 +/- 6.15 RLU, ***p=3.03x10^{-5}; Na 10mM: 142.12 +/- 11.85 RLU, *p=0.012; UAS-PI31: 133.37 +/- 10.48 RLU, *p=0.027; RNAi PI31 108.67 +/- 6.34 RLU, p=0.281; RNAi PI31 + Na 10mM: 122.11 +/- 24.693 RLU, p=0.422; PI31DHbyX: 119.967 +/- 12.281 RLU, p= 0.208; PI31DHbYX + Na 10mM : 130.739 +/- 9.033 RLU, *p=0.017).

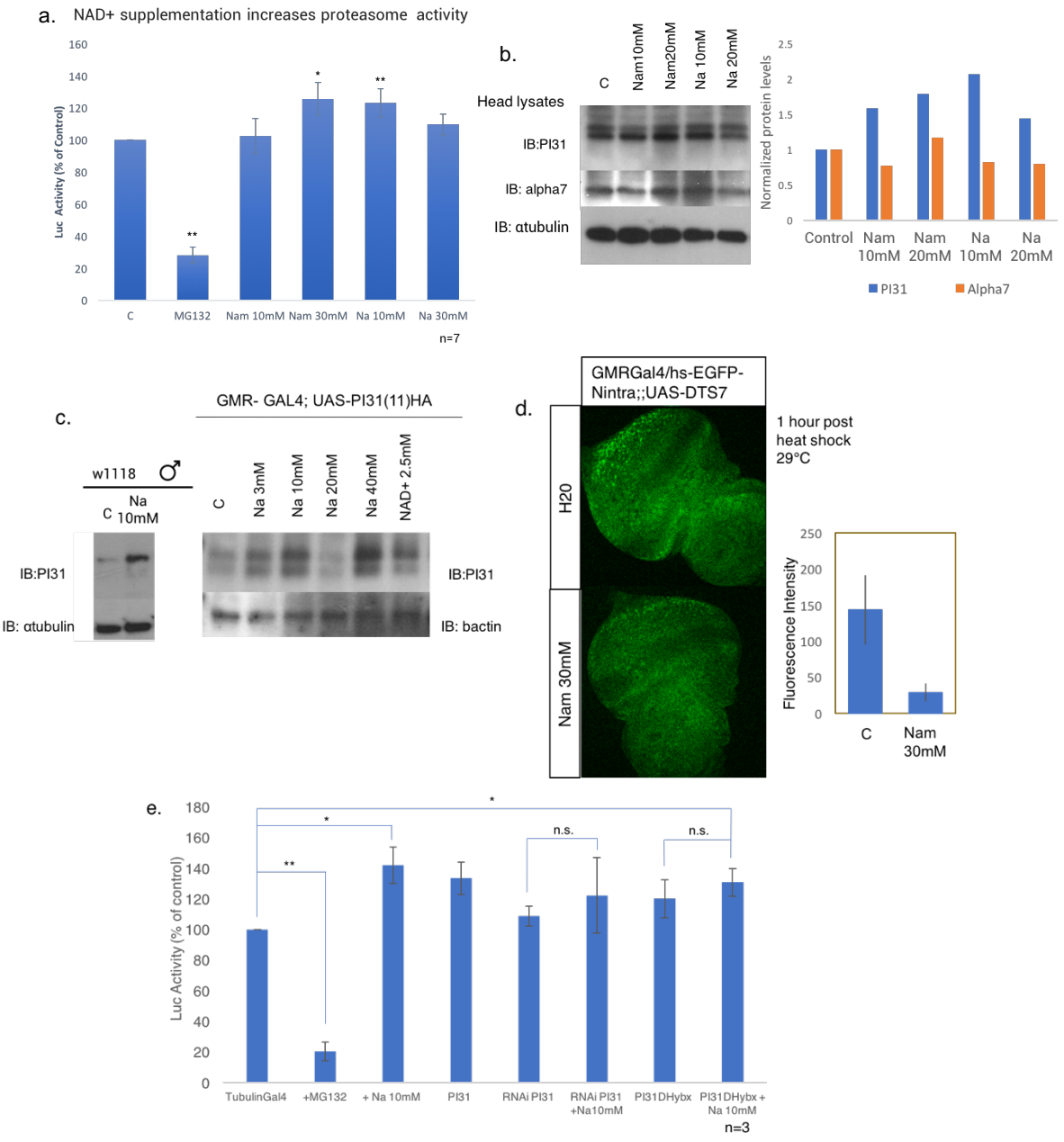
a.
NAD+ supplementation increases proteasome activity
Luc Activity (% of Control)
C
MG132
Nam 10mM
Nam 30mM
Na 10mM
Na 30mM
n=7
b.
C
Nam10mM
Nam20mM
Na 10mM
Na 20mM
Head lysates
IB:PI31
IB: alpha7
IB: αtubulin
Normalized protein levels
Control
Nam 10mM
Nam 20mM
Na 10mM
Na 20mM
PI31
Alpha7
c.
GMR- GAL4; UAS-PI31(11)HA
w1118 ♂
C
Na 10mM
C
Na 3mM
Na 10mM
Na 20mM
Na 40mM
NAD+ 2.5mM
IB:PI31
IB: αtubulin
IB:PI31
IB: bactin
d.
GMRGal4/hs-EGFP-Nintra;;UAS-DTS7
H20
Nam 30mM
1 hour post heat shock 29°C
Fluorescence Intensity
C
Nam 30mM
e.
Luc Activity (% of control)
TubulinGal4
+MG132
+ Na 10mM
PI31
RNAi PI31
RNAi PI31 +Na10mM
PI31DHybx
PI31DHybx + Na 10mM
n.s.
n.s.
n=3

3.3.2 Proteasome activity and DmPI31 levels increase with dietary restriction

Dietary restriction is thus far the only non-genetic application that has been reported to extend lifespan across several species. Dietary restriction (DR) is shown to ameliorate age-related proteasome decline in some tissues (Dasuri et al., 2009; Li et al., 2008; Zhang et al., 2007c) as well as increase NAD+ levels (Banerjee et al., 2012)(Lin et al., 2000). However, the mechanism by which proteasome activity is altered under DR is yet to be determined. Since, DR increases NAD+, I first sought to determine whether DR can also induce an increase in dmPI31 levels. In this case, DR is defined as yeast restriction from 3% to 0.25% while the composition of molasses is unchanged. *Drosophila* whole body male or head lysates expressing mcherry-dmPI31 under the PI31 endogenous promoter were fed control or DR food as embryos and resolved on SDS-page gel and immunoblotted for dmPI31. Head lysates showed a modest increase in dmPI31 expression while whole body lysates showed no change when normalized to controls (Figure 3.3d). Interestingly, the increase in dmPI31 is associated with a reduced expression of α7 which also occurs in whole body DR fed flies (Figure 3.3d). It is noteworthy to add that DR restricted flies are comparably smaller than their control fed counterparts. This may point to developmental transcriptional changes that occur during DR that alter the expression of core proteasome subunits. Head lysates do not distinguish between dmPI31 in the brain, eye, or muscle cells. To differentiate between the tissues in the head, larva brains expressing mCherry-dmPI31 under the PI31 endogenous promoter were fed on control or DR food. Confocal z-stack projections show increased mCherry-dmPI31 under DR than under control fed lines. The localization of PI31 does not appear altered and still co-localizes with cells expressing deadpan (Dpn), the neuroblast marker (Figure 3.3a-c). Wild-type fly lysates subject to DR food were assayed for proteasome activity using the in vitro assay and showed increased proteasome

activity in both head and whole-body fractions however only the whole-body lysates showed a significant increase in activity (compared to Control whole body: 4202.61 +/- 44.12 RLU, MG132:4202.61+/- 44.12 RLU, **p=0.007; DR whole body: 5032.53 +/- 48.54 RLU, **p=0.002; Control heads: 2294.74 +/- 152.23 RLU; DR heads: 2505.34 +/- 52.95 RLU, p=0.21) (Figure 3.3e). Given, this result it may be that the ratio between α7 and dmPI31 is important for increased proteasome activity during DR or that the short term effected of DR is more pronounced in tissues outside the head, like muscle or intestine. These results show that proteasome activity is regulated under DR and the dmPI31 pathway may participate to regulate proteasomes under these conditions in the brain.

Figure 3.3 DR increases dmPI31 expression and proteasome activity

Confocal z-projections of larval brains showing an increase in PI31::mcherry-PI31 upon dietary restriction by means of yeast restriction. (a) Control 3rd instar larval brains showing mcherry background fluorescence (red) and counter stained with anti-Dpn (green) to mark neuroblasts within the CB, OLs. The merged image shows DAPI staining of all nuclei. (b) Control fed 3rd instar larval brains expressing mcherry-PI31 under the PI31 endogenous promoter. Z-projections show PI31 expression in the CB and VNC that co-expresses with anti-Dpn (green) staining. (c) 3rd instar larva fed on a DR diet show increased mcherry-PI31 expression compared to control fed larva with anti-Dpn (green) again staining neuroblasts. (d) Western blot analysis from adult fed flies shows DmPI31 protein levels increase upon rearing on DR food compared to control in head lysates but not in whole body. The 20S proteasome subunit, alpha7, show decreased expression on DR diet compared to control in both head and wholebody lysates. (e) Lysates from adult flies on DR diets showed an increase in proteasome activity. Total protein from either whole body males or heads only were extracted and proteasome activity was measured using the fluorogenic-peptide hydrolysis at 10min. Values were normalized to amount of tubulin determined by western analysis and plotted as relative luminescence unites (RLU). MG132 was used as a control for specificity of proteasome activity. Error bars are the result of 3 intendent assays. Statistical analysis was carried out using a two-tailed, paired, t test, (compared to Control whole body: 4202.61 +/- 44.12 RLU, MG132:4202.61+/- 44.12 RLU, **p=0.007; DR whole body: 5032.53 +/- 48.54 RLU, **p=0.002; Control heads: 2294.74 +/- 152.23 RLU; DR heads: 2505.34 +/- 52.95 RLU, p=0.21).

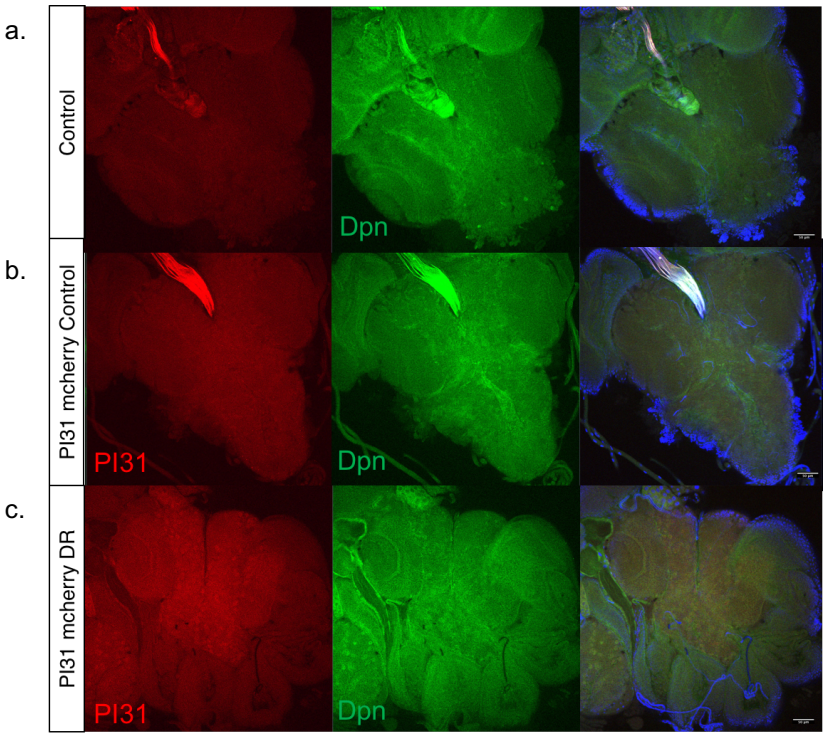
a.
Control
Dpn
b.
PI31 mcherry Control
PI31
Dpn
c.
PI31 mcherry DR
PI31
Dpn

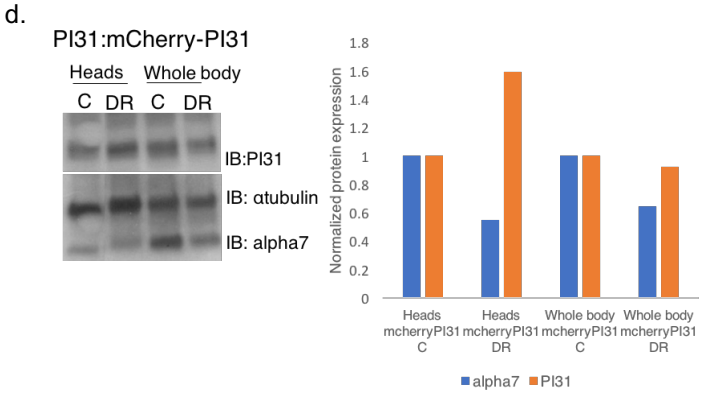
d.
PI31:mCherry-PI31
Heads
Whole body
C DR C DR
IB:PI31
IB: αtubulin
IB: alpha7
Normalized protein expression
1.8
1.6
1.4
1.2
1
0.8
0.6
0.4
0.2
0
Heads mcherryPI31 C
Heads mcherryPI31 DR
Whole body mcherryPI31 C
Whole body mcherryPI31 DR
alpha7
PI31

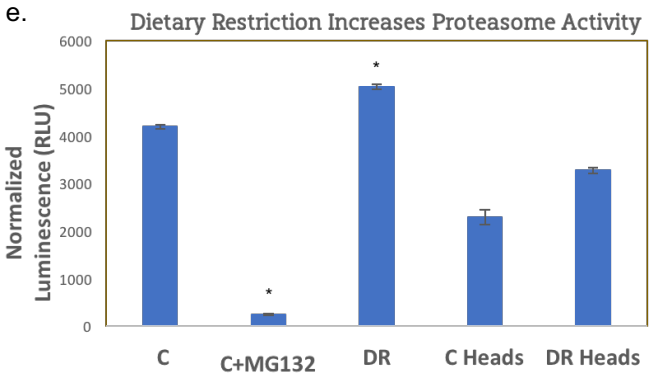
e.
Dietary Restriction Increases Proteasome Activity
Normalized Luminescence (RLU)
6000
5000
4000
3000
2000
1000
0
*
*
C
C+MG132
DR
C Heads
DR Heads

3.3.3 NAD+ repletion increases proteasome assembly

Given that proteasome activity is shown to increase under Na, Nam, and DR conditions and the limitation of the *in vitro* assay to distinguish between 20S and 26S activity, I examined whether subsequent changes in proteasome assembly are a contributing factor. Proteasome complexes from wildtype flies that were fed either Nam or Na, were separated in their native conformation using gel electrophoresis and blotted for the proteasome subunit, α7 which incorporates into 20S and 26S proteasomes. Total protein concentration was measured using the BCA assay, normalized, and equal amounts of protein were loaded for each condition. To determine whether Na and Nam supplementation could increase proteasome activity specifically in the brain, head lysates were collected from wildtype fed flies and subjected to native analysis. Blotting the membrane after transfer with the 20S subunit α7 showed that feeding with Nam or Na increased overall 26S assembly but Nam at 20mM and Na at 10mM showed the greatest increase in 26S proteasome assembly compared to controls (Figure 3.4a). As an internal control, 26S proteasome complexes were normalized to the amount of 20S and in this case Na 10mM showed the greatest increase in 26S/20S ratio. This condition however also resulted in a loss of 20S amounts which may be due to toxicity (Figure 3.4a'). Considering that NAD+ is also a major redox substrate, Na may initially cause an imbalance in the NADH/NAD+ ratio tipping the scales toward oxidative stress, which has been shown to cause proteasome disassembly (Livnat-Levanon et al., 2014). To test whether these proteasomes have increased catalytic activity, I performed an in-gel proteasome peptidase assay where cleavage of suc-LLVY-AMC results in fluorescence that can resolve the activity contributed to different proteasome species. I show that feeding with 20mM Nam and 10mM Na increases 26S activity consistent with increased assembly (Figure 3.4a). 20S proteasome activity in-gel can also be assayed with the addition of

0.02% SDS, which opens the "gate" of the core particle to allow entry of substrates. Nam 20 and Na 10 again show the greatest increase in 20S activity compared to control (Figure 3.4a).

One possible mechanism by which Nam and Na supplementation increases proteasome activity is through TNKS mediated ADP-ribosylation of PI31. Increasing NAD+ increases substrate availability for TNKS, which may lead to increased ADP-ribosylation of PI31 and an increase in proteasome assembly. Since, *dmPI31* mutants live to the larval stage, I tested whether feeding mutant larval could increase proteasome assembly. Interestingly, dmPI31 mutants show less double capped 26S proteasomes and also show a smaller intermediary form that still maintains catalytic activity (Figure 3.4b) but feeding does not change the levels of 26S proteasome complexes. 20S proteasome amounts are also not significantly different between control and Nam fed lines (Figure 3.4b') but the 20S proteasomes under control fed larval show reduced 20S activity but upon feeding 20S activity is restored. This could point to dmPI31 having a role in maintaining 20S proteasome stability and upon feeding NAD+ precursors could confer enhanced stability. It is reported that NADH, the reduced form of NAD+, can stabilize proteasomes independent of ATP (Tsvetkov et al., 2014) thus supplementation with precursors could also lead to enhanced stability. Consistent with other results in this study, Na fed *PI31* mutant larva have decrease proteasome amounts and activity suggesting this condition may be toxic (Figure 3.4b). Thus, the increase in proteasome assembly seen with NAD+ supplementation is dependent on the presence of dmPI31 and could be through a mechanism that enhances proteasome stability.

Figure 3.4 26S proteasome assembly increases upon NAD+ repletion

(a) Proteasome complexes from head lysates from male and female flies fed NAD+ precursors for 10 days PE were resolve in their native assemblies. Blotting for anti-alpha7, a 20S proteasome subunit, labels the 20S CP as well as single capped (RPCP) and double capped (RP2CP) proteasomes. Upon feeding with NAD+ precursors, 26S proteasome assembly is increased compared to control. (a') Nam 20mM and Na 10mM showed the greatest increase in 26S assembly compared to controls while Na 10mM and Na 20mM show the greatest increase in 26S/20S ratio. (a) Using a fluorogenic peptide (LLVY-AMC), the activity of resolved proteasomes can be assayed in-gel and activities resulting from single capped versus double capped proteasomes determined. 26S proteasomes are more active compared to control in head lysates from flies that were fed on Nam 20mM and Na 10mM consistent with these concentrations increasing 26S assembly. 20S proteasome activity in-gel can also be assayed with the addition of 0.02% SDS, which opens the "gate" of the core particle to allow entry of substrates. Nam 20mM and Na 10mM again show the greatest increase in 20S activity compared to control. (b) *DmPI31* null mutant larva were lysed and proteins resolved in their native conformation to assay proteasome complexes after feeding on NAD+ precursors. *DmPI31* mutants show less double capped 26S proteasomes and also show a smaller intermediary form that still maintains catalytic activity. (b') 26S proteasome amounts do not change significantly between control and Nam fed lines. (b) In-gel activity assays show 26S proteasome activity does not increase upon feeding but Na 10mM shows reduced activity. 20S proteasomes under control fed larval lack 20S activity but upon feeding 20S activity is restored, this could be due to insufficient gate opening.

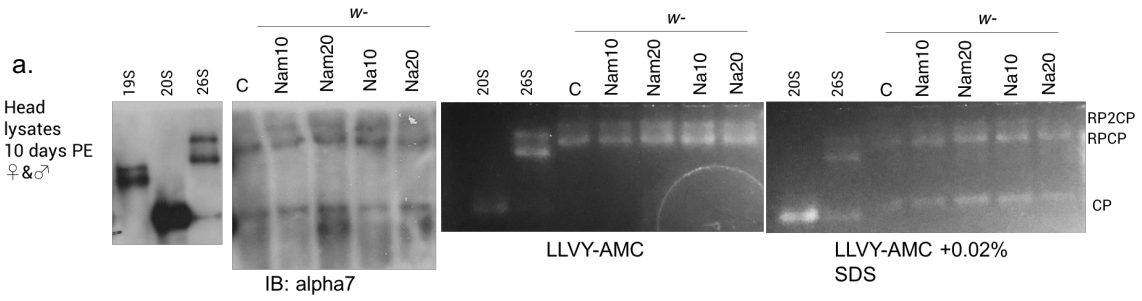

a'.

Proteasome assembly

	20S %	26S %	26S/20S %
C	100.00	100.00	100.00
Nam 10	108.49	197.99	182.49
Nam 20	157.35	235.10	149.41
Na 10	73.35	284.01	387.20
Na 20	102.13	224.44	219.75

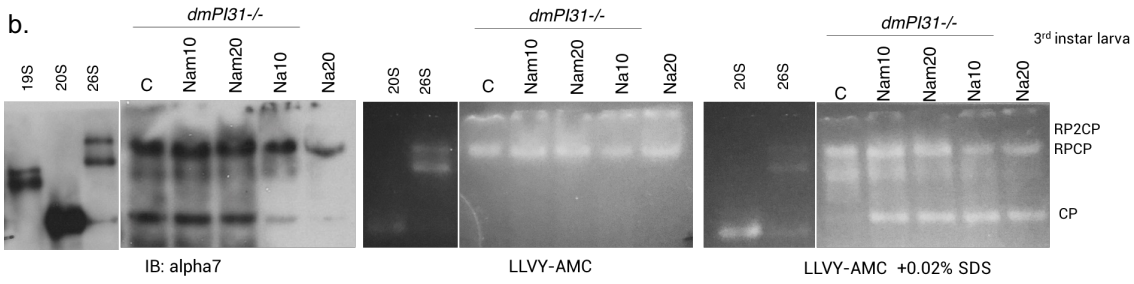

b'.

Proteasome assembly

	20S %	26S %	26S/20S %
C	100.00	100.00	100.00
Nam10	94.56	104.43	110.44
Nam20	79.59	107.39	134.92
Na 10	27.07	106.39	393.05
Na 20	6.02	37.83	628.29

3.3.4 Mutations in Nmnat, an essential NAD+ synthase, cause defects in proteasome activity

To validate that NAD+ levels play a role in regulating DmPI31 levels, I genetically targeted the NAD+ salvage pathway using mutants for *Nmnat*, an essential enzyme that catalyzes the final step in NAD+ synthesis (Figure 1.3). *Nmnat* mutants are lethal before the 1st instar larval stage so mitotic clones were generated in the eye using an eye specific flippase. These clones reveal a marked decrease in DmPI31 levels in both 3rd instar larvae and adult stages, with photoreceptor axons beginning to degenerate in adults (Figure 3.5a-b). Published reports have indicated that *Nmnat* mutant photoreceptor clones do not display any developmental defects. Instead, aged and light stimulated retina show progressive degeneration that can be significantly suppressed in flies that are dark reared (Zhai et al., 2006). Thus, loss of dmPI31 likely proceeds axon degeneration and is a possible mechanism by which protein load exceeds protein degradation and leads to degeneration. Upon overexpression of Nmnat in the *Nmnat* mutant background, dmPI31 expression levels are rescued (Figure 3.5c) indicating Nmnat levels are important for dmPI31 expression. To test whether loss of Nmnat results in defective proteasome activity, I again subject fly lysates to the *in vitro* proteasome activity assay. Using the Tubulin-Gal4, Tubulin-Gal80 temperature sensitive driver various transgenes were driven in the whole body of flies at 25°C. RNAi mediated knockdown of PI31, TNKS, and Nmnat decreased proteasome activity but neither PI31 nor Nmnat overexpression increased proteasome activity compared to control at this temperature. The proteasome inhibitor MG132 was used to control for proteasome specific activity (Figure 3.6a). These results suggest that loss of Nmnat results in decrease proteasome activity which may be due to loss of dmPI31 expression. To test this result, flies co-expressing UAS-PI31 and UAS-RNAi-Nmnat in *Drosophila* eye under the GMR-Gal4 driver were dissected and stained for levels of HA-PI31. Consistent with the *Nmnat* mutant clone results, loss of Nmnat leads to decreased dmPI31 expression while photoreceptor axons remain intact (Figure

3.6b). To determine whether Nmnat alone is sufficient to increase proteasome activity, I tested whether Nmnat overexpression could rescue proteasome impairment caused by mutant proteasome subunits DTS5 and DTS7. At high temperatures, these mutants are dominant and inhibit proteasome activity leading to a rough eye phenotype (Figure 3.7a), which can be rescued by overexpression of dmPI31 (Figure 3.7b). Overexpression of Nmnat suppresses the decreased size of the eye caused by DTS5/DTS7 but the external eye morphology remains rough (Figure 3.7c). In addition, feeding 30mM Na is not sufficient to alter the external rough eye phenotype (Figure 3.7f). Neither RNAi nor enzymatically inactive Nmnat suppressed the phenotype (Figure 3.7d,e) suggesting either that NAD+ levels are not sufficiently enhanced or that DTS5/DTS7 mutant proteasomes do not require ADP-riboslyated PI31. Indeed, overexpression of PI31ΔHbYX in this mutant background rescues the DTS5 phenotype (not shown), suggesting that TNKS-mediated ADP-ribosylation is not needed or that TNKS can bind PI31 *in vivo* independent of the HbYX motif.

To determine whether the loss of PI31 seen with loss of Nmnat is due to a physical interaction, I cloned FLAG-tagged NmnatC and HA tagged-dmPI31 and transfected them in human 293 cells. Total lysate when blotted for either HA or FLAG showed successful expression of these plasmids (Figure 3.8). However, upon IP with HA to pull down PI31 no FLAG antibody was detected in the pull down (Figure 3.8) indicating that PI31 and NmnatC do not interact under these conditions. However, there are two other major isoforms of Nmnat that should also be tested that differ in the splicing of the last 3 exons and have been shown to localize to distinct cellular compartments. Isoform PD, which is cytoplasmic is shown to have refolding chaperone-like properties and suppress the neurodegeneration caused by polyglutamine expanded ataxin-1 (Ruan et al., 2015). Since, no physical interaction was observed I tested whether loss of NAD+ is contributing to loss of dmPI31 in the *Nmnat* mutant clones. By feeding flies with *Nmnat* photoreceptor clones either 20mM or 40mM nicotinamide, I observe an increase in mean HA-PI31 expression in mutant clones (Figure 3.9a).

Several clonal patches were tested for each condition and this increase is shown to be significant and dose dependent (Wild-type control fed: 31.32 +/- 2.61 RFU; *Nmnat* clone control fed: 16.08 +/- 0.92 RFU, ***p=8.6x10^{-5}; *Nmnat* clone Nam 20: 19.07 +/- 1.01, *p=0.04; *Nmnat* clone Nam 40: 20.57 +/- 1.21 RFU, **p=0.007) (Figure 3.9b). Since, *Nmnat* mutants still produce a truncated form of the protein that has the NMN binding domain in the N-terminus intact it is possible that residual activity is still present. However, a functional null allele with the first 4 exons deleted was also tested and still caused the loss of dmPI31 expression (not shown). Whether DmPI31 expression can be rescued with NAD+ supplementation in these clones has not yet been tested. This future experiment could determine whether the loss of DmPI31 is dependent on NAD+ synthesis, shared intermediate binding to Nmnat, or a general stress response by affected neurons.

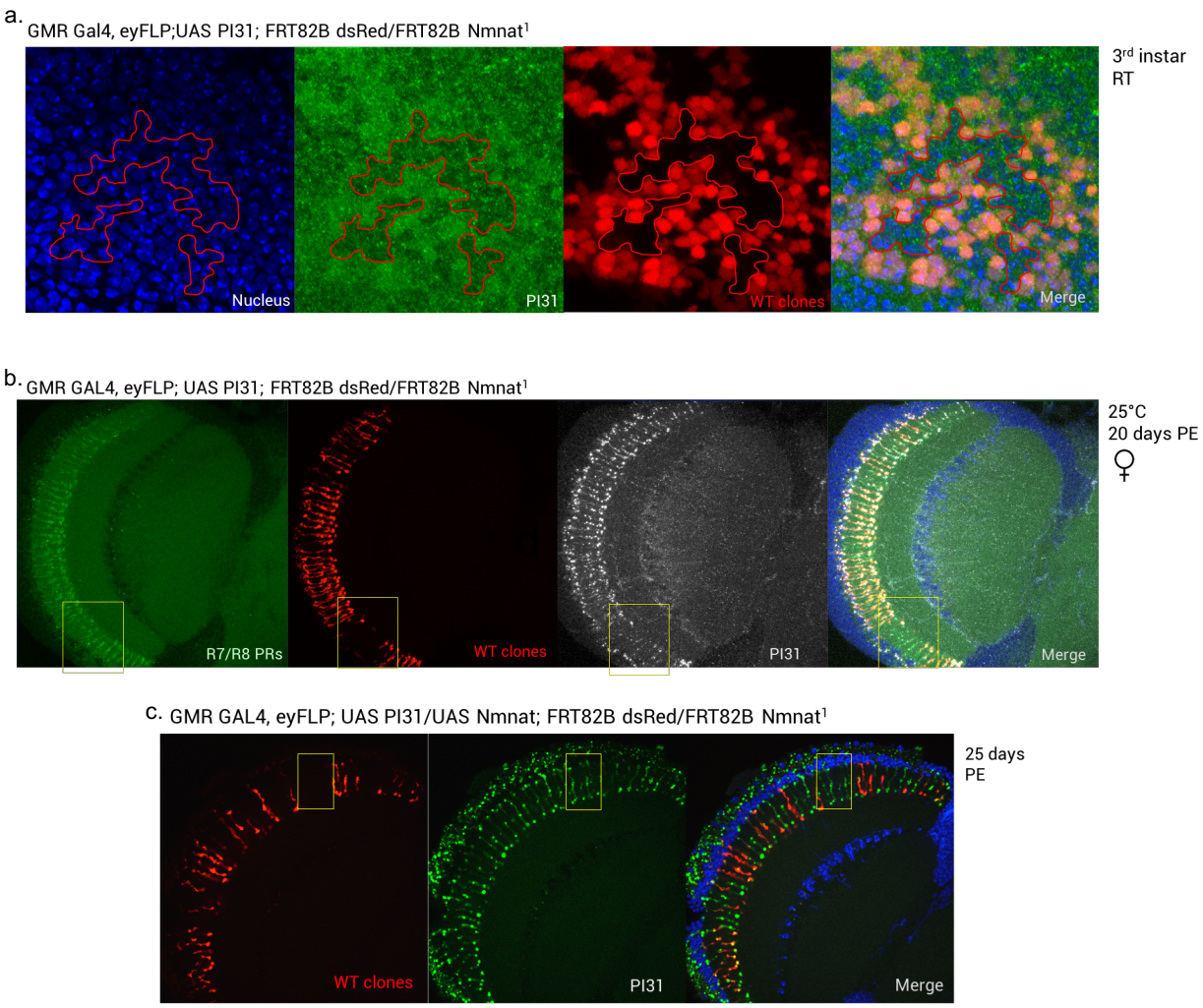

Figure 3.5 Nmnat mutants display less dmPI31 in photoreceptor cells

Mosaic clones of mutant *Nmnat*^{1} were generated in the *Drosophila* larval eye discs and adult photoreceptor axons by driving eye specific flippase. (a) HA tagged PI31 was driven in 3rd instar larva eye discs under the GMR-Gal4 driver. Nmnat mutant clones, outlined in red, show less HA-PI31 expression although Nmnat clones do not show any developmental defects. (b) Adult optic lobes with *Nmnat*^{1} mutant clones boxed in yellow. These clones display signs of axon degeneration at 20 days PE accompanied by less HA-PI31 expression (white). Staining with anti-chaoptin (green) marks all R7/R8 photoreceptor axons while dsRed marks only wild-type clones. (c) Optic lobes with mosaic clones of mutant *Nmnat*^{1} in 25 day old flies generated using eyeless-flippase. HA-PI31 expression can be rescued in *Nmnat*^{1} mutant clones, boxed in yellow, by overexpression of Nmnat driven by GMR-Gal4.

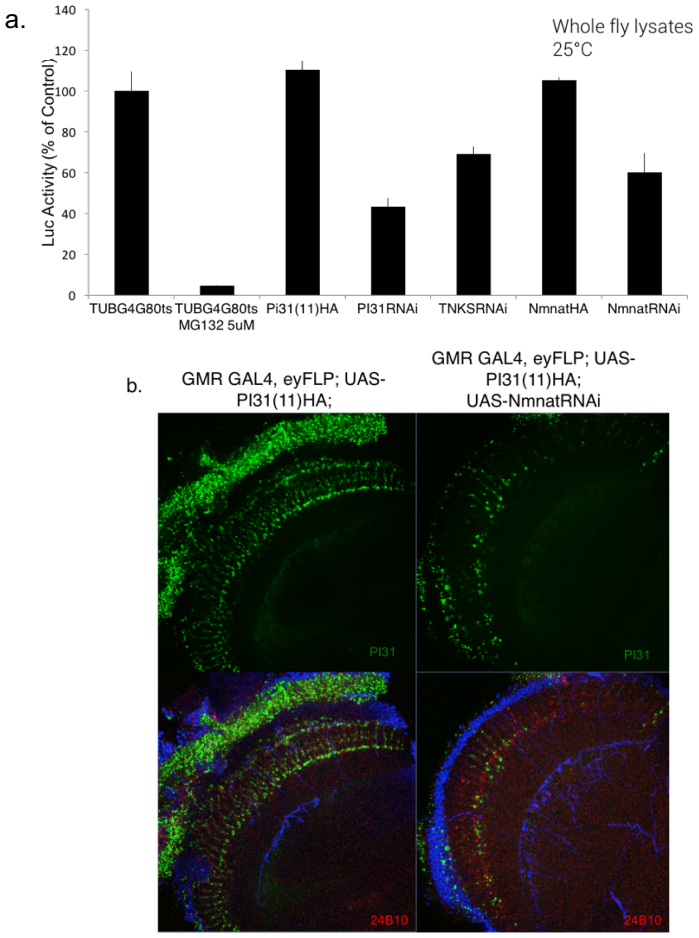

Figure 3.6 Knockdown of Nmnat leads to defects in proteasome activity

(a) *In vitro* proteasome activity assay on whole fly lysates from lines expressing indicated transgenes under Tubulin-Gal4, Tubulin-Gal80 temperature sensitive driver at 25°C. RNAi mediated knockdown of PI31, TNKS, and Nmnat decreased proteasome activity. Neither PI31 nor Nmnat overexpression increased proteasome activity compared to control. The proteasome inhibitor MG132 was used to control for proteasome specific activity. (b) Confocal images of optic lobe z-projections from flies UAS- PI31 lines and lines co-expressing UAS-PI31 and UAS-RNAi-Nmnat under the GMR-Gal4 driver. DmPI31 expression is decreased in Nmnat knockdown background while photoreceptor axons remain intact as indicated by anti-24B10 (red) staining.

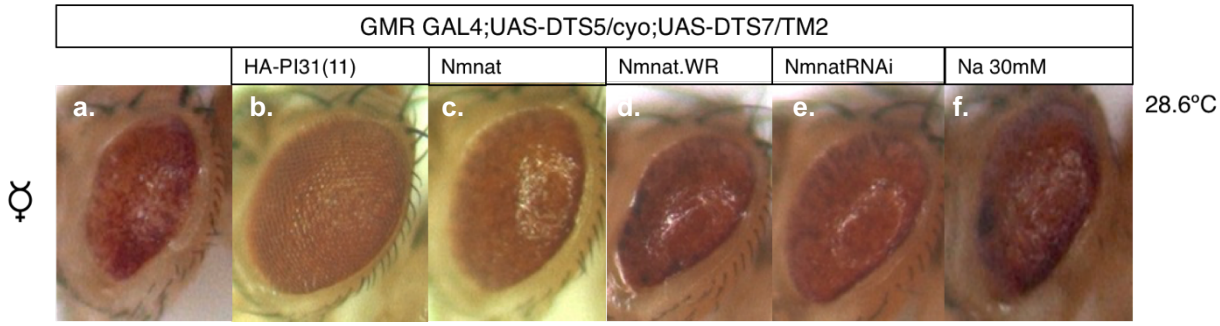

Figure 3.7 Nmnat is sufficient to suppress eye phenotypes caused by mutant proteasomes
(a) Eye phenotypes from female flies expressing the temperature sensitive DTS5 and DTS7 mutations in the proteasome under the GMR-Gal4 driver at 28.6°C. (a) These mutations are dominant and inhibit proteasome activity leading to a rough eye phenotype. (b) Overexpression of dmPI31 in this background rescues this eye phenotype. (c) Overexpression of Nmnat in this background suppresses the eye phenotypes and the size of the eye increases but the morphology remains rough. (d) Enzymatically inactive Nmnat.WR and (e) RNAi for Nmnat do not show significant difference in eye morphology compared to DTS5/DTS7 background. (f) Feeding DTS5/DTS7 flies throughout development on Na 30mM is not sufficient to alter the external rough eye phenotype.

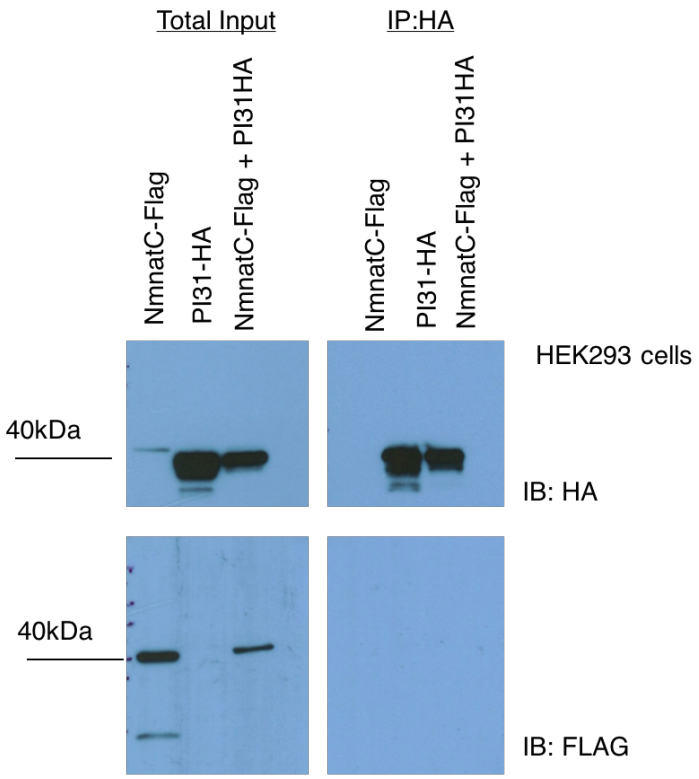

Figure 3.8 DmPI31 does not show a physical interaction with NmnatC

Human 293 cells were transfected with either FLAG-tagged NmnatC isoform, HA tagged-dmPI31, or co-transfected. Total lysate input blotted for HA shows expression of HA-PI31 in cells transfected with HA-PI31 alone or co-transfected with NmnatC. Blotting against anti-Flag shows expression after transfection of Nmnat in total lysates. Using HA magnetic beads, HA-PI31 was pulled down however, no Flag tagged protein was detected to co-IP with HA-PI31, suggesting PI31 does not physically interact with NmnatC. However, PI31 is known to be cleaved at its C-terminus and NmnatC may be protecting PI31 from this cleavage.

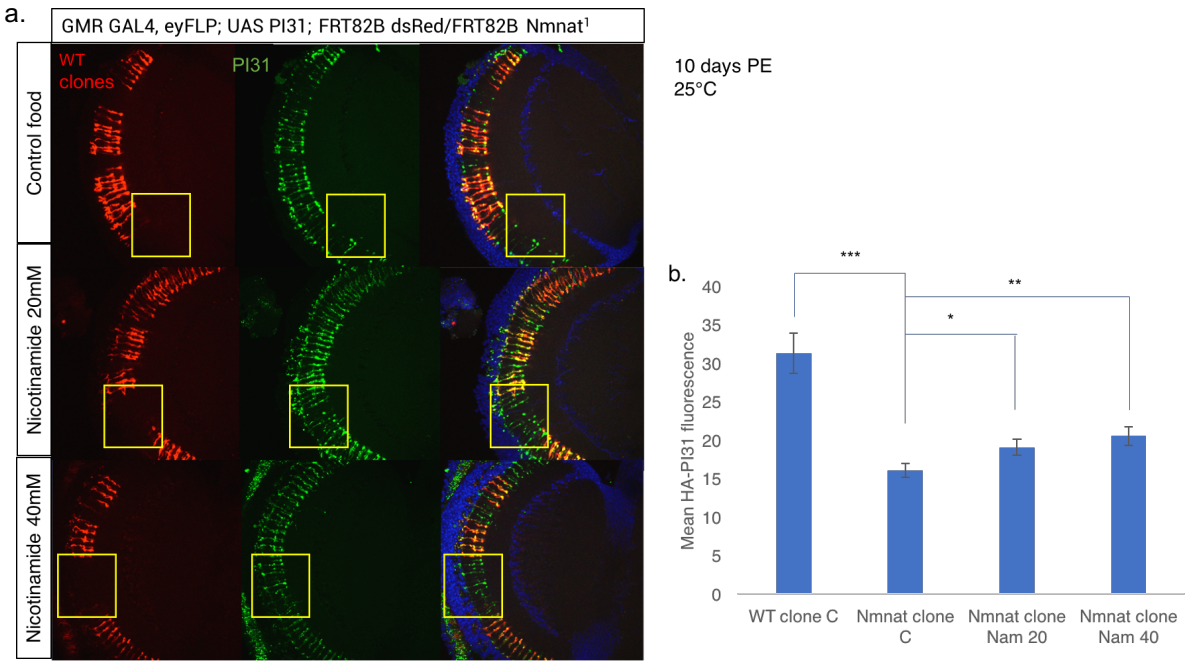

Figure 3.9 Nam partially rescues dmPI31 expression in photoreceptor axons

(a) Mosaic clones of mutant *Nmnat*^{1} were generated in the *Drosophila* adult photoreceptor axons by driving eye specific flippase. These flies were put on 20mM or 40mM Nam supplemented instant food at 1 day PE and flipped once to new food before dissection at 10 days PE. Nmnat mutant clones show less HA-PI31 expression that can be significantly increased upon feeding with increasing amounts of Nam. (b) Quantification of HA-PI31 fluorescent signal in wild type versus Nmnat mutant clones fed on control or Nam supplemented diets. A significant increase in seen upon supplementation of both Nam 20mM and Nam 40mM. (Wild-type control fed: 31.32 +/- 2.61 RFU; *Nmnat* clone control fed: 16.08 +/- 0.92 RFU, ***p=8.6x10^{-5}; *Nmnat* clone Nam 20: 19.07 +/- 1.01, *p=0.04; *Nmnat* clone Nam 40: 20.57 +/- 1.21 RFU, **p=0.007)

3.4 Discussion

Both NAD+ levels and proteasome assembly have been shown to decline with age ((Tonoki et al., 2009; Gomes et al., 2013). This connection suggests a hypothesis whereby loss of NAD+ during aging can decrease proteasome activity and lead to the accumulation of abnormal proteins seen in aging and age-related disorders. It's intriguing to think of proteasomes in direct communication with the metabolic status of the cell via NAD+ dependent ADP-ribosylation of dmPI31. In a means to test this hypothesis, I have found that NAD+ precursors can increase proteasome activity, dmPI31 protein levels, and proteasome assembly. The activity of the proteasome under NAD+ supplementation is dependent on expression of full length PI31 as knockdown of PI31 or overexpression of PI31ΔHbYX does not cause significant changes between fed states. However, attempts to pull down the ADP-ribosylated form of dmPI31 in adult flies were not successful. This could be due to technical difficulties but more intriguingly may mean that this modification is only abundant during specific developmental time points and possibly localized to distinct subcellular locations in discreet amounts ie possibly at the synapse. In this way, ADP-ribosylation of DmPI31 could serve as a metabolic switch to regulate proteasome activity in different cellular compartments based on the local NAD+ pools available. In fact, NAD+ in not able to move between compartments (van Roermund et al., 1995) and different NAD+ pools have been shown to behave independently of one another to maintain cellular homeostasis after stress (Yang et al., 2007). However, until recently tools to study the subcellular distribution of distinct NAD+ pools were lacking or relied on NAD+ consumption by PARP1 as a read out (Dölle et al., 2009; Hung et al., 2011; Cambronne et al., 2016; VanLinden et al., 2017). These tools can now be adapted to Drosophila and used alongside existing tools to measure proteasome activity *in vivo* to determine the affect of subcellular NAD+ pools on

proteasome activity.

The finding that dietary restriction (DR) is also able to increase proteasome activity *in vitro* and increase DmPI31 expression in the larval brain is in line with DR increasing NAD+ levels. I find that proteasome activity is not significantly altered in the brain compared to whole body. Similarly, other studies have found that 26S proteasome activity is lower in the brain than liver, brain proteasomes display less plasticity, and DR preserves 26S proteasome activity (Dasuri et al., 2009). This is intriguing since DR is the only non-genetic way to extend lifespan across several species. These results point to a quality control mechanism that is preserved with age during increased states of NAD+ to maintain proteostasis. Our findings that the essential neuronal maintenance factor, Nmnat, regulates DmPI31 protein levels *in vivo*, does not interact with dmPI31, and does not itself significantly impact proteasome function point to a signaling pathway or intermediate binding partner. Indeed, evidence points to a signaling event mediated by NAD+ as NAD+ supplementation can increase DmPI31 levels in an *Nmnat* mutant background. The recovery of DmPI31 could also be due to increased health of the axons provided by NAD+ in a pathway different than that of Nmnat.

NAD+ in addition to being a substrate for NAD+ consuming enzymes also plays a major role in redox reactions involved in cellular respiration. Although I find that NAD+ increases proteasome activity, DmPI31, and proteasome assembly, I cannot rule out the possibility that these effects are mediated through the generation of more ATP. 26S proteasome mediated degradation is an ATP dependent process requiring ATP during ubiquitination of substrates, substrate unfolding, substrate hydrolysis, and 26S assembly (Majetschak, 2013). However, the reduced form of NAD+, NADH has been shown to bind directly to 26S proteasomes via a putative NADH binding motif (G*x*G*xx*G) and maintain their stability independent of ATP. It is

also possible that feeding NAD+ precursors increases NADH in the cell and contributes to increased proteasome assembly by maintaining 26S proteasome integrity (Tsvetkov et al., 2014). The sum of these findings indicate that 26S proteasomes are metabolically regulated and that contexts where NAD+ levels are compromised could lead to insufficient proteasome activity that manifests in various phenotypes such as aging and neurodegeneration.

3.5 Materials and Methods

Fly stocks and recipes for nutrient supplementation

Oregon-R and *w1118* flies were used as controls. Hs-N^{intra}EGFP, DTS5, and DTS7 were given as kind gifts by John Belote. All Nmnat stocks were generated by Hugo Bellen's lab and deposited in Bloomington with stock numbers Nmnat.WR (39700), Nmnat (39699), NmnatRNAi (29402). Fly food was generated by adding 36g Baker's dried active yeast, 87.5 g corn meal, and 10g agar to 1.2L distilled H_20. Mixture was boiled for 10min to allow agar to dissolve and then 83ml of molasses was added and mixture was allowed to boil for 10 additional minutes with continuous stirring. While stirring food was cooled to 65°C and 8.3mL 30% Tegosept and 0.89mL propionic acid were added along with indicated concentration of Na or Nam. Food was aliquoted into empty fly vials and allowed to solidify and cool to room temperature before flies were distributed onto food. Extra food was stored at 4°C until needed and brought to room temperature prior to addition of flies. All lines were grown at 25°C in a 12hr light/dark cycle incubator.

In vitro proteasome activity assay

Heads or whole-body tissue samples from indicated genotypes were prepared in PIPES lysis buffer (50mM PIPES, 1mM $MgCl_2$, 50mM $NaCl_2$, 2mM EGTA, and 2mM fresh ATP) by

homogenizing tissue using pellet pestle motor and spinning samples in table top centrifuge for 20min at 4°C. Supernatant was taken and protein concentration measured with BCA assay (Pierce BCA Protein Assay Kit- Thermo Scientific). 50-75ug of protein was mixed at a 1:1 ratio with the Proteasome-Glo chymotrypsin reagent (Promega G8621) according to manufacture details. MG132 (UBPBio, F1101), a proteasome inhibitor, was incubated with control samples as a readout for proteasome specific signal. Reactions were done in triplicate in a 96 well plate and read on Spectramax M-2 microplate reader. Statistical analysis was done by averaging experimental replicates, normalizing to controls, and taking activity as a percentage of control over several assays. Error bars represent 7 separate experiments all normalized to their respective controls.

***In vivo* proteasome activity assay and immunostaining**

To assess the *in vivo* activity of the proteasome, degradation of EGFP-N^{intra} was monitored in the presence of dominant proteasome subunit mutants. Hs-EGFP-N^{intra} lines were crossed to UAS-DTS7 and propagated for a stable line. These lines were fed Na 30mM and late 3^{rd} instar were heat shocked by placing larva in an Eppendorf tube in a 37°C water bath for 30min. Larva were then placed at 25°C and allowed to recover for 1 hour before dissection and fixation. Tissues were mounted with Vectashield plus DAPI and imaged on the confocal microscope. Statistical analysis was done by measuring fluorescence intensity in ImageJ and comparing control non fed vs fed larva.

Native gels and in gel peptidase activity

Head or whole body lysates were homogenized using a pellet pestle motor in native lysis buffer (50mM Tris- HCL pH 8.0, 5mM $MgCl_2$, 0.5mM EDTA, and fresh 2mM ATP, 0.2% NP40,

Protease inhibitor cocktail (Roche, 11873580001) and phosphatase inhibitor (ThermoFisher Scientific 78442). Samples were spun down at 4°C in table top centrifuge at max speed and supernatant was taken and measure for protein concentration using BCA assay. Native running buffer was prepared as followed and cooled to 4°C (450mM Tris, 450mM Boric acid, 5mM EDTA, and 25mM $MgCl_2$, 0.5mM ATP, and 0.5mM DTT). 40ug of samples were loaded 1:1 with native sample buffer (Bio-Rad, 161-0738) onto 3-8% Criterion XT Tris-Acetate Gels along with 3ug purified bovine 19S (A1301), 20S (A1401), and 26S (A1201) as loading controls from UBPBio. Electrophoresis was carried out for 1 hour at RT at 50V and then continued at 4°C for 6 hours at 120V. Protein transfer was done using PVDF 0.45um pore membranes (Millipore) in Tris-Glycine buffer without methanol for 3hours at 12V at RT using Genie Electrophoretic Transfer apparatus. Afterward, membranes were blocked with 5% milk in PBST (Tween-20) overnight at 4°C. Membranes were incubated with primary antibodies anti-alpha7 (1:500) a-Rpt3(1:500) both from Enzo for 1 hour at RT, washed 3X, and incubated with secondary antibody a-mouse-HRP (1:2500), then washed 3X. Membranes were developed using Western Lighting ECL blotting reagent (Perkin Elmer) using Kodak Biomax MR film.

For native in-gel activity assays, native gels were run to completion but before transfer were washed with Buffer A (50mM Tris-HCl ph 7.5, 150mM NaCl, 5mM $MgCl_2$, 10% glycerol) and the incubated with developing buffer (50mM Tris-HCl ph 7.5, 150mM NaCl, 5mM $MgCl_2$, 1mM ATP, 100uM Suc-LLVY-AMC) at 30°C for 30min with light shaking. Gel was exposed to illumination at 365nm and imaged using iPhone 6. To assay 20S CP activity gel was exposed to developing buffer plus the addition of 20% SDS for 30min at 30°C. Visualized again at 365nm and then washed with buffer A before transfer proceeded.

Western blotting

Protein samples from either *in vitro* activity assays or native gel analysis were taken and 20ug of protein loaded with 10uL of SDS red loading buffer. Proteins were resolved on 4-20% mini-protean TGX precast gels and electrophoresis was carried out for 1.5hour at 100V. Transfer was done using PVDF membrane 0.45um pore size in Tris-Glycine buffer plus 20% methanol for 1.5hour at 100V in 4°C. Membranes were blocked in 5% milk and stained with primary antibodies, a-tubulin (1:1000) or a-βactin (1:1000) for 1hour, washed 3X, incubated with secondary, and developed using ECL Western blotting detection reagent.

Cell culture of S2 cells and HEK293 cells

S2 cells were grown at RT in sterile conditions using Schneider's cell medium with 10% heat inactivated FBS, and antibiotics. Cells were split periodically. Before transient transfection cells were split to 70% confluency and lipofectamine and recombinant DNA of GST-PI31 given as a gift by Yetis Gultekin, were allowed to incubate and form complexes for 30min at RT. In the meantime, S2 cells were put in serum free low antibiotic and transfection reagent was added dropwise all over petri dish with cells. This was incubated for 4 hours at which point cells were incubated with fresh media.

Nmnat and dmPI31 co-immunoprecipitation

TOPO cloning was used to generate plasmids and transfect them into HEK 293 cells. Cationic lipid reagent (20 µl of Lipofectamine 2000; Invitrogen) was diluted in serum-free media (Opti-MEM; Invitrogen) for transfection in HEK293 cells (100 mm dish). Following a 5 hr incubation, the medium was replaced with Dulbecco's modified Eagle's medium (Invitrogen) supplemented

with 10% fetal bovine serum (FBS). Transfected cells were harvested in PBS 48 hr following the addition of serum-containing media. The cells were then lysed by repeated freeze/thaw cycles in 600 µl of lysis buffer (20 mM HEPES-KOH [pH 7.6], 200 mM KCl, 0.5mM EDTA, 10% glycerol, 1% Triton X-100 and protease inhibitor cocktail [Complete; Roche]) that contained RNase A (50 µg/ml; Sigma-Aldrich). Cell debris was pelleted by centrifugation, and the protein concentration in the supernatant was determined with the Bio-Rad assay. Primers for NmnatC isoform that were used are as follows F-ATGATTGTGAAAATCAGCTGGC and R-CTAAAGTTGCACTTGGGAAATC with Flag tag GACTACAAAGACGATGACGACAAG.
HA- PI31 plasmid was a gift from Yetis Gultekin.

Brain dissections and immunofluorescence

GMR Gal4, eyFLP;sco/scyo;FRT82B dsRED lines were crossed with either FRT82B Nmnat^{1} (24886) or FRT82B Nmnat$^{\Delta 4790\text{-}1}$ (39698) and mitotic clones were generated in the photoreceptor axons and PE flies were fed C, 20mM Nam, or 40mM Nam supplemented instant Drosophila medium plus yeast for 10 days. Adult brains where dissected and fixed in 4% PFA for 40min and blocked in 2% BSA. Primary antibody a-mouse HA (1:1000, Sigma) was used for incubation at 4°C overnight, tissues were washed 3X in PBST, and secondary Donkey anti-mouse FITC (1:500) was added and incubated for 4 hours at 4°C. Tissues were washed 3X and mounted in Vectashield plus DAPI before being imaged on Zeiss confocal microscope at 63X.

4. DmPI31 increases proteasome activity to suppress degeneration in a Drosophila model for Spinocerebellar Ataxia-Type 1 (SCA1)

4.1 Summary

Neurodegenerative diseases such as Alzheimer's, Parkinson's, Huntington's, and Spinocerebellar ataxias (SCAs) share a characteristic feature, the accumulation of ubiquitin-conjugated proteins into aggregates. This suggests that the affected neurons initiated clearance of abnormal proteins by tagging with ubiquitin, but proteasome-mediated degradation subsequently failed. In this chapter, I explore the impact of upregulating proteasomes via the DmPI31 pathway on neurodegeneration in the poly-glutamine disease, Spinocerebellar Ataxia Type-1(SCA1). Using a *Drosophila* model for SCA1 that expresses human ataxin-1 with an extended 82 glutamine repeat (hAtx-1[82Q]), I demonstrate that poly-ubiquitinated proteins do indeed accumulate in this model and that DmPI31 and NAD+ repletion are sufficient to suppress this accumulation. Additionally, DmPI31 alleviates degenerative phenotypes associated with overexpression of hAtx-1[82Q] in the eye. Lastly, I explore the possibility that dmPI31 rescues these phenotypes by altering the localization of proteasomes. These studies suggest that dmPI31 may be a therapeutically promising target for the treatment of neurodegenerative diseases.

4.2 Rationale

The autosomal dominant poly-glutamine disease, Spinocerebellar ataxia type-1(SCA1), is the result of an abnormal CAG trinucleotide repeat of 39 or more in the ATXN1 gene. ATXN1 is conserved across several species including humans, mice, and *Drosophila* but its exact function

is unknown. It is clear however, that the mutant ataxin-1 protein accumulates into nuclear inclusions along with Hsp70, ubiquitin, and proteasomes in SCA1 (Cummings et al., 1998; Fernandez-Funez et al., 2000). Furthermore, selective degradation of mutant ataxin-1 requires the ubiquitin-proteasome pathway (Fernandez-Funez et al., 2000; Lee and Goldberg, 2010; Persengiev et al., 2012). Using a short lived enhanced green fluorescent protein (d2EGFP), one group showed that mutant ataxin-1(82Q) causes d2EGFP to accumulate as the result of proteasome impairment (Park et al., 2005). In *Drosophila*, proteasome impairment by the dominant temperature sensitive Pros26.1 mutation (DTS5), enhances the neurodegeneration caused by expanded ataxin-1. However, whether other proteasome subunits and interactors can modify SCA1 phenotypes is unknown, since much of the work is focused around ubiquitin-like modifiers and chaperones (Ding et al., 2016; Lee and Goldberg, 2010; Nagashima et al., 2011; Parfitt et al., 2009). One protein that was found to act as a chaperone and ameliorate SCA1 induced neurodegeneration in *Drosophila* is NMNAT. Overexpression of NMNAT or enzyme-inactive NMNAT (NMNAT-WR) partially suppressed the degenerative phenotypes produced hAtx-1[82Q] and are recruited to aggregates *in vivo*. Still, in cultured cells insoluble aggregates accumulate upon treatment with the proteasome inhibitor, MG132. These aggregates still accumulate when co-transfected with NMNAT in the presence of MG132, although at lower levels (Zhai et al., 2008). This points to NMNAT promoting hAtx-1[82Q] degradation at least partially through a proteasome-mediated pathway.

In the previous chapter, I showed that NMNAT can modulate both proteasome activity and DmPI31 levels. Thus, I hypothesized that DmPI31 may also act to partially suppress neurodegeneration in SCA1 flies. Here, I describe the suppression of poly-ubiquitinated proteins and degenerative phenotypes in SCA1 by overexpression of DmPI31. I investigate

whether this suppression is through increased activity of proteasomes, increased degradation of hAtx-1[82Q], or localization. The results point toward increased hAtx-1[82q] degradation and localalization of proteasomes being key. In addition, I show that NAD+ repletion is also able to reduce the accumulation of poly-ubiquitinated proteins and this suggests a possible parallel pathway that works in addition to enzymatically inactive NMNAT to reduce SCA1 toxicity.

4.3 Results

4.3.1 DmPI31 suppresses toxicity induced by human Ataxin-1

The established model for *SCA1* in Drosophila was generated by cloning *SCA1* cDNAs differing in the length of their poly-glutamine expansion into the Drosophila pUAST vector. These cDNAs encode for full length human ataxin-1 with either a 30-glutamine repeat (wild-type isoform) or an 82-glutamine expansion (disease relevant isoform). Both transgenic lines result in progressive neurodegenerative phenotypes although the severity is diminished and time of onset delayed in hAtx-1[30Q]. Moreover, wild-type *Drosophila* ataxin-1 (dAtx-1) overexpressed under UAS control in the retina results in a rough eye phenotype, pointing to the amount of accumulated ataxin-1 being significant for disease phenotypes in addition to glutamine repeat length (Fernandez-Funez et al., 2000; Zhai et al., 2008).

Here, my goal was to determine whether overexpression of DmPI31 is sufficient to lessen the burden of ataxin-1 accumulation in SCA1 through increased proteasome activity. Using the Gal4/UAS system, I drove expression of four different ataxin-1 transgenes in the *Drosophila* retina under the glass multimer reporter (GMR). Consistent with previous reports, I show that overexpression of dAtx-1 results in a rough eye phenotype that is rescued with overexpression of NMNAT (Figure 4.1a) (Zhai et al., 2008). Overexpressing both full-length DmPI31 and C-

terminal truncated dmPI31ΔHbYX rescued the small and rough eye phenotype caused by dAtx-1(Figure 4.1a) in a manner comparable to NMNAT. Similarly, both DmPI31 and DmPI31ΔHbYX were able to rescue the rough eye phenotype caused by overexpression of hAtx-1[30Q] (Figure 4.1b). Two transgenic lines for hAtx-1[82Q] with different chromosomal insertions were used to test whether DmPI31 was sufficient to rescue the severe eye phenotypes caused by the expanded human isoform. Both lines cause a severe degenerative phenotype but hAtx-1[82Q] on the 3rd chromosome gives a more severe phenotype than the insertion on the X chromosome. However, DmPI31 and DmPI31ΔHbYX are able to improve the external retinal phenotypes in both cases comparable to overexpression of NMNAT. It is of note that PI31ΔHbYX contributes to an enhanced suppression compared to full length DmPI31. This may be due to lower expression levels of the truncated form since another DmPI31 insertion (10a) that is expressed at low levels shows even further suppression (Figure 4.1d). The HbYX domain at the C-terminal end of DmPI31 is thought to operate by allowing DmPI31 to dock onto 20S proteasomes in a manner similar to the HbYX motifs used by proteasome activators (Smith et al., 2007b; Kusmierczyk et al., 2011). This motif was also shown to be essential for full 26S activation conferred by DmPI31 and be necessary for TNKS and 19S assembly chaperone binding to DmPI31 (Bader et al., 2011; Cho-Park and Steller, 2013). So, how does the HbYX deleted DmPI31 lead to more suppression rather than an enhancement of the retinal phenotype? To better understand this phenotype, I tested knockdown of TNKS in the hAtx-1[82Q] background. Using a UAS driven RNAi for TNKS, the phenotype of the retinae is aggravated with many more necrotic spots consistent with reports that TNKS knockdown enhances proteasome inhibition. Surprisingly, RNAi of PI31 suppresses toxicity of SCA1 counter to its role as a proteasome activator. This may be due to incomplete knockdown of PI31 and/or a stress

response that results in more proteasome activity when proteasomes are inhibited (Meiners et al., 2003). However, rescue of SCA1 retinal phenotype may be dependent on fine-tuned levels of DmPI31 which may explain why knockdown and an insertion with less expression are able to enhance suppression. Knockdown of two other proteasome subunits α6 and α7 cause enhancement of the SCA1 phenotype (not shown). Together, these data show that proteasome activity is indeed essential for suppressing the toxicity of SCA1 and that the dmPI31/TNKS pathway positively mediates suppression.

To further validate these findings, I prepared cryostat sections of *Drosophila* heads for immunofluorescence detection of retinal structures. 10um slices of whole heads were taken and stained for anti-chaoptin (24b10) to mark photoreceptors, anti-HA, and DAPI to label DNA in nuclei. Consistent with published data, SCA1 causes severe retinal degeneration see in the internal structure resulting in collapse of the retina and short disorganized photoreceptor staining (Figure 4.2b). Overexpressing DmPI31 in this background does not rescue retinal collapse but organization of photoreceptors is slightly improved (Figure 4.2c). In these sections overexpressed DmPI31 is seen to localize primarily in the retina and lamina in distinct puncta but also shows some expression in the R7 and R8 photoreceptor axons. Similar to the improvement in eternal eye morphology DmPI31ΔHbYX shows a slight improvement in retinal collapse with photoreceptor organization appearing more organized compared to hAtx-1[82Q] (Figure 4.2d). To better assay degeneration in the eye, I prepared whole mount retinal dissections and visualized photoreceptors by staining with rhodopsin-1 or armadillo, the Drosophila homolog of βcatenin, and phalloidin, to label F-actin rich rhabdomeres. Preliminary results of confocal z-stack projections show that overexpression of hAtx-1[82Q] causes rhadomeres to degenerate as early as 4 days post eclosion. Staining with phalloidin shows rhabodmere

disorganization and loss while anti-armadillo, which stains cell membranes, reveals the extent of disorganization. Bristle cells and pigment cells are cluster together, membranes are not continuous, and many cells appear to have burst (Figure 4.3a). Overexpression of DmPI31 rescued some of the disorganization and rhabdomere loss as indicated by phalloidin staining. Staining with armadillo still revealed disruptions in membrane structure and pigment cell degeneration however, overall membrane structure was improved (Figure 4.3b). Thus, taken together these results indicate that although some degeneration is still present, overexpression of dmPI31 in the Ataxin-1[82Q] mutant background can suppress disruptions in rhabodmere organization. The physiological consequences of this improvement are still being explored.

Figure 4.1.DmPI31 overexpression partially suppresses degenerative phenotypes in a *Drosophila* model for SCA1

Eye exterior morphology (a-d) of flies overexpressing (a) wild-type *Drosophila* Atx-1, (b) wild-type human ataxin-1 with a 30Q repeat, (c) 82Q expanded mutant human ataxin-1 on the 3rd chromosomes and (d) 82Q human ataxin-1 on the X chromosome. In each case, dmPI31 overexpression suppresses the phenotypes along with dmPI31ΔHbYX comparable to overexpression of NMNAT. Interestingly, (c) RNAi for TNKS show enhanced toxicity while RNAi for PI31 appears to suppress toxicity. (d) Lowered expression of full length dmPI31 also enhances suppression of mutant eye phenotype cause by hAtx-1[82Q] which may point to compensatory mechanisms being responsible for the eye phenotypes that result from RNAi for dmPI31.

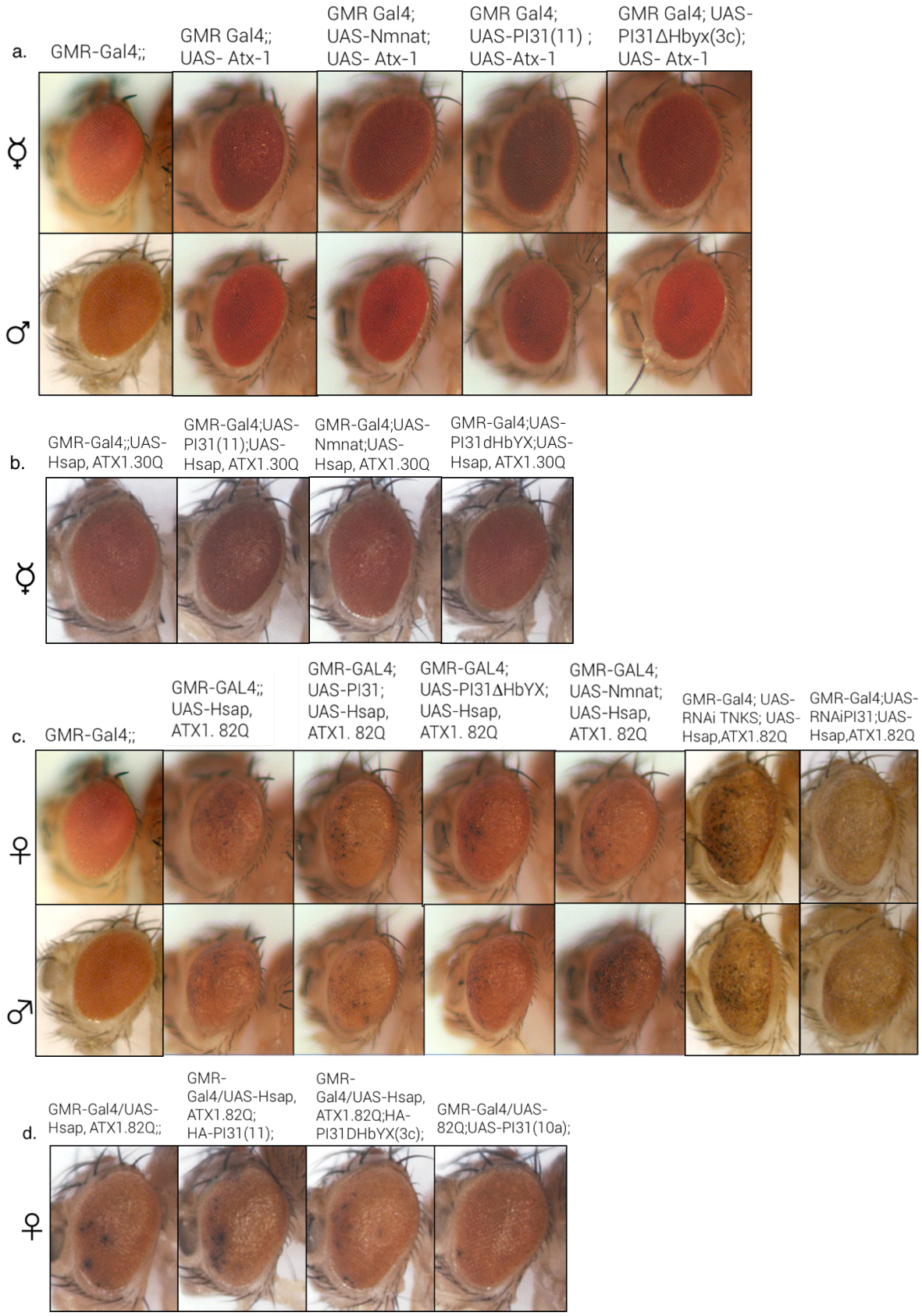
a.
GMR-Gal4;;
GMR Gal4;; UAS- Atx-1
GMR Gal4; UAS-Nmnat; UAS- Atx-1
GMR Gal4; UAS-PI31(11) ; UAS-Atx-1
GMR Gal4; UAS-PI31ΔHbyx(3c); UAS- Atx-1
♀
♂
b.
GMR-Gal4;;UAS-Hsap, ATX1.30Q
GMR-Gal4;UAS-PI31(11);UAS-Hsap, ATX1.30Q
GMR-Gal4;UAS-Nmnat;UAS-Hsap, ATX1.30Q
GMR-Gal4;UAS-PI31dHbYX;UAS-Hsap, ATX1.30Q
♀
c.
GMR-Gal4;;
GMR-GAL4;; UAS-Hsap, ATX1. 82Q
GMR-GAL4; UAS-PI31; UAS-Hsap, ATX1. 82Q
GMR-GAL4; UAS-PI31ΔHbYX; UAS-Hsap, ATX1. 82Q
GMR-GAL4; UAS-Nmnat; UAS-Hsap, ATX1. 82Q
GMR-Gal4; UAS-RNAi TNKS; UAS-Hsap,ATX1.82Q
GMR-Gal4;UAS-RNAiPI31;UAS-Hsap,ATX1.82Q
♀
♂
d.
GMR-Gal4/UAS-Hsap, ATX1.82Q;;
GMR-Gal4/UAS-Hsap, ATX1.82Q; HA-PI31(11);
GMR-Gal4/UAS-Hsap, ATX1.82Q;HA-PI31DHbYX(3c);
GMR-Gal4/UAS-82Q;UAS-PI31(10a);
♀

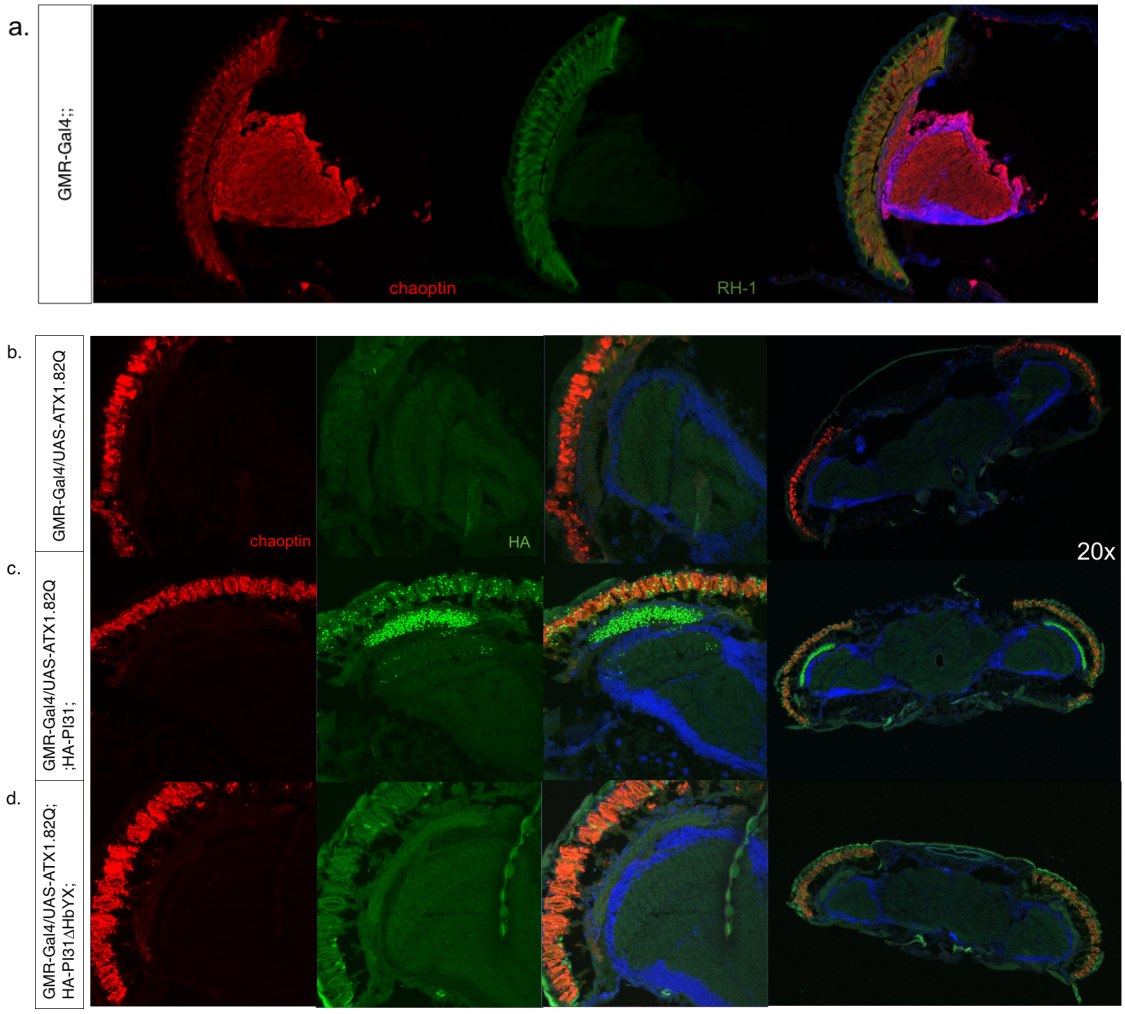

Figure 4.2. Retinal sections reveal partial suppression of ataxin-1 internal eye degeneration by dmPI31

(a-d) 10um frozen sections from *Drosophila* retina were stained with chaoptin (red) and (a)RH-1 or (b-d) anti-HA. Vertical sections show marked degeneration of rhabdomeres in lines overexpressing (b) hAtx-1[82] that can be partially suppressed with overexpression of (c) full length HA-dmPI31, which results in more organized rhabdomeres. HA staining shows dmPI31 localizes highly in the retina, lamina, and R7/R8 photoreceptor axons. (d) Overexpression of HA-PI31ΔHbYX shows even more suppression with some rhabdomere length returning and improved organization. Images are taken at 63X or 20X where indicated.

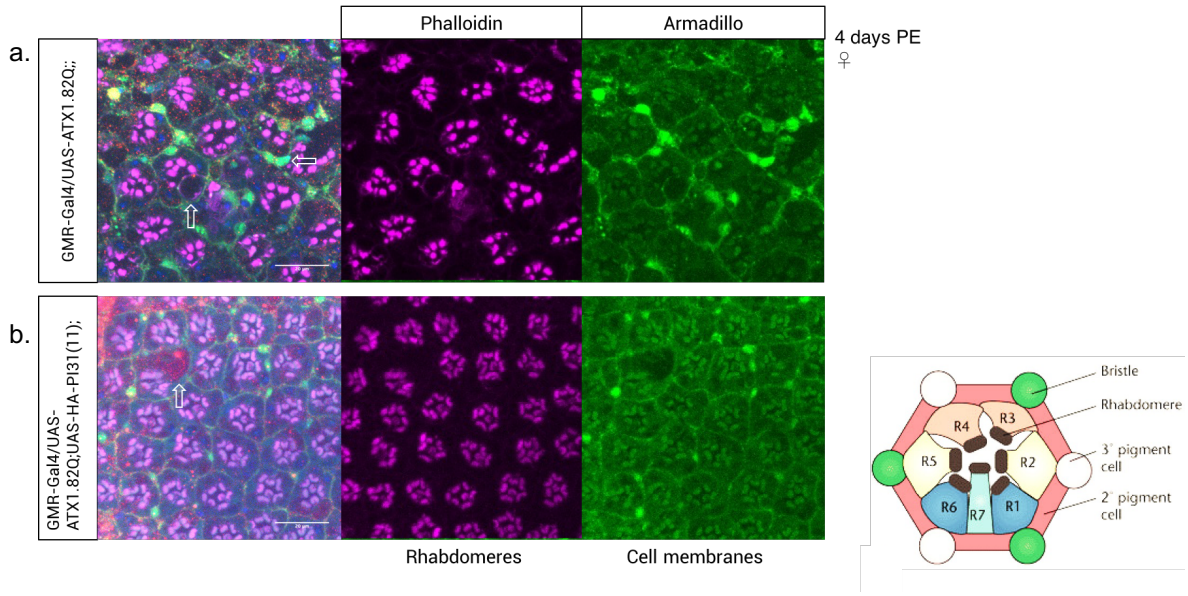

Figure 4.3 DmPI31 suppresses photoreceptor degeneration and improves retinal organization

(a-b) 4-day old whole mount retina were stained for phalloidin (purple) and anti-armadillo (green) to mark rhabdomeres and cell membranes respectively. (a) In hAtx-1[82Q] retina, ommatidial organization is severely affected and rhabdomeres are shown to degenerate as in indicated by lack of phalloidin staining. Bristle and pigment cells also cluster and many cells show a "burst" phenotype (see white arrow). (b) Overexpression of dmPI31 results in an improvement in the organization of the retina as indicated by phalloidin staining. However, armadillo staining shows pigment and bristle cells are still unorganized and degenerate as well as the persistence of the "burst" phenotype seen with expanded ataxin alone.

4.3.2 DmPI31 increases degradation of polyubiquitinated proteins in a Drosophila model for SCA1

To determine whether proteasome activity is enhanced in SCA1 flies expressing dmPI31, I first assayed whether polyubiquitinated proteins faithfully accumulate in the SCA1 mutant background. To do this, whole mount brains were dissected and stained for conjugated ubiquitin (anti-FK2) as a readout of proteasome activity. In SCA1 mutants, FK2 accumulates compared to GMRGal4 control indicating a defect in proteasome mediated degradation consistent with other reports (Figure 4.4a,b). Co-expression with either dmPI31 or dmPI31ΔHbYX reduced FK2 staining to near control levels (Figure 4.3c,d). ImageJ was used to quantify the fluorescence intensity relative to the area for each genotype and the reduction in FK2 staining in the dmPI31 and dmPI31ΔHbYX background are shown to be significant (Figure 4.4e). The majority of FK2 accumulates in the cells of the medulla cortex but can also be seen in the R7 and R8 photoreceptor axons.

How does DmPI31 mediated clearance of ubiquitinated proteins in SCA1? It could be that enhanced assembly of 26S proteasomes mediates clearance of toxic hAtx-1[82]. This does not give a simple explanation for the increased rescue seen when overexpressing PI31ΔHbYX, since TNKS and 19S assembly chaperone binding require the HbYX domain (Cho-Park and Steller, 2013). To determine the extent of hAtx-1[82Q] clearance, head lysates were resolved on SDS-PAGE gel and subject to western blot analysis. Anti-atxain 1 antibody showed a slight accumulation compared to no expression control in fly lysates overexpressing the human expanded protein (Figure 4.5a). The band that is seen in control is likely due to the antibody recognizing endogenous *Drosophila* ataxin-1. In lysates that overexpress PI31, ataxin-1 levels are modestly reduced which can account for the lower levels of poly-ub proteins that are seen *in*

vivo. However, PI31ΔHbYX which showed a stronger suppression of FK2 did not show reductions in Atx-1 levels. The α7 subunit of the proteasome does not show a change in expression levels between expanded ataxin-1 alone or with the PI31 transgenes (Figure 4.5a). To address whether proteasome assembly is affected, I turned to native gel analysis to determine whether changes in proteasome assembly could account for the rescue. Preliminary results show no significant difference in proteasome assembly in head lysates from 25 day old flies (Figure 4.5b). The amount of proteasome activity assayed by in gel activity showed no difference between hAtx-1[82Q] and those line crossed with PI31 or PI31ΔHbYX. However, double capped proteasomes are not detectable at this protein concentration and thus a more concentrated protein sample may distinguish between different amounts of assembly.

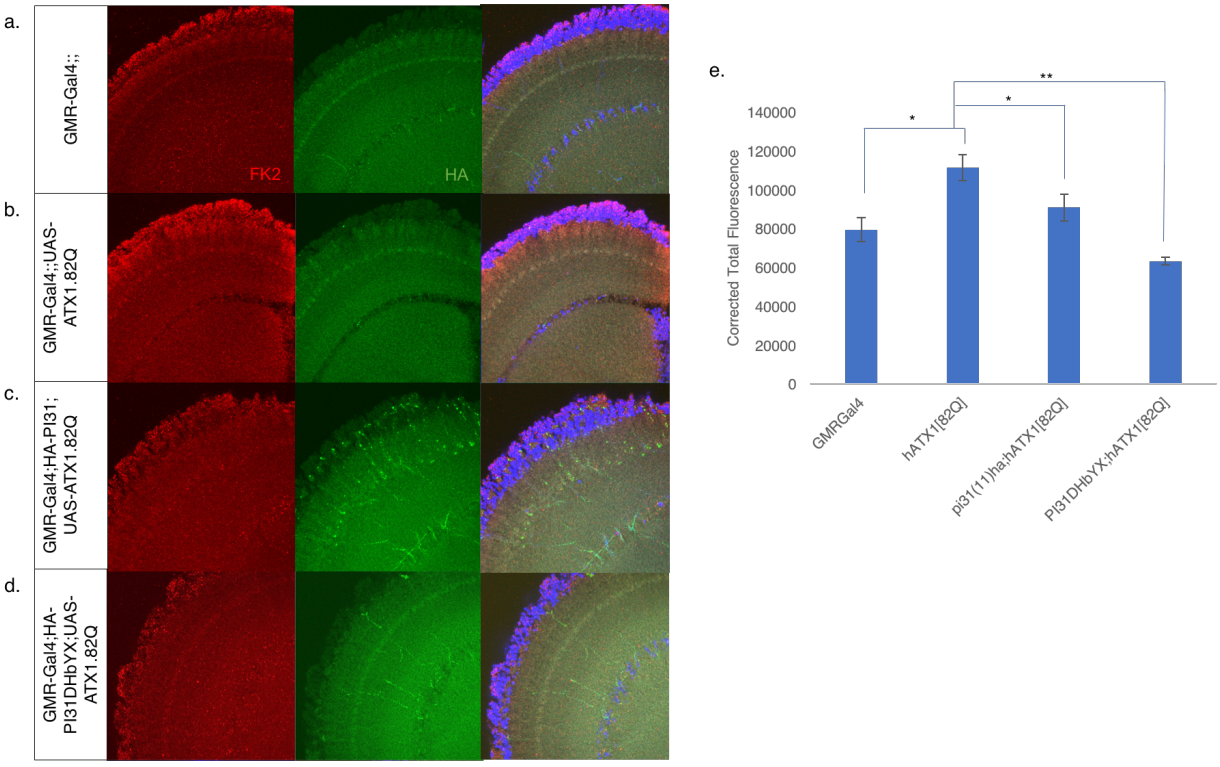

Figure 4.4 DmPI31 relieves the accumulation of polyubiquitinated proteins in SCA1

(a-d) Whole mount adult brains were assayed for the accumulation of ubiquitin conjugated proteins by staining with FK2 antibody and imaging by confocal microscopy. (a) Control lines show slight accumulation of FK2 and HA autofluorescent signal with (b) marked accumulation of FK2 in the hAtx-1[82Q] overexpression background. (c) Co-expression of HA-PI31 or (d) HA-PI31ΔHbYX significantly reduces the accumulation of FK2. (c) HA-PI31 is highly expressed in the R7/R8 photoreceptor axons while HA-PI31ΔHbYX is not expressed at high levels. (e) Quantification of FK2 signal in z-projections of the optic lobe. Bars represent the corrected total fluorescence and statistical analysis was carried out on a total of 5 heads. (GMR Gal4 : 79348. 8 +/- 6181.3 ; hAtx-1[82Q] :111488.3 +/- 6781.5, p=0.042; PI31 hAtx-1[82Q] : 90821.60 +/-6919.3,*p=0.064; PI31DHbYX hAtx-1[82Q]: 63164.7 +/- 1891, **p=0.0019). Significance was carried out with a two-tailed, paired, t test.

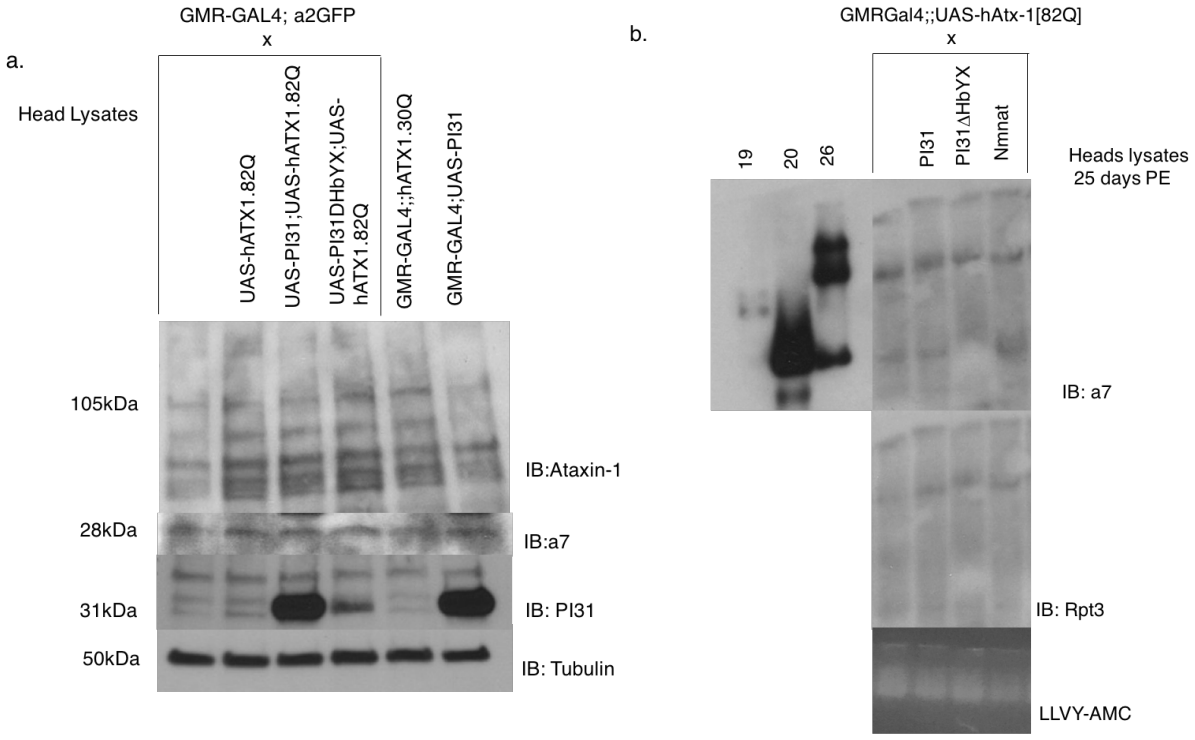

Figure 4.5 DmPI31 overexpression causes Atx-1 degradation but not increased proteasome assembly

(a) Western blot analysis from hAtx-1[82Q] fly head lysates show slight accumulation of atxain-1 antibody compared to no expression control at 105kDa. The band that is seen in the control is likely due to the antibody recognizing endogenous *Drosophila* ataxin-1. In lysates that overexpress PI31, ataxin-1 levels are modestly reduced but PI31ΔHbYX did not reduce Atx-1 levels. Wild-type human ataxin-1[30Q] also shows accumulation but overexpression of dmPI31 alone shows ataxin-1 levels similar to control. The alpha7 subunit of the proteasome does not show a change in expression levels between expanded ataxin alone or with the dmPI31 transgenes. (b) Native gel analysis of head lysates from 25 day old flies. Blotting with alpha7 or Rpt3 did not show marked differences between proteasome assembly in any of the cases that result in partial suppression of SCA1 phenotypes.

4.3.3 PI31 may alter localization of proteasomes in neurodegenerative models

The suppression of neurodegenerative phenotypes may also depend upon the localization of mutant proteins, chaperones, and proteasomes. For instant, the neuroprotective ability of Nmnat in the SCA1 model was found to be the result of different splice variants that translate into proteins with different localization. The cytoplasmic isoform of Nmnat was found to confer neuroprotection and is the major splice variant under stress conditions in neurons (Ruan et al., 2015). PI31 may also alter local proteasome activity and contribute to the suppression of SCA1 phenotypes. In SCA1, it was observed that the GFP tagged alpha2 subunit of the proteasome displays altered localization compared to controls (Figure 4.6). In controls, α2 appears in puncta localized near the giant glial cells of the medulla (Figure 4.6a). However, in hAtx-1[82Q] very few puncta remain possibly pointing to a shift to a more diffuse distribution (Figure 4.6b). Previous western analysis on these flies did not show a difference between another alpha subunit α7 thus leading to the interpretation of localization being altered.

In a *Drosophila* model for Parkinson's disease (PD), the missense mutations found in α-synuclein (A53T, A30P, E46K) that lead to early onset familial PD, lead to similar symptoms in the fly. These include loss of climbing ability, progressive loss of dopaminergic neurons and the formation of inclusion bodies (Feany and Bender, 2000). Unpublished data from Dolor Ferres Marco, a former postdoc in the Steller lab, shows that the progressive loss of climbing ability of A53T lines can be recused by overexpression of PI31ΔHbYX but not by full length PI31 (Figure 4.7a). PI31 itself is shown to be essential to maintain climbing ability with age consistent with previous finding that loss of PI31 results in decreased lifespan (Figure 4.7a orange line). To determine the cause of this difference between full length and HbYX deleted PI31, I looked at the localization of both in an A53T α-synuclein background. Expression of all transgenes was

driven by the pan neuronal driver nervana2. Interestingly, these transgenes show different localization in the optic lobe of flies. While full length PI31 is expressed at high levels and mostly nuclear, HbYX deleted PI31 expression is mostly cytoplasmic, similar to the neuroprotective form of Nmnat (Figure 4.7b-c). More studies within the affected dopaminergic neurons of this model will need to be tested but these preliminary results point to these two different transgenes being expressed in different locals which may explain the differences in neuroprotection seen in PD and SCA1 models. Preliminary results to assay the localization of PI31 in SCA1 and degradation of hAtx-1[82Q] show that overexpression of full length PI31 is sufficient to lower total hAtx-1[82Q] accumulation (Figure 4.8). This was expected since western blot analysis verified decreased expression of hAtx-1[82Q]. However, whether PI31ΔHbYX truncated will result in the altered expression of expanded ataxin-1 is yet to be determined. Western blot results show that hAtx-1[82Q] does not decrease in a PI31ΔHbYX background so determining the localization of both proteins may give clues to how PI31ΔHbYX confers more protection.

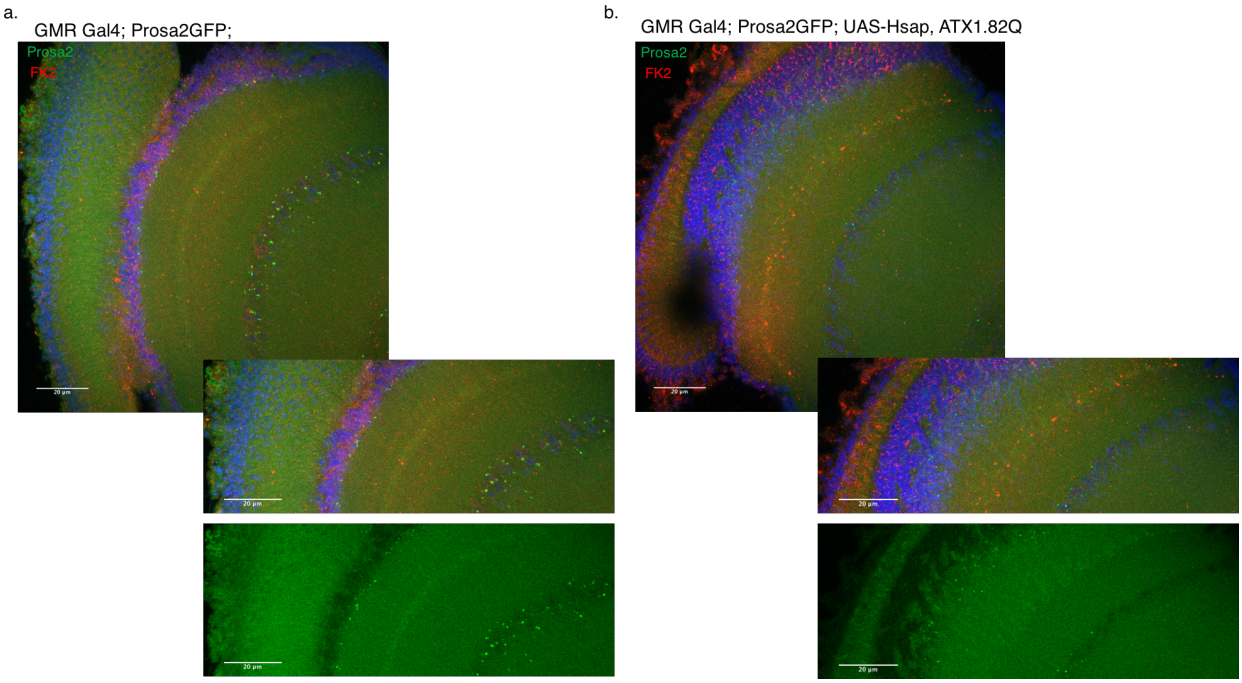

Figure 4.6 Expanded Atx-1 causes a shift in proteasome localization

(a-b) Whole mount brains expressing the GFP tagged alpha2 subunit of the proteasome under its endogenous promoter were fixed, stained for FK2, and imaged on a confocal microscope. (a) In the control optic lobe, alpha2-GFP is highly expressed in distinct cells within the medulla as puncta. FK2 (red) does not show substantial staining. (b) Upon overexpression of hAtx-1[82Q] in these lines, FK2 (red) shows marked accumulation in both retina and R7/R8 photoreceptor axons. Here, alpha2-GFP also becomes localized to the medulla cortex and expression is more diffuse.

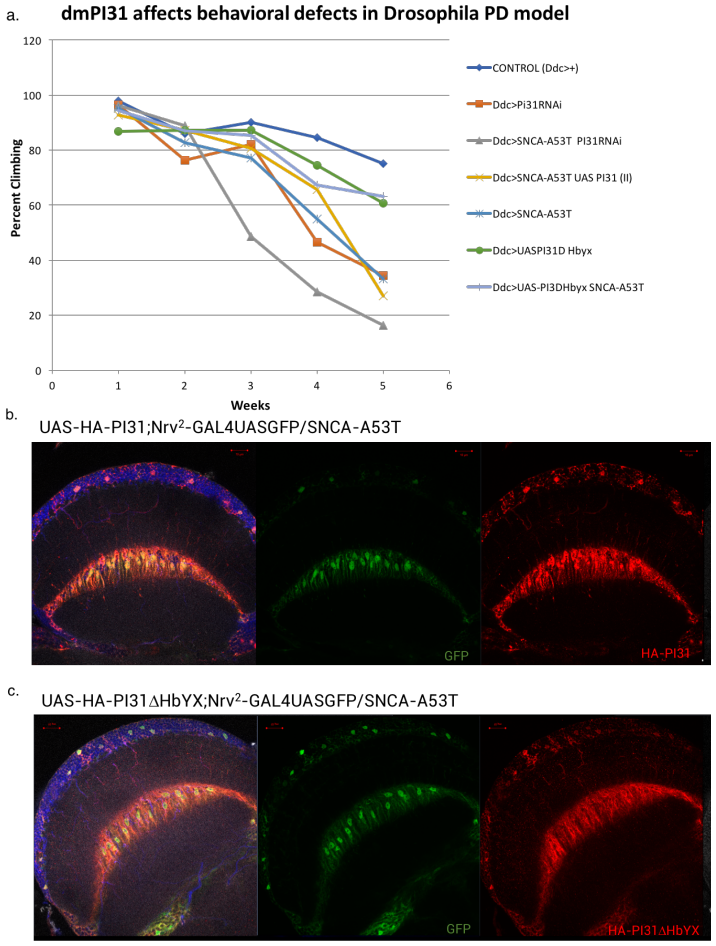

Figure 4.7 Overexpression of dmPI31ΔHbYX rescues climbing ability in a Drosophila PD model and shifts localization of PI31 to the cytoplasm

(a) Climbing assay of *Drosophila* Parkinson's disease model expressing the A53T α–synuclein mutation. These flies (teal) show progressive loss of climbing ability that is rescued with co-expression of PI31DHbYX (light blue). Co-expression with full length PI31 (yellow) did not rescue the climbing ability and RNAi of PI31 (grey) enhances loss of climbing ability. (b) Overexpression of full length dmPI31 in the A53T mutant background shows PI31(red) localized primarily in the nucleus while (c) overexpression of PI31DHbYX shifts localization to the cytoplasm. GFP marks cells highly expressing nervana-Gal4 driver.

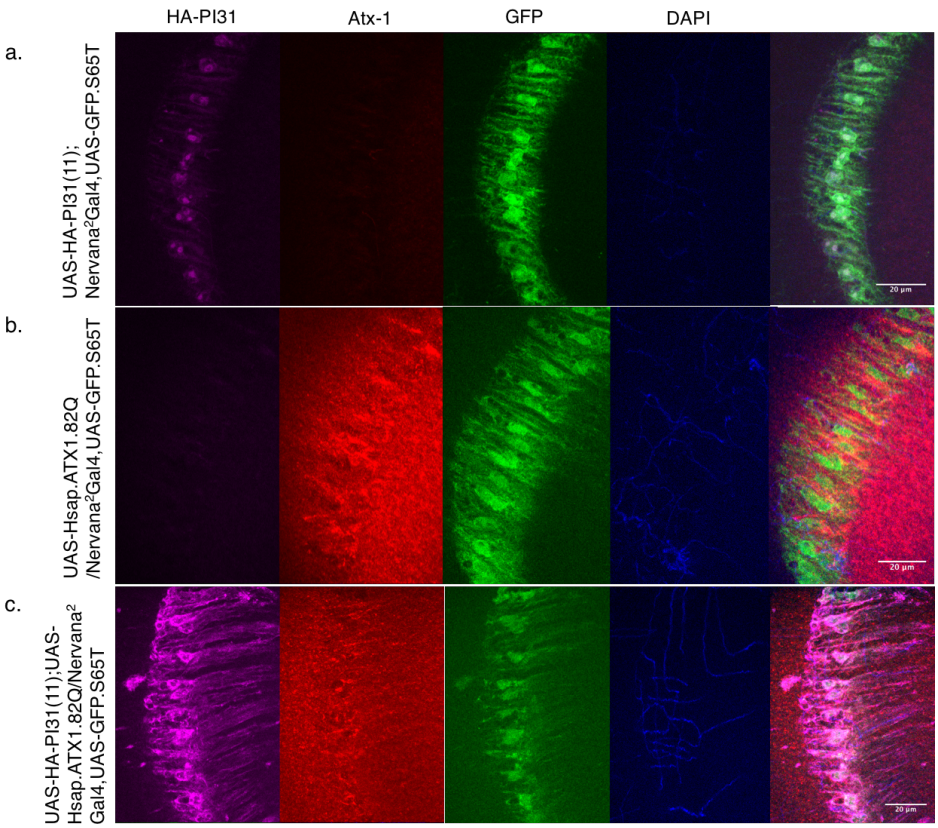

Figure 4.8 Overexpression of DmPI31 *in vivo* reduces Atx-1 accumulation and shows nuclear localization of Atx-1 puncta

(a) Overexpression of dmPI31 alone shows PI31 highly expressed to the giant glial cells in the medulla. This staining overlaps with the nervana2 Gal4 driven expression of GFP. (b) Lines expressing hAtx-1[82Q] alone show marked accumulation of Atx-1 signal that can be suppressed with (c) co-expression of dmPI31.

4.4 Discussion

Spinocerebellar Ataxia Type-1 is a neurodegenerative polyglutamine disease that is characterized by the accumulation of mutant ataxin-1 into nuclear inclusions positive for UPS components and chaperones. The pathogenesis of disease has also been show to display aberrant proteasome function (Cummings et al., 1998; Park et al., 2005). Here, it is shown that dmPI31, an essential proteasome regulator, suppresses degenerative phenotypes associated with the disease. Overexpression of DmPI31 increases the degradation of polyubiquitinated proteins but the exact mechanisms by through which it acts to suppress degeneration remains to be shown. Interestingly, the truncated PI31ΔHbYX shows greater suppression of degenerative phenotypes leading to questions how DmPI31 acts to regulate the UPS in this context. This is especially relevant since both mutant and wild-type ataxin-1 are ubiquitinated at similar rates *in vitro* but the mutant protein remains highly resistant to degradation (Cummings et al., 1999). To determine what may contribute to these difference, preliminary results show that proteasome assembly is not significantly impacted while pointing toward local proteasome activity as being important. DmPI31 and the HbYX deleted protein have different subcellular localizations in a model for Parkinson's disease but their localization in the SCA1 model remain to be resolved. Still, these results show that driving DmPI31 expression suppresses the accumulation of ataxin-1 *in vivo*. Further studies are needed to determine how PI31ΔHbYX acts on these puncta and whether cytoplasmic or nuclear proteasome activity is more critical.

Also, whether or not this suppression is due to a functional NAD+ salvage pathway remains to be shown. Previous reports show that overexpression of Nmnat, an essential NAD+ salvage enzyme, was sufficient to suppress degeneration in SCA1. In addition, the

enzymatically inactive form also offered mild suppression (Zhai et al., 2008). The yeast homologs of NMNAT, NMA1 and NMA2, were also able to suppress proteotoxicity in neurodegenerative models of disease but interestingly other components of the NAD+ salvage pathway such as QNS1, PNC1, and NPT1 also protected. Disruption of NPT1 in an NMA1 or NMA2 overexpression background still suppressed toxicity caused by 103Q suggesting a functional salvage pathway is not needed. However, these results don't negate the presence of compensatory pathways for NAD+ biosynthesis or the idea of parallel pathways mediating both chaperone and UPS activity as essential. The preliminary results that were gathered here showed a slight decrease in polyubiquitinated proteins in flies fed for 5 days on 20mM Na but whether or not this suppression relies on DmPI31 remains to be determined. Also, whether further clearance can be achieved in flies overexpressing DmPI31 and under NAD+ repletion may implicate modification of DmPI31 as essential for increased proteasome activity under stress. To test this, DmPI31ΔHbYX transgenic lines can be subject to NAD+ repletion and the amount of cleared polyubiquitinated proteins compared to full length DmPI31.

These findings hint at a pathway with the ability to suppress the pathogenesis of SCA1 that may also translate to improving proteotoxicity in other polyglutamine diseases. The exact mechanism by which toxicity is suppressed with overexpression of DmPI31 remains to be determined. It is intriguing, however, to envision a means by which neurons may be able to localize proteasome activity by differential modification of the proteasome regulator, DmPI31.

4.5 Materials and Methods

Fly stocks and culturing

Drosophila SCA1 models for hAtx-1[82Q] on the X (39740) and 3rd chromosomes (33818) were obtained from Bloomington along with UAS-Atx-1 (39741). All other lines used in this chapter are previously described in other sections.

Crytostat sections of Drosophila heads

Frozen sections were taken according to the following protocol (Helfrich-Förster, 2007).Working quickly, whole heads from indicated genotypes are removed from body and proboscis is removed. These heads are placed in 4% PFA overnight at 4°C and washed 3X the next day in PBST. Heads are then subject to a sucrose gradient 5%, 10%, 25% sucrose. Heads were allowed to sink and then transferred to OCT medium in a cryostat chuck that was then quickly frozen by dipping into a dry ice/ethanol bath. Section were kept at -80°C until reading to section at which time 10um sections were taken. Ribbons of sections were placed on glass slides and fixed for an additional 10min in 4% PFA, washed 3X, blocked with 2% BSA, and immunostained with primary antibody on top of glass slides with plastic coverslips. Primary antibodies a-chaoptin (1:100, 24b10 DSHB), a-RH1 (1:100, 4C5 DSHB), Donkey a-rabbit-HA (1:1000). Images were taken on confocal microscope.

Whole mount retinal dissections and immunostaining

Protocol from (Hsiao et al., 2012) was followed for the dissection of whole mount retinae. Briefly, retinae were carefully removed from adult heads and placed in 4% PFA for 40min on ice. At this point it is crucial to remove the lamina very carefully and wash retina 3X in PBST.

Primary antibody staining is done in PCR tubes to reduce volume. The following antibodies were used a-armadillo (1:100, N27A1 DSHB) and Alexa Fluor 647 Phallodin from CST (1:500). Washed 3X and incubated with secondary antibody a-mouse FITC (1:500) before another wash and mounting by preparing 'bridges' so that retina are not folded while imaging.

Whole mount brain dissections and immunostaining

Whole mount brain dissections are done in the same manner as in Chapter 2. Here however, FK2 antibody was used at (1:500) and a-HA rabbit (1:500). Alpha2GFP brains were also dissected and stained for FK2. Images were quantified using ImageJ by measuring the corrected fluorescence intensity. Human ataxin-1 antibody was obtained from Cell Signaling (2177S) and used at dilution (1:200).

Western blots

Head only lysates were homogenized in lysis buffer (20 mM HEPES-KOH [pH 7.6], 200 mM KCl, 0.5mM EDTA, 10% glycerol, 1% Triton X-100 and protease inhibitor cocktail [Complete; Roche]) and spun in a microcentrifuge for 15min at 4°C. Protein concentration was measured using BCA assay and normalized. 45ug protein was added along with 1X SDS sample buffer and proteins were resolved for 1.5hour at 100V in 4-20% precast gels. Transfer was done at 4°C for 1.2 hours at 100V using PVDF membranes and tris-glycine buffer plus 20% methanol. After transfer, membrane was blocked and primary antibodies were incubated each for 1 hour. The same membrane was stripped and blocked between each antibody. Anti-Ataxin-1 (1:500), a-alpha7 (1:500), a-PI31 generated in the lab by Yetis Gultekin (1:2500), and a-tubulin (1:2500) were used.

Native gels

Preliminary native gel analysis was run on heads collected from the indicated genotypes in the same fashion as in Chapter 3.

5. Future Perspectives

5.1 Insights into the in vivo function of DmPI31

Several *in vivo* functions of DmPI31 in *Drosophila* neurons were uncovered in this study including maintenance of AZs, motor neuron morphology, and photoreceptor axons. However, results from this study imply that DmPI31 also has developmental roles in maintaining proteasome activity to regulate degradation of cell cycle components. Yet, the cause of lethality of *dmPI31* mutants remains to be uncovered. The expansion of Dpn positive cells within the larval brain point to serious defects in cell cycle control that could lead to apoptosis and a simple way to test this hypothesis is by TUNEL assay since cleaved DCP-1 showed a slight accumulation. However, the post mitotic effects of loss of DmPI31 remain of major interest as it still remains to be seen whether the primary mechanism by which DmPI31 acts to regulate proteasome activity is through increased assembly. Global changes in proteasome assembly from whole head lysates show increased assembly upon NAD+ repletion that was dependent on DmPI31 but ADP-ribosylated DmPI31 was not detected in adult flies. However, these modification may be small compared to the global changes and may not reflect the amount of proteasome regulation going on at particular locales, such as at the synapse. Thus, looking into DmPI31 localization may provide critical insight into its major function as a proteasome regulator. Indeed, ongoing studies in our lab point to DmPI31 being a direct transporter of proteasomes to distal parts of the axon. However, how this movement is regulated, what prompts the movement of proteasomes, and whether movement relies on ADP-ribosylation is still unclear.

In addition, an understanding of how DmPI31 itself is regulated will provide key insights into when this protein may be active. From the data presented in this thesis it is clear that

DmPI31 can be regulated by nutritional status but whether this occurs as a result of post-translational modification or transcriptional regulation was not resolved. Uncovering transcription factors that may act on DmPI31 could provide insight into when this protein is active. Whether PI31 binding to the proteasome is also still unknown. How can this protein with an intact HbYX motif bind to 20S and still activate 26S? It is possible that modification of DmPI31 results in cleavage of the C-terminal end of this protein to relieve 20S inhibition in vivo but the N-terminal end maintains interaction with 26S and aids in its stability. Cleavage of DmPI31 C-terminus is under active investigation in our lab and previously reported to be involved in its stability (Bader et al., 2011).

5.2 Changes in NAD+ metabolism with age and declining proteostasis

Both NAD+ levels and proteasome assembly have been shown to decline with age which makes for an intriguing hypothesis about why many neurodegenerative diseases are late-onset. A decline in NAD+ could lead to a steady decline in proteostasis with age leading to neurodegeneration. Indeed, these studies give attention to this hypothesis, as I show that NAD+ leads to increased proteasome activity. Others have shown that boosting NAD+ levels can suppress neurodegeneration and here I have shown that NAD+ repletion can suppress the accumulation of polyubiquitinated proteins. However, the direct mechanism of these observations remains to be uncovered. NAD+ is involved in a variety of cellular processes including the production of ATP, thus it is possible that maintenance of neurons by proteasome activity is an indirect effect of more ATP production. Whether this increase proteasome activity by NAD+ is dependent on ADP-ribosylated PI31 is currently being explored, but small amounts

the of ADP-ribosylated form only in distinct compartment may prove uncovering a mechanism challenging.

Although Nmnat can rescue neurodegeneration independent of its NAD+ synthase activity, it does not rule out that increased NAD+ does not further suppress phenotypes. Thus it would be interesting to see whether overexpression of Nmnat in combination with overexpression of DmPI31 or upon NAD+ repletion can further suppress the phenotypes caused in the *Drosophila* SCA1 model. Parallel pathways are likely to exist that mediate neuronal health via maintenance of proteostasis since loss of proteostasis is detrimental.
Parallel pathways, NAD+ supplements, neuronal health via maintenance of proteostasis

5.3 DmPI31-mediated proteasome regulation in maintaining neuronal health

The cumulative results of these studies show that DmPI31, an essential proteasome regulator, has the ability to directly affect proteasome activity *in vivo*. The role of DmPI31 and the reported and implied post-translational modifications that it undergoes make it an excellent candidate for small molecule compounds that could regulate proteasome activity under certain conditions. Bortezomib, a proteasome inhibitor, inactivates proteasomes globally and thus results in the unwanted side effect of peripheral neuropathy. However, targeting PI31 may bypass these effects depending upon the post-translation modification that is targeted.

It is becoming apparent that DmPI31 may play an essential role is proteasome localization from my work and other work in the lab. What is interesting is that neurons may use DmPI31 to move proteasomes to required compartments in addition to them functioning to properly assemble proteasomes. The location of endogenous DmPI31 in photoreceptor axons implies that a mechanism exists to transport proteasomes to these distant compartments. Once their

destination is reached, subcellular NAD+ pools could act to increase proteasome assembly at these distinct locations, and this mechanism could function to maintain synapses and promote neuronal health. New tools that are being developed will allow for identification of subcellular NAD+ pools in vivo which will guide our understanding of where ADP-ribosylation of DmPI31 is likely having the most benefit. The whole story about how DmPI31 acts on proteasome activity is still to be clear up but ultimately will lead to a better understanding of how proteostasis is maintained throughout the aging processes in neurons and will open the field up to explore 26S proteasome regulation even further.

6. References

Alano, C.C., Garnier, P., Ying, W., Higashi, Y., Kauppinen, T.M., and Swanson, R.A. (2010). NAD+ depletion is necessary and sufficient for PARP-1 - mediated neuronal death. J. Neurosci. Off. J. Soc. Neurosci. *30*, 2967–2978.

Alé, A., Bruna, J., Herrando, M., Navarro, X., and Udina, E. (2015). Toxic effects of bortezomib on primary sensory neurons and Schwann cells of adult mice. Neurotox. Res. *27*, 430–440.

Ali, Y.O., Ruan, K., and Zhai, R.G. (2011). NMNAT suppresses Tau-induced neurodegeneration by promoting clearance of hyperphosphorylated Tau oligomers in a Drosophila model of tauopathy. Hum. Mol. Genet. *21*, 237–250.

Anderson, R.M., Bitterman, K.J., Wood, J.G., Medvedik, O., and Sinclair, D.A. (2003). Nicotinamide and PNC1 govern lifespan extension by calorie restriction in Saccharomyces cerevisiae. Nature *423*, 181–185.

Aradska, J., Bulat, T., Sialana, F.J., Birner-Gruenberger, R., Erich, B., and Lubec, G. (2015). Gel-free mass spectrometry analysis of Drosophila melanogaster heads. PROTEOMICS *15*, 3356–3360.

Araki, T., Sasaki, Y., and Milbrandt, J. (2004). Increased Nuclear NAD Biosynthesis and SIRT1 Activation Prevent Axonal Degeneration. Science *305*, 1010–1013.

Arbeitman, M.N., Furlong, E.E.M., Imam, F., Johnson, E., Null, B.H., Baker, B.S., Krasnow, M.A., Scott, M.P., Davis, R.W., and White, K.P. (2002). Gene expression during the life cycle of Drosophila melanogaster. Science *297*, 2270–2275.

Bader, M., Arama, E., and Steller, H. (2010). A novel F-box protein is required for caspase activation during cellular remodeling in Drosophila. Dev. Camb. Engl. *137*, 1679–1688.

Bader, M., Benjamin, S., Wapinski, O.L., Smith, D.M., Goldberg, A.L., and Steller, H. (2011). A Conserved F Box Regulatory Complex Controls Proteasome Activity in Drosophila. Cell *145*, 371–382.

Banerjee, K.K., Ayyub, C., Ali, S.Z., Mandot, V., Prasad, N.G., and Kolthur-Seetharam, U. (2012). dSir2 in the Adult Fat Body, but Not in Muscles, Regulates Life Span in a Diet-Dependent Manner. Cell Rep. *2*, 1485–1491.

Barthelme, D., and Sauer, R.T. (2012). Identification of the Cdc48•20S proteasome as an ancient AAA+ proteolytic machine. Science *337*, 843–846.

Belenky, P., Bogan, K.L., and Brenner, C. (2007). NAD+ metabolism in health and disease. Trends Biochem. Sci. *32*, 12–19.

de Bie, P., and Ciechanover, A. (2011). Ubiquitination of E3 ligases: self-regulation of the ubiquitin system via proteolytic and non-proteolytic mechanisms. Cell Death Differ. *18*, 1393–1402.

Bingol, B., and Schuman, E.M. (2006). Activity-dependent dynamics and sequestration of proteasomes in dendritic spines. Nature *441*, 1144–1148.

Brent, J., Werner, K., and McCabe, B.D. (2009a). Drosophila larval NMJ immunohistochemistry. J. Vis. Exp. JoVE.

Brent, J.R., Werner, K.M., and McCabe, B.D. (2009b). Drosophila Larval NMJ Dissection. J. Vis. Exp. JoVE.

Cambronne, X.A., Stewart, M.L., Kim, D., Jones-Brunette, A.M., Morgan, R.K., Farrens, D.L., Cohen, M.S., and Goodman, R.H. (2016). Biosensor reveals multiple sources for mitochondrial NAD^+. Science *352*, 1474–1477.

Cascio, P., Call, M., Petre, B.M., Walz, T., and Goldberg, A.L. (2002). Properties of the hybrid form of the 26S proteasome containing both 19S and PA28 complexes. EMBO J. *21*, 2636–2645.

Castro, A., Bernis, C., Vigneron, S., Labbé, J.-C., and Lorca, T. (2005). The anaphase-promoting complex: a key factor in the regulation of cell cycle. Oncogene *24*, 314–325.

Chen, D., Frezza, M., Schmitt, S., Kanwar, J., and Dou, Q.P. (2011). Bortezomib as the first proteasome inhibitor anticancer drug: current status and future perspectives. Curr. Cancer Drug Targets *11*, 239–253.

Chen, L., Thiruchelvam, M.J., Madura, K., and Richfield, E.K. (2006). Proteasome dysfunction in aged human alpha-synuclein transgenic mice. Neurobiol. Dis. *23*, 120–126.

Chondrogianni, N., Tzavelas, C., Pemberton, A.J., Nezis, I.P., Rivett, A.J., and Gonos, E.S. (2005). Overexpression of proteasome beta5 assembled subunit increases the amount of proteasome and confers ameliorated response to oxidative stress and higher survival rates. J. Biol. Chem. *280*, 11840–11850.

Cho-Park, P.F., and Steller, H. (2013). Proteasome Regulation by ADP-Ribosylation. Cell *153*, 614–627.

Chu-Ping, M., Slaughter, C.A., and DeMartino, G.N. (1992). Purification and characterization of a protein inhibitor of the 20S proteasome (macropain). Biochim. Biophys. Acta *1119*, 303–311.

Clemen, C.S., Marko, M., Strucksberg, K.-H., Behrens, J., Wittig, I., Gärtner, L., Winter, L., Chevessier, F., Matthias, J., Türk, M., et al. (2015). VCP and PSMF1: Antagonistic regulators of proteasome activity. Biochem. Biophys. Res. Commun. *463*, 1210–1217.

Coleman, M.P., and Perry, V.H. (2002). Axon pathology in neurological disease: a neglected therapeutic target. Trends Neurosci. *25*, 532–537.

Coux, O., Tanaka, K., and Goldberg, A.L. (1996). Structure and Functions of the 20S and 26S Proteasomes. Annu. Rev. Biochem. *65*, 801–847.

Cummings, C.J., Mancini, M.A., Antalffy, B., DeFranco, D.B., Orr, H.T., and Zoghbi, H.Y. (1998). Chaperone suppression of aggregation and altered subcellular proteasome localization imply protein misfolding in SCA1. Nat. Genet. *19*, 148–154.

Cummings, C.J., Reinstein, E., Sun, Y., Antalffy, B., Jiang, Y., Ciechanover, A., Orr, H.T., Beaudet, A.L., and Zoghbi, H.Y. (1999). Mutation of the E6-AP Ubiquitin Ligase Reduces Nuclear Inclusion Frequency While Accelerating Polyglutamine-Induced Pathology in SCA1 Mice. Neuron *24*, 879–892.

Dasuri, K., Zhang, L., Ebenezer, P., Liu, Y., Fernandez-Kim, S.O., and Keller, J.N. (2009). Aging and Dietary Restriction Alter Proteasome Biogenesis and Composition in the Brain and Liver. Mech. Ageing Dev. *130*, 777–783.

De La Mota-Peynado, A., Lee, S.Y.-C., Pierce, B.M., Wani, P., Singh, C.R., and Roelofs, J. (2013). The proteasome-associated protein Ecm29 inhibits proteasomal ATPase activity and in vivo protein degradation by the proteasome. J. Biol. Chem. *288*, 29467–29481.

Di Fonzo, A., Dekker, M.C.J., Montagna, P., Baruzzi, A., Yonova, E.H., Correia Guedes, L., Szczerbinska, A., Zhao, T., Dubbel-Hulsman, L.O.M., Wouters, C.H., et al. (2009). FBXO7 mutations cause autosomal recessive, early-onset parkinsonian-pyramidal syndrome. Neurology *72*, 240–245.

Ding, Y., Adachi, H., Katsuno, M., Sahashi, K., Kondo, N., Iida, M., Tohnai, G., Nakatsuji, H., and Sobue, G. (2016). BIIB021, a synthetic Hsp90 inhibitor, induces mutant ataxin-1 degradation through the activation of heat shock factor 1. Neuroscience *327*, 20–31.

Dölle, C., Niere, M., Lohndal, E., and Ziegler, M. (2009). Visualization of subcellular NAD pools and intra-organellar protein localization by poly-ADP-ribose formation. Cell. Mol. Life Sci. *67*, 433–443.

Dourlen, P., Levet, C., Mejat, A., Gambis, A., and Mollereau, B. (2013). The Tomato/GFP-FLP/FRT Method for Live Imaging of Mosaic Adult Drosophila Photoreceptor Cells. J. Vis. Exp. JoVE.

Egger, B., Chell, J.M., and Brand, A.H. (2008). Insights into neural stem cell biology from flies. Philos. Trans. R. Soc. B Biol. Sci. *363*, 39–56.

Elhassan, Y.S., Philp, A.A., and Lavery, G.G. (2017). Targeting NAD+ in Metabolic Disease: New Insights Into an Old Molecule. J. Endocr. Soc. *1*, 816–835.

Feany, M.B., and Bender, W.W. (2000). A Drosophila model of Parkinson's disease. Nature *404*, 394–398.

Fernandez-Funez, P., Nino-Rosales, M.L., de Gouyon, B., She, W.C., Luchak, J.M., Martinez, P., Turiegano, E., Benito, J., Capovilla, M., Skinner, P.J., et al. (2000). Identification of genes that modify ataxin-1-induced neurodegeneration. Nature *408*, 101–106.

Gillingwater, T.H., Haley, J.E., Ribchester, R.R., and Horsburgh, K. (2004). Neuroprotection After Transient Global Cerebral Ischemia in Wlds Mutant Mice. J. Cereb. Blood Flow Metab. *24*, 62–66.

Glickman, M.H., and Ciechanover, A. (2002). The Ubiquitin-Proteasome Proteolytic Pathway: Destruction for the Sake of Construction. Physiol. Rev. *82*, 373–428.

Gomes, A.P., Price, N.L., Ling, A.J.Y., Moslehi, J.J., Montgomery, M.K., Rajman, L., White, J.P., Teodoro, J.S., Wrann, C.D., Hubbard, B.P., et al. (2013). Declining NAD+ Induces a Pseudohypoxic State Disrupting Nuclear-Mitochondrial Communication during Aging. Cell *155*, 1624–1638.

Gray, D.A., Tsirigotis, M., and Woulfe, J. (2003). Ubiquitin, proteasomes, and the aging brain. Sci. Aging Knowl. Environ. SAGE KE *2003*, RE6.

Gregori, L., Fuchs, C., Figueiredo-Pereira, M.E., Van Nostrand, W.E., and Goldgaber, D. (1995). Amyloid beta-protein inhibits ubiquitin-dependent protein degradation in vitro. J. Biol. Chem. *270*, 19702–19708.

Groll, M., Bajorek, M., Köhler, A., Moroder, L., Rubin, D.M., Huber, R., Glickman, M.H., and Finley, D. (2000). A gated channel into the proteasome core particle. Nat. Struct. Biol. *7*, 1062–1067.

Grubbs, N., Leach, M., Su, X., Petrisko, T., Rosario, J.B., and Mahaffey, J.W. (2013). New Components of Drosophila Leg Development Identified through Genome Wide Association Studies. PLoS ONE *8*.

Gu, Y., Xu, K., Torre, C., Samur, M., Barwick, B.G., Rupji, M., Arora, J., Neri, P., Kaufman, J., Nooka, A., et al. (2018). 14-3-3ζ binds the proteasome, limits proteolytic function and enhances sensitivity to proteasome inhibitors. Leukemia *32*, 744–751.

Guarente, L., and Picard, F. (2005). Calorie Restriction— the SIR2 Connection. Cell *120*, 473–482.

Guerrero, C., Milenkovic, T., Przulj, N., Kaiser, P., and Huang, L. (2008). Characterization of the proteasome interaction network using a QTAX-based tag-team strategy and protein interaction network analysis. Proc. Natl. Acad. Sci. *105*, 13333–13338.

Hamilton, A.M., and Zito, K. (2013). Breaking it down: the ubiquitin proteasome system in neuronal morphogenesis. Neural Plast. *2013*, 196848.

Han, S.K., Lee, D., Lee, H., Kim, D., Son, H.G., Yang, J.-S., Lee, S.-J.V., Kim, S., Han, S.K., Lee, D., et al. (2016). OASIS 2: online application for survival analysis 2 with features for the analysis of maximal lifespan and healthspan in aging research. Oncotarget *7*, 56147–56152.

Heinrichs, A. (2009). Protein degradation: Assembly from the base.

Helfrich-Förster, C. (2007). Immunohistochemistry in Drosophila: sections and whole mounts. Methods Mol. Biol. Clifton NJ *362*, 533–547.

Hirano, H., Kimura, Y., and Kimura, A. (2016). Biological significance of co- and post-translational modifications of the yeast 26S proteasome. J. Proteomics *134*, 37–46.

Homem, C.C.F., and Knoblich, J.A. (2012). Drosophila neuroblasts: a model for stem cell biology. Development *139*, 4297–4310.

Hsiao, H.-Y., Johnston, R.J., Jukam, D., Vasiliauskas, D., Desplan, C., and Rister, J. (2012). Dissection and Immunohistochemistry of Larval, Pupal and Adult Drosophila Retinas. J. Vis. Exp. JoVE.

Hsu, M.-T., Guo, C.-L., Liou, A.Y., Chang, T.-Y., Ng, M.-C., Florea, B.I., Overkleeft, H.S., Wu, Y.-L., Liao, J.-C., and Cheng, P.-L. (2015). Stage-Dependent Axon Transport of Proteasomes Contributes to Axon Development. Dev. Cell *35*, 418–431.

Hung, Y.P., Albeck, J.G., Tantama, M., and Yellen, G. (2011). Imaging Cytosolic NADH-NAD+ Redox State with a Genetically Encoded Fluorescent Biosensor. Cell Metab. *14*, 545–554.

Janse, D.M., Crosas, B., Finley, D., and Church, G.M. (2004). Localization to the Proteasome Is Sufficient for Degradation. J. Biol. Chem. *279*, 21415–21420.

Jia, H., Li, X., Gao, H., Feng, Z., Li, X., Zhao, L., Jia, X., Zhang, H., and Liu, J. (2008). High doses of nicotinamide prevent oxidative mitochondrial dysfunction in a cellular model and improve motor deficit in a Drosophila model of Parkinson's disease. J. Neurosci. Res. *86*, 2083–2090.

Kreko-Pierce, T., and Eaton, B.A. (2017). The Drosophila LC8 homolog cut up specifies the axonal transport of proteasomes. J Cell Sci *130*, 3388–3398.

Kruegel, U., Robison, B., Dange, T., Kahlert, G., Delaney, J.R., Kotireddy, S., Tsuchiya, M., Tsuchiyama, S., Murakami, C.J., Schleit, J., et al. (2011). Elevated proteasome capacity extends replicative lifespan in Saccharomyces cerevisiae. PLoS Genet. *7*, e1002253.

Kumar, B., Kim, Y.-C., and DeMartino, G.N. (2010). The C terminus of Rpt3, an ATPase subunit of PA700 (19 S) regulatory complex, is essential for 26 S proteasome assembly but not for activation. J. Biol. Chem. *285*, 39523–39535.

Kusmierczyk, A.R., Kunjappu, M.J., Kim, R.Y., and Hochstrasser, M. (2011). A Conserved 20S Proteasome Assembly Factor Requires a C-terminal HbYX Motif for Proteasomal Precursor Binding. Nat. Struct. Mol. Biol. *18*, 622–629.

Lee, D.H., and Goldberg, A.L. (2010). Hsp104 is essential for the selective degradation in yeast of polyglutamine expanded ataxin-1 but not most misfolded proteins generally. Biochem. Biophys. Res. Commun. *391*, 1056–1061.

Leggett, D.S., Hanna, J., Borodovsky, A., Crosas, B., Schmidt, M., Baker, R.T., Walz, T., Ploegh, H., and Finley, D. (2002). Multiple Associated Proteins Regulate Proteasome Structure and Function. Mol. Cell *10*, 495–507.

Lehmann, S., Loh, S.H.Y., and Martins, L.M. (2016). Enhancing NAD+ salvage metabolism is neuroprotective in a PINK1 model of Parkinson's disease. Biol. Open *6*, 141–147.

Lehmann, S., Loh, S.H.Y., and Martins, L.M. (2017). Enhancing NAD(+) salvage metabolism is neuroprotective in a PINK1 model of Parkinson's disease. Biol. Open *6*, 141–147.

Li, F., Zhang, L., Craddock, J., Bruce-Keller, A.J., Dasuri, K., Nguyen, A., and Keller, J.N. (2008). Aging and dietary restriction effects on ubiquitination, sumoylation, and the proteasome in the heart. Mech. Ageing Dev. *129*, 515–521.

Li, X., Lonard, D.M., Jung, S.Y., Malovannaya, A., Feng, Q., Qin, J., Tsai, S.Y., Tsai, M.-J., and O'Malley, B.W. (2006). The SRC-3/AIB1 coactivator is degraded in a ubiquitin- and ATP-independent manner by the REGgamma proteasome. Cell *124*, 381–392.

Li, X., Thompson, D., Kumar, B., and DeMartino, G.N. (2014). Molecular and Cellular Roles of PI31 (PSMF1) Protein in Regulation of Proteasome Function. J. Biol. Chem. *289*, 17392–17405.

Lin, S.-J., Defossez, P.-A., and Guarente, L. (2000). Requirement of NAD and SIR2 for Life-Span Extension by Calorie Restriction in Saccharomyces cerevisiae. Science *289*, 2126–2128.

Linford, N.J., Bilgir, C., Ro, J., and Pletcher, S.D. (2013). Measurement of Lifespan in Drosophila melanogaster. JoVE J. Vis. Exp. e50068–e50068.

Liu, J., Wang, Y., Li, L., Zhou, L., Wei, H., Zhou, Q., Liu, J., Wang, W., Ji, L., Shan, P., et al. (2013). Site-specific Acetylation of the Proteasome Activator REGγ Directs Its Heptameric Structure and Functions. J. Biol. Chem. *288*, 16567–16578.

Livnat-Levanon, N., Kevei, É., Kleifeld, O., Krutauz, D., Segref, A., Rinaldi, T., Erpapazoglou, Z., Cohen, M., Reis, N., Hoppe, T., et al. (2014). Reversible 26S proteasome disassembly upon mitochondrial stress. Cell Rep. *7*, 1371–1380.

Livneh, I., Cohen-Kaplan, V., Cohen-Rosenzweig, C., Avni, N., and Ciechanover, A. (2016). The life cycle of the 26S proteasome: from birth, through regulation and function, and onto its death. Cell Res. *26*, 869–885.

Lőw, P., Varga, Á., Pircs, K., Nagy, P., Szatmári, Z., Sass, M., and Juhász, G. (2013). Impaired proteasomal degradation enhances autophagy via hypoxia signaling in Drosophila. BMC Cell Biol. *14*, 29.

Ma, J., Katz, E., and Belote, J.M. (2002). Expression of proteasome subunit isoforms during spermatogenesis in Drosophila melanogaster. Insect Mol. Biol. *11*, 627–639.

Mack, T.G.A., Reiner, M., Beirowski, B., Mi, W., Emanuelli, M., Wagner, D., Thomson, D., Gillingwater, T., Court, F., Conforti, L., et al. (2001). Wallerian degeneration of injured axons and synapses is delayed by a Ube4b/Nmnat chimeric gene. Nat. Neurosci. *4*, 1199–1206.

Majetschak, M. (2013). Regulation of the proteasome by ATP: implications for ischemic myocardial injury and donor heart preservation. Am. J. Physiol. Heart Circ. Physiol. *305*, H267-278.

McCay, C.M., Crowell, M.F., and Maynard, L.A. (1935). The Effect of Retarded Growth Upon the Length of Life Span and Upon the Ultimate Body Size One Figure. J. Nutr. *10*, 63–79.

McClure, J.M., Wierman, M.B., Maqani, N., and Smith, J.S. (2012). Isonicotinamide enhances Sir2 protein-mediated silencing and longevity in yeast by raising intracellular NAD+ concentration. J. Biol. Chem. *287*, 20957–20966.

Meiners, S., Heyken, D., Weller, A., Ludwig, A., Stangl, K., Kloetzel, P.-M., and Krüger, E. (2003). Inhibition of Proteasome Activity Induces Concerted Expression of Proteasome Genes and *de Novo* Formation of Mammalian Proteasomes. J. Biol. Chem. *278*, 21517–21525.

Morris, M.C., Evans, D.A., Bienias, J.L., Scherr, P.A., Tangney, C.C., Hebert, L.E., Bennett, D.A., Wilson, R.S., and Aggarwal, N. (2004). Dietary niacin and the risk of incident Alzheimer's disease and of cognitive decline. J. Neurol. Neurosurg. Psychiatry *75*, 1093–1099.

Mouchiroud, L., Houtkooper, R.H., Moullan, N., Katsyuba, E., Ryu, D., Cantó, C., Mottis, A., Jo, Y.-S., Viswanathan, M., Schoonjans, K., et al. (2013). The NAD(+)/Sirtuin Pathway Modulates Longevity through Activation of Mitochondrial UPR and FOXO Signaling. Cell *154*, 430–441.

Murata, S., Yashiroda, H., and Tanaka, K. (2009). Molecular mechanisms of proteasome assembly. Nat. Rev. Mol. Cell Biol. *10*, 104–115.

Nagashima, Y., Kowa, H., Tsuji, S., and Iwata, A. (2011). FAT10 protein binds to polyglutamine proteins and modulates their solubility. J. Biol. Chem. *286*, 29594–29600.

Nedelsky, N.B., Todd, P.K., and Taylor, J.P. (2008). Autophagy and the ubiquitin-proteasome system: collaborators in neuroprotection. Biochim. Biophys. Acta *1782*, 691–699.

Neuburger, P.J. (2006). A Genetic Suppressor of Two Dominant Temperature-Sensitive Lethal Proteasome Mutants of Drosophila melanogaster Is Itself a Mutated Proteasome Subunit Gene. Genetics *173*, 1377–1387.

Ocampo, A., Liu, J., and Barrientos, A. (2013). NAD+ salvage pathway proteins suppress proteotoxicity in yeast models of neurodegeneration by promoting the clearance of misfolded/oligomerized proteins. Hum. Mol. Genet. *22*, 1699–1708.

Otero, M.G., Alloatti, M., Cromberg, L.E., Almenar-Queralt, A., Encalada, S.E., Pozo Devoto, V.M., Bruno, L., Goldstein, L.S.B., and Falzone, T.L. (2014). Fast axonal transport of the

proteasome complex depends on membrane interaction and molecular motor function. J. Cell Sci. *127*, 1537–1549.

Parfitt, D.A., Michael, G.J., Vermeulen, E.G.M., Prodromou, N.V., Webb, T.R., Gallo, J.-M., Cheetham, M.E., Nicoll, W.S., Blatch, G.L., and Chapple, J.P. (2009). The ataxia protein sacsin is a functional co-chaperone that protects against polyglutamine-expanded ataxin-1. Hum. Mol. Genet. *18*, 1556–1565.

Park, Y., Hong, S., Kim, S.-J., and Kang, S. (2005). Proteasome function is inhibited by polyglutamine-expanded ataxin-1, the SCA1 gene product. Mol. Cells *19*, 23–30.

Park, Y., Hong, S., Kim, S.-J., and Kang, S. Proteasome Function Is Inhibited by Polyglutamine-expanded Ataxin-1, the SCA1 Gene Product. Mol. Cells *19*, 23–30.

Pathare, G.R., Nagy, I., Bohn, S., Unverdorben, P., Hubert, A., Körner, R., Nickell, S., Lasker, K., Sali, A., Tamura, T., et al. (2012). The proteasomal subunit Rpn6 is a molecular clamp holding the core and regulatory subcomplexes together. Proc. Natl. Acad. Sci. U. S. A. *109*, 149–154.

Patrick, G.N. (2006). Synapse formation and plasticity: recent insights from the perspective of the ubiquitin proteasome system. Curr. Opin. Neurobiol. *16*, 90–94.

Persengiev, S., Kondova, I., and Bontrop, R.E. (2012). Functional Annotation of Small Noncoding RNAs Target Genes Provides Evidence for a Deregulated Ubiquitin-Proteasome Pathway in Spinocerebellar Ataxia Type 1. J. Nucleic Acids *2012*.

Piterman, R., Braunstein, I., Isakov, E., Ziv, T., Navon, A., Cohen, S., and Stanhill, A. (2014). VWA domain of S5a restricts the ability to bind ubiquitin and Ubl to the 26S proteasome. Mol. Biol. Cell *25*, 3988–3998.

van Roermund, C.W., Elgersma, Y., Singh, N., Wanders, R.J., and Tabak, H.F. (1995). The membrane of peroxisomes in Saccharomyces cerevisiae is impermeable to NAD(H) and acetyl-CoA under in vivo conditions. EMBO J. *14*, 3480–3486.

Rogers, I., Kerr, F., Martinez, P., Hardy, J., Lovestone, S., and Partridge, L. (2012). Ageing Increases Vulnerability to Aβ42 Toxicity in Drosophila. PLoS ONE *7*.

Ruan, K., Zhu, Y., Li, C., Brazill, J.M., and Zhai, R.G. (2015). Alternative splicing of Drosophila Nmnat functions as a switch to enhance neuroprotection under stress. Nat. Commun. *6*.

Savulescu, A.F., and Glickman, M.H. (2011). Proteasome activator 200: the heat is on.. Mol. Cell. Proteomics MCP *10*, R110.006890.

Schmidt, M., and Finley, D. (2013). Regulation of proteasome activity in health and disease. Biochim. Biophys. Acta.

Selkoe, D.J. (2002). Alzheimer's disease is a synaptic failure. Science *298*, 789–791.

Sha, Z., and Goldberg, A.L. (2014). Proteasome-Mediated Processing of Nrf1 Is Essential for Coordinate Induction of All Proteasome Subunits and p97. Curr. Biol. *24*, 1573–1583.

Shim, S.M., Lee, W.J., Kim, Y., Chang, J.W., Song, S., and Jung, Y.-K. (2012). Role of S5b/PSMD5 in Proteasome Inhibition Caused by TNF-α/NFκB in Higher Eukaryotes. Cell Rep. *2*, 603–615.

Smith, D.M., Chang, S.-C., Park, S., Finley, D., Cheng, Y., and Goldberg, A.L. (2007a). Docking of the Proteasomal ATPases' Carboxyl Termini in the 20S Proteasome's α Ring Opens the Gate for Substrate Entry. Mol. Cell *27*, 731–744.

Smith, D.M., Chang, S.-C., Park, S., Finley, D., Cheng, Y., and Goldberg, A.L. (2007b). Docking of the Proteasomal ATPases' Carboxyl Termini in the 20S Proteasome's α Ring Opens the Gate for Substrate Entry. Mol. Cell *27*, 731–744.

Snyder, H., Mensah, K., Theisler, C., Lee, J., Matouschek, A., and Wolozin, B. (2003). Aggregated and monomeric alpha-synuclein bind to the S6' proteasomal protein and inhibit proteasomal function. J. Biol. Chem. *278*, 11753–11759.

Stadtmueller, B.M., and Hill, C.P. (2011). Proteasome Activators. Mol. Cell *41*, 8–19.

Stefanis, L., Larsen, K.E., Rideout, H.J., Sulzer, D., and Greene, L.A. (2001). Expression of A53T mutant but not wild-type alpha-synuclein in PC12 cells induces alterations of the ubiquitin-dependent degradation system, loss of dopamine release, and autophagic cell death. J. Neurosci. Off. J. Soc. Neurosci. *21*, 9549–9560.

Sümegi, M., Hunyadi-Gulyás, É., Medzihradszky, K.F., and Udvardy, A. (2003). 26S proteasome subunits are O-linked N-acetylglucosamine-modified in Drosophila melanogaster. Biochem. Biophys. Res. Commun. *312*, 1284–1289.

Szlanka, T., Haracska, L., Kiss, I., Deák, P., Kurucz, É., Andó, I., Virágh, E., and Udvardy, A. (2003). Deletion of proteasomal subunit S5a/Rpn10/p54 causes lethality, multiple mitotic defects and overexpression of proteasomal genes in Drosophila melanogaster. J. Cell Sci. *116*, 1023–1033.

Tai, H.-C., Besche, H., Goldberg, A.L., and Schuman, E.M. (2010). Characterization of the Brain 26S Proteasome and its Interacting Proteins. Front. Mol. Neurosci. *3*.

Tai, H.-C., Serrano-Pozo, A., Hashimoto, T., Frosch, M.P., Spires-Jones, T.L., and Hyman, B.T. (2012). The synaptic accumulation of hyperphosphorylated tau oligomers in Alzheimer disease is associated with dysfunction of the ubiquitin-proteasome system. Am. J. Pathol. *181*, 1426–1435.

Tokumoto, T., Yamashita, M., Tokumoto, M., Katsu, Y., Horiguchi, R., Kajiura, H., and Nagahama, Y. (1997). Initiation of Cyclin B Degradation by the 26S Proteasome upon Egg Activation. J. Cell Biol. *138*, 1313–1322.

Tomaru, U., Takahashi, S., Ishizu, A., Miyatake, Y., Gohda, A., Suzuki, S., Ono, A., Ohara, J., Baba, T., Murata, S., et al. (2012). Decreased proteasomal activity causes age-related phenotypes and promotes the development of metabolic abnormalities. Am. J. Pathol. *180*, 963–972.

Tonoki, A., Kuranaga, E., Tomioka, T., Hamazaki, J., Murata, S., Tanaka, K., and Miura, M. (2009). Genetic evidence linking age-dependent attenuation of the 26S proteasome with the aging process. Mol. Cell. Biol. *29*, 1095–1106.

Tsai, N.-P. (2014). Ubiquitin proteasome system-mediated degradation of synaptic proteins: An update from the postsynaptic side. Biochim. Biophys. Acta BBA - Mol. Cell Res. *1843*, 2838–2842.

Tsakiri, E.N., Sykiotis, G.P., Papassideri, I.S., Terpos, E., Dimopoulos, M.A., Gorgoulis, V.G., Bohmann, D., and Trougakos, I.P. (2013). Proteasome dysfunction in Drosophila signals to an Nrf2-dependent regulatory circuit aiming to restore proteostasis and prevent premature aging. Aging Cell *12*, 802–813.

Tsvetkov, P., Myers, N., Eliav, R., Adamovich, Y., Hagai, T., Adler, J., Navon, A., and Shaul, Y. (2014). NADH binds and stabilizes the 26S proteasomes independent of ATP. J. Biol. Chem. *289*, 11272–11281.

Um, J.W., Im, E., Lee, H.J., Min, B., Yoo, L., Yoo, J., Lübbert, H., Stichel-Gunkel, C., Cho, H.-S., Yoon, J.B., et al. (2010). Parkin directly modulates 26S proteasome activity. J. Neurosci. Off. J. Soc. Neurosci. *30*, 11805–11814.

VanLinden, M.R., Niere, M., Nikiforov, A.A., Ziegler, M., and Dölle, C. (2017). Compartment-Specific Poly-ADP-Ribose Formation as a Biosensor for Subcellular NAD Pools. Methods Mol. Biol. Clifton NJ *1608*, 45–56.

Verdin, E. (2015). NAD^+ in aging, metabolism, and neurodegeneration. Science *350*, 1208–1213.

Verma, R., Chen, S., Feldman, R., Schieltz, D., Yates, J., Dohmen, J., and Deshaies, R.J. (2000). Proteasomal Proteomics: Identification of Nucleotide-sensitive Proteasome-interacting Proteins by Mass Spectrometric Analysis of Affinity-purified Proteasomes. Mol. Biol. Cell *11*, 3425–3439.

Vernace, V.A., Arnaud, L., Schmidt-Glenewinkel, T., and Figueiredo-Pereira, M.E. (2007). Aging perturbs 26S proteasome assembly in Drosophila melanogaster. FASEB J. *21*, 2672–2682.

Vilchez, D., Morantte, I., Liu, Z., Douglas, P.M., Merkwirth, C., Rodrigues, A.P.C., Manning, G., and Dillin, A. (2012). RPN-6 determines C. elegans longevity under proteotoxic stress conditions. Nature *489*, 263–268.

Vilchez, D., Saez, I., and Dillin, A. (2014). The role of protein clearance mechanisms in organismal ageing and age-related diseases. Nat Commun *5*.

Wang, J., Zhai, Q., Chen, Y., Lin, E., Gu, W., McBurney, M.W., and He, Z. (2005). A local mechanism mediates NAD-dependent protection of axon degeneration. J. Cell Biol. *170*, 349–355.

Wang, S., Xing, Z., Vosler, P.S., Yin, H., Li, W., Zhang, F., Signore, A.P., Stetler, R.A., Gao, Y., and Chen, J. (2008). Cellular NAD Replenishment Confers Marked Neuroprotection Against Ischemic Cell Death Role of Enhanced DNA Repair. Stroke J. Cereb. Circ. *39*, 2587–2595.

Wang, X., Chemmama, I.E., Yu, C., Huszagh, A., Xu, Y., Viner, R., Block, S.A., Cimermancic, P., Rychnovsky, S.D., Ye, Y., et al. (2017). The Proteasome-Interacting Ecm29 Protein Disassembles the 26S Proteasome in Response to Oxidative Stress. J. Biol. Chem. jbc.M117.803619.

Weberruss, M.H., Savulescu, A.F., Jando, J., Bissinger, T., Harel, A., Glickman, M.H., and Enenkel, C. (2013). Blm10 facilitates nuclear import of proteasome core particles. EMBO J. *32*, 2697–2707.

Winborn, B.J., Travis, S.M., Todi, S.V., Scaglione, K.M., Xu, P., Williams, A.J., Cohen, R.E., Peng, J., and Paulson, H.L. (2008). The deubiquitinating enzyme ataxin-3, a polyglutamine disease protein, edits Lys63 linkages in mixed linkage ubiquitin chains. J. Biol. Chem. *283*, 26436–26443.

Wójcik, C., and DeMartino, G.N. (2003). Intracellular localization of proteasomes. Int. J. Biochem. Cell Biol. *35*, 579–589.

Xiang, L., and He, G. (2011). Caloric Restriction and Antiaging Effects. Ann. Nutr. Metab. *58*, 42–48.

Yang, B.-J., Han, X.-X., Yin, L.-L., Xing, M.-Q., Xu, Z.-H., and Xue, H.-W. (2016). *Arabidopsis* PROTEASOME REGULATOR1 is required for auxin-mediated suppression of proteasome activity and regulates auxin signalling. Nat. Commun. *7*, 11388.

Yang, H., Yang, T., Baur, J.A., Perez, E., Matsui, T., Carmona, J.J., Lamming, D.W., Souza-Pinto, N.C., Bohr, V.A., Rosenzweig, A., et al. (2007). Nutrient-Sensitive Mitochondrial NAD+ Levels Dictate Cell Survival. Cell *130*, 1095–1107.

Yashiroda, H., Toda, Y., Otsu, S., Takagi, K., Mizushima, T., and Murata, S. (2015). N-Terminal α7 Deletion of the Proteasome 20S Core Particle Substitutes for Yeast PI31 Function. Mol. Cell. Biol. *35*, 141–152.

Yoshino, J., Mills, K.F., Yoon, M.J., and Imai, S. (2011). Nicotinamide Mononucleotide, a Key NAD+ Intermediate, Treats the Pathophysiology of Diet- and Age-Induced Diabetes in Mice. Cell Metab. *14*, 528–536.

Zaiss, D.M.W., Standera, S., Holzhütter, H., Kloetzel, P.-M., and Sijts, A.J.A.M. (1999). The proteasome inhibitor PI31 competes with PA28 for binding to 20S proteasomes. FEBS Lett. *457*, 333–338.

Zhai, R.G., Cao, Y., Hiesinger, P.R., Zhou, Y., Mehta, S.Q., Schulze, K.L., Verstreken, P., and Bellen, H.J. (2006). Drosophila NMNAT maintains neural integrity independent of its NAD synthesis activity. PLoS Biol. *4*, e416.

Zhai, R.G., Zhang, F., Hiesinger, P.R., Cao, Y., Haueter, C.M., and Bellen, H.J. (2008). NAD synthase NMNAT acts as a chaperone to protect against neurodegeneration. Nature *452*, 887–891.

Zhang, F., Su, K., Yang, X., Bowe, D.B., Paterson, A.J., and Kudlow, J.E. (2003). O-GlcNAc Modification Is an Endogenous Inhibitor of the Proteasome. Cell *115*, 715–725.

Zhang, F., Hu, Y., Huang, P., Toleman, C.A., Paterson, A.J., and Kudlow, J.E. (2007a). Proteasome Function Is Regulated by Cyclic AMP-dependent Protein Kinase through Phosphorylation of Rpt6. J. Biol. Chem. *282*, 22460–22471.

Zhang, F., Paterson, A.J., Huang, P., Wang, K., and Kudlow, J.E. (2007b). Metabolic Control of Proteasome Function. Physiology *22*, 373–379.

Zhang, H., Ryu, D., Wu, Y., Gariani, K., Wang, X., Luan, P., D'Amico, D., Ropelle, E.R., Lutolf, M.P., Aebersold, R., et al. (2016). NAD+ repletion improves mitochondrial and stem cell function and enhances life span in mice. Science aaf2693.

Zhang, L., Li, F., Dimayuga, E., Craddock, J., and Keller, J.N. (2007c). Effects of aging and dietary restriction on ubiquitination, sumoylation, and the proteasome in the spleen. FEBS Lett. *581*, 5543–5547.

Zheng, Q., Huang, T., Zhang, L., Zhou, Y., Luo, H., Xu, H., and Wang, X. (2016). Dysregulation of Ubiquitin-Proteasome System in Neurodegenerative Diseases. Front. Aging Neurosci. *8*.

Zhu, S., Wildonger, J., Barshow, S., Younger, S., Huang, Y., and Lee, T. (2012). The bHLH repressor Deadpan regulates the self-renewal and specification of Drosophila larval neural stem cells independently of Notch. PloS One *7*, e46724.